
[All ETDs from UAB](#)

[UAB Theses & Dissertations](#)

2005

Effects of passivation on surface properties of titanium and titanium alloys.

Donald William Petersen
University of Alabama at Birmingham

Follow this and additional works at: <https://digitalcommons.library.uab.edu/etd-collection>

Recommended Citation

Petersen, Donald William, "Effects of passivation on surface properties of titanium and titanium alloys." (2005). *All ETDs from UAB*. 5425.
<https://digitalcommons.library.uab.edu/etd-collection/5425>

This content has been accepted for inclusion by an authorized administrator of the UAB Digital Commons, and is provided as a free open access item. All inquiries regarding this item or the UAB Digital Commons should be directed to the [UAB Libraries Office of Scholarly Communication](#).

EFFECTS OF PASSIVATION ON SURFACE PROPERTIES OF TITANIUM AND
TITANIUM ALLOYS

by

DONALD WILLIAM PETERSEN

A DISSERTATION

Submitted to the graduate faculty of The University of Alabama at Birmingham,
in partial fulfillment of the requirements for the degree of
Doctor of Philosophy

BIRMINGHAM, ALABAMA

2005

UMI Number: 3187882

Copyright 2005 by
Petersen, Donald William

All rights reserved.

INFORMATION TO USERS

The quality of this reproduction is dependent upon the quality of the copy submitted. Broken or indistinct print, colored or poor quality illustrations and photographs, print bleed-through, substandard margins, and improper alignment can adversely affect reproduction.

In the unlikely event that the author did not send a complete manuscript and there are missing pages, these will be noted. Also, if unauthorized copyright material had to be removed, a note will indicate the deletion.

UMI[®]

UMI Microform 3187882

Copyright 2006 by ProQuest Information and Learning Company.

All rights reserved. This microform edition is protected against unauthorized copying under Title 17, United States Code.

ProQuest Information and Learning Company
300 North Zeeb Road
P.O. Box 1346
Ann Arbor, MI 48106-1346

Copyright by
Donald William Petersen
2005

ABSTRACT OF DISSERTATION
GRADUATE SCHOOL, UNIVERSITY OF ALABAMA AT BIRMINGHAM

Degree PhD Program Biomedical Engineering

Name of Candidate Donald William Petersen

Committee Chair Jack E. Lemons

Title Effects of Passivation on Surface Properties of Titanium and Titanium Alloys

The goal of these studies was to determine the effects of different passivation parameters on the surface oxide, corrosion, and biological properties of clinically relevant titanium and titanium alloys (commercially pure Ti, Ti-6Al-4V, and Ti-15Mo). The main focus was on nitric acid passivation and the parameters of passivation time and nitric acid concentration and temperature, as well as the effect of ultrasonication and the addition of titanium ions to the nitric acid solution. The surface topography, oxide characteristics, corrosion properties, chemistry, and biological responses were systematically examined for variously passivated titanium and titanium alloys.

Nitric-acid-passivated and heat-treated samples exhibited similar corrosion properties, which were significantly better than those of non passivated samples were. The heat-treated samples had significantly thicker oxides (8.8-16.8 nm) than the nitric-acid-passivated groups did (3.0-5.4 nm).

The effect of passivation time was dependent on nitric acid concentration. Higher concentrations and temperatures improved the protective properties of the oxides. Alloy elements were found throughout the oxides with varying compositional gradients due to the different passivation treatments. Observed gradients were associated with Electrochemical Impedance Spectroscopy parameters oxide homogeneity and oxide resistance.

Biological responses were similar for all groups. The rougher Ti-15Mo surfaces resulted in higher cell numbers at the initial time period.

Ultrasonication and addition of titanium ions did not alter the corrosion properties of the treated materials. Surface chemistry analyses showed ultrasonication to reduce the percentages of aluminum and molybdenum at the outer surfaces of Ti-6Al-4V and Ti-15Mo, respectively. Electrochemical Impedance Spectroscopy spectra for the ultrasonic and titanium ion groups exhibited two phase angle maximums, which indicated the presence of a dual-layer oxide with a porous outer oxide on top of a dense barrier layer. Biological responses were similar for all groups.

Thus, passivation was shown to improve the corrosion resistance of titanium and titanium alloys. Passivation parameters were shown to affect the protective properties, and these effects were linked to changes in the chemistry and uniformity of the oxide. All materials and surface treatments exhibited excellent corrosion properties and cellular attachment and proliferation.

DEDICATION

I dedicate this dissertation to my children, Rhett, Devan, and Julia.

ACKNOWLEDGMENTS

First, I acknowledge my advisor, Dr. Jack Lemons. I am deeply honored and grateful to have had the opportunity to be a student of one of the “godfathers” of biomaterials. Dr. Lemons’ knowledge, patience, and kindness are legendary, and I am extremely fortunate to have worked with him. I thank him.

I also thank my committee members, Dr. Linda Lucas, Dr. Robin Griffin, Dr. Charles Prince, and Dr. John Cuckler, for their support and expert advice. Thanks go to Dr. Earl Ada for his help with testing and analysis. Special thanks go to Klaus Krause for his editorial advice with the manuscripts. I acknowledge some of the people at University of Alabama, Birmingham who have made my academic and personal experiences special: Laura Clark, Martha Wilkins, Jeff Best, Jon Mosley, Joel Bumgardner, Joo Ong, Preston Beck, Krishna Venugopalan, and many others. I gratefully acknowledge the financial support of Wright Medical Technology and Alvarado Orthopedic Research.

I especially acknowledge my parents and family. Their support and love through all the years have been a blessing for me. Special thanks go to my mom for always being my number 1 fan and to my dad for encouraging me to ask questions and then to go to work to find the answers.

Finally, I thank my wife, Paige, for all her love and support. I would not have been able to finish this without her. Also, a big thank-you goes to my children, Rhett, Devan, and Julia, for providing me with the inspiration to try to make a difference.

TABLE OF CONTENTS

	<i>Page</i>
ABSTRACT.....	iii
DEDICATION.....	v
ACKNOWLEDGMENTS	vi
LIST OF TABLES.....	ix
LIST OF FIGURES	xii
LIST OF ABBREVIATIONS.....	xvi
INTRODUCTION	1
Clinical Relevance	5
Dissertation Organization	6
Hypotheses.....	6
COMPARATIVE EVALUATIONS OF SURFACE CHARACTERISTICS OF CP TITANIUM, TI-6AL-4V AND TI-15MO-2.8NB-0.2SI (TIMETAL® 21SRX).....	9
EFFECTS OF NITRIC ACID PASSIVATION PARAMETERS ON TITANIUM AND TITANIUM ALLOYS RELATED TO CORROSION, SURFACE CHEMISTRY, AND CELL CULTURE PART I EFFECTS OF NITRIC ACID CONCENTRATION, TEMPERATURE, AND TIME.....	40
EFFECTS OF NITRIC ACID PASSIVATION PARAMETERS ON TITANIUM AND TITANIUM ALLOYS RELATED TO CORROSION, SURFACE CHEMISTRY, AND CELL CULTURE PART II EFFECTS OF UTILIZING ULTRASONICATION, TITANIUM IONS IN SOLUTION, AND DIFFERENT SURFACE MORPHOLOGIES.....	115

TABLE OF CONTENTS (Continued)

	<i>Page</i>
SUMMARY DISCUSSION	172
Hypotheses	172
Future Research	188
CONCLUSIONS.....	190
GENERAL LIST OF REFERENCES	192

LIST OF TABLES

<i>Table</i>	<i>Page</i>
COMPARATIVE EVALUATIONS OF SURFACE CHARACTERISTICS OF CP TITANIUM, Ti-6Al-4V AND Ti-15Mo-2.8Nb-0.2Si (TIMETAL® 21SRX)	
1	List of Titanium and Titanium Alloys Used in This Study13
2	Surface Treatments Used in This Study.....14
3	Average Oxide Thickness (nm), $n = 2$18
4	Average Ecorr results (mV), $n = 3$19
5	Average Icorr results (nA/cm^2), $n = 3$19
6	Average Ipass results (nA/cm^2), $n = 3$20
EFFECTS OF NITRIC ACID PASSIVATION PARAMETERS ON TITANIUM AND TITANIUM ALLOYS RELATED TO CORROSION, SURFACE CHEMISTRY, AND CELL CULTURE PART I EFFECTS OF NITRIC ACID CONCENTRATION, TEMPERATURE, AND TIME	
1	Passivation Parameters Used for Nitric Acid Passivation Treatments47
2	Summary of Effect of Time of Nitric Acid Passivation on Impedance and Capacitive Behavior as Determined by Using Spectra From Nyquist and Bode Plots52
3	EIS Parameters Q, n, and Rp Results for cpTi.....55
4	EIS Parameters Q, n, and Rp Results for Ti-6Al-4V56
5	EIS Parameters Q, n, and Rp Results for Ti-15Mo.....57

LIST OF TABLES (Continued)

<i>Table</i>	<i>Page</i>
6 Ecorr, Icorr, and Ipass Results for cpTi	61
7 Ecorr, Icorr, and Ipass Results for Ti-6Al-4V	62
8 Ecorr, Icorr, and Ipass Results for Ti-15Mo	63
9 Surface Composition (at%) by XPS Analysis of Various Passivation Treatment Groups of cpTi After Different Etch Times	64
10 Surface Composition (at%) by XPS Analysis of Various Passivation Treatment Groups of Ti-6Al-4V After Different Etch Times	65
11 Surface Composition (at%) by XPS Analysis of Various Passivation Treatment Groups of Ti-15Mo After Different Etch Times	66
12 Percentage of Oxidation States for cpTi, Ti-6Al-4C, and Ti-15Mo After Different Nitric Acid Passivation Treatments	70
13 Ti/O Ratios for cpTi, Ti-6Al-4V, and Ti-15Mo at Different Etch Times: Effect of 10% and 40% Nitric Acid Concentrations	81
14 Ionic Radii of Titanium, Aluminum, Vanadium, and Molybdenum	85
<p>EFFECTS OF NITRIC ACID PASSIVATION PARAMETERS ON TITANIUM AND TITANIUM ALLOYS RELATED TO CORROSION, SURFACE CHEMISTRY, AND CELL CULTURE</p> <p>PART II</p> <p>EFFECTS OF UTILIZING ULTRASONICATION, TITANIUM IONS IN SOLUTION, AND DIFFERENT SURFACE MORPHOLOGIES</p>	
1 Passivation Methods and Parameters Used	121
2 Qp, np, and Rp Values for cpTi, Ti-6Al-4V, and Ti-15Mo	131
3 Qpor, npor, and Rpor Values for cpTi, Ti-6Al-4V, and Ti-15Mo	132
4 Q, n, and Rp Results for 60- and 600-Grit Groups	133
5 Ecorr, Icorr, and Ipass Results for cpTi, Ti-6Al-4V, and Ti-15Mo	135

LIST OF TABLES (Continued)

<i>Table</i>	<i>Page</i>
6 Ecorr, Icorr, and Ipass Results for 60- and 600-Grit Groups.....	136
7 Activation Times for cpTi, Ti-6Al-4V, and Ti-15Mo Passivation Treatment Groups.....	137
8 Surface Composition (at%) by XPS Analysis of Various Passivation Treatment Groups of cpTi After Different Etch Times	138
9 Surface Composition (at%) by XPS Analysis of Various Passivation Treatment Groups of Ti-6Al-4V After Different Etch Times	139
10 Surface Composition (at%) by XPS Analysis of Various Passivation Treatment Groups of Ti-15Mo After Different Etch Times	140
11 Percentage of Oxidation States for cpTi, Ti-6Al-4V, and Ti-15Mo After Different Nitric Acid Passivation Treatments.....	143
12 Cell Number Results for the Different Treatment Groups at Different Time Points: Percentage of Control (Tissue Culture Plastic)	144
13 Proliferation Results for the Different Treatment Groups at Different Time Periods: Percentage of Control (Tissue Culture Plastic)	145

LIST OF FIGURES

<i>Figure</i>	<i>Page</i>
COMPARATIVE EVALUATIONS OF SURFACE CHARACTERISTICS OF CP TITANIUM, Ti-6Al-4V AND Ti-15Mo-2.8Nb-0.2Si (TIMETAL® 21SRX)	
1	Representative microstructure for cpTi showing equiaxed alpha grains (original magnification x200)33
2	Representative microstructure for Ti64 showing dual phase alpha-beta grains (original magnification x200)34
3	Representative microstructure for 21SRx showing equiaxed beta grains (original magnification x200)35
4	Representative AES spectra of Passivated 21SRx sample after Ar ion sputter36
5	Representative polarization curves for cpTi in the Cleaned, Passivated, and Heat Treated conditions37
6	Representative polarization curves for Ti-6Al-4V in the Cleaned, Passivated, and Heat Treated conditions38
7	Representative polarization curves for 21SRx in the Cleaned, Passivated, and Heat Treated conditions39
EFFECTS OF NITRIC ACID PASSIVATION PARAMETERS ON TITANIUM AND TITANIUM ALLOYS RELATED TO CORROSION, SURFACE CHEMISTRY, AND CELL CULTURE PART I EFFECTS OF NITRIC ACID CONCENTRATION, TEMPERATURE, AND TIME	
1	Nyquist plot for cpTi treatment groups95
2	Bode phase angle plot for cpTi treatment groups96

LIST OF FIGURES (Continued)

<i>Figure</i>	<i>Page</i>
3 Nyquist plot for Ti-6Al-4V treatment groups.....	97
4 Bode phase angle plot for Ti-6Al-4V treatment groups	98
5 Nyquist plot for Ti-15Mo treatment groups.....	99
6 Bode phase angle plot for Ti-15Mo treatment groups	100
7 The Q, n, and Rp results for cpTi as a function of passivation time.....	101
8 The Q, n, and Rp results for Ti64 as a function of passivation time	102
9 The Q, n, and Rp results for Ti-15Mo as a function of passivation time.....	103
10 Percentage change between Q, n, and Rp values of groups passivated in 20°C nitric acid and those values of groups passivated in 50°C nitric acid (n = 3).....	104
11 Percentage change between Q, n, and Rp values of groups passivated in 10% nitric acid and those values of groups passivated in 40% nitric acid (n = 3).....	105
12 Ti/O ratio results for the different cpTi treatment groups.....	106
13 Normalized Al wt% and V wt% results for the different Ti-6Al-4V treatment groups.....	107
14 Normalized Mo wt% results for the different Ti-15Mo treatment groups.....	108
15 XPS high-resolution Ti 2p spectra for passivated cpTi (top), Ti-6Al-4V (middle) and Ti-15Mo (bottom) samples (40% nitric acid at 20°C for 1 h)	109
16 Attachment results after 1, 4, and 24 h of incubation	110
17 Attachment results after 3 and 7 days of incubation.....	111
18 Proliferation results for 1 to 4 h and 4 to 24 h of incubation	112
19 Proliferation results for 1 to 3 days and 3 to 7 days of incubation	113
20 Representative SEM micrographs of cpTi (top), Ti-6Al-4V (middle), and Ti-15Mo (bottom) material with 600-grit finish in the Clean condition (original magnification x1000)	114

LIST OF FIGURES (Continued)

<i>Figure</i>	<i>Page</i>
<p>EFFECTS OF NITRIC ACID PASSIVATION PARAMETERS ON TITANIUM AND TITANIUM ALLOYS RELATED TO CORROSION, SURFACE CHEMISTRY, AND CELL CULTURE PART II EFFECTS OF UTILIZING ULTRASONICATION, TITANIUM IONS IN SOLUTION, AND DIFFERENT SURFACE MORPHOLOGIES</p>	
1	Representative SEM micrographs of cpTi material with 60-grit and 600-grit finish in the Clean condition (original magnification of top and bottom micrographs x1000)161
2	Representative SEM micrographs of Ti-6Al-4V material with 60-grit and 600-grit finish in the Clean condition (original magnification of top and bottom micrographs x1000)162
3	Representative SEM micrographs of Ti-15Mo material with 60-grit and 600-grit finish in the Clean condition (original magnification of top and bottom micrographs x1000)163
4	SEM micrographs of cpTi and Ti-15Mo materials with 600-grit finish that had been passivated with 40% nitric acid with the addition of 160 mg Ti/liter. Micrographs show pit-like features that were more prevalent and larger on the surfaces of the 160Ti groups (original magnifications of top and bottom Micrographs x1000).....164
5	Phase angle Bode plot for two Ti-6Al-4V-40%-Ultrasonic samples.....165
6	Representative activation curves for cpTi (cp) and Ti-6Al-4V (64) samples from all the treatment groups.....166
7	Depth profiles of elemental composition in the surface region for ultrasonically passivated cpTi, Ti-6Al-4V, and Ti-15Mo167
8	Normalized percentage of aluminum in the surface region for the different treatment groups of Ti-6Al-4V as a function of etch time.....168
9	Normalized percentage of vanadium in the surface region for the different treatment groups of Ti-6Al-4V as a function of etch time.....169
10	Normalized percentage of molybdenum in the surface region for the different treatment groups of Ti-15Mo as a function of etch time.....170

LIST OF FIGURES (Continued)

<i>Figure</i>	<i>Page</i>
11 Representative Ti 2p high-resolution spectra for cpTi (top), Ti-6Al-4V (middle), and Ti-15Mo (bottom) samples that had been passivated ultrasonically (40% nitric acid at 20°C for 1 h)	171

LIST OF ABBREVIATIONS

AES	Auger electron microscopy
ASTM	American Society for Testing and Materials
C	capacitor
CPE	constant-phase element
cpTi	commercially pure titanium
E _{corr}	corrosion potential
EEC	equivalent electrical circuit
EIS	electrochemical impedance spectroscopy
FBS	fetal bovine serum
HBSS	Hanks' Balanced Salt Solution
I _{corr}	corrosion rate at the maximum corrosion potential
I _{pass}	passive current density
PBS	phosphate buffer saline
R _p	oxide resistance
R _s	system resistance
SCE	standard calomel electrode
SEM	scanning electron microscopy
XPS	X-ray photoelectron spectroscopy

INTRODUCTION

In 1738, M. V. Lomonosov first reported the phenomenon of passivation.¹ In the course of conducting corrosion experiments on iron in nitric acid, Lomonosov found that the rate of iron dissolution did not increase uniformly with increasing nitric acid concentration, but instead dropped drastically and remained low with further concentration increases.¹ In Lomonosov's "Dissertation on the Action of Chemical Solvents in General," he states, "when using strong spirits of niter for the dissolution of metals, dissolution soon stops because the solvent ceases to act".² Since then, the effects of passivation have been the topic of many studies in the scientific community.

Metals that exhibit the type of behavior described by Lomonosov are known as passive metals. Titanium is one such metal. The passive property of titanium stems from the fact that it is a reactive metal and on exposure to oxygen instantaneously oxidizes and forms a thin oxide layer. The oxide layer, in turn, isolates the metal from the environment and thus prevents further oxidation. The oxide film that forms instantly is often referred to as a natural or native oxide. For titanium, the native oxides are typically 3-5 nm thick and have an amorphous structure.^{3,4} Although thin, the native oxides provide excellent corrosion resistance.⁵⁻⁷

However, titanium can be further passivated (i.e., made more corrosion resistant) by subjecting it to other surface treatments. Heat treating, boiling in water, and treating with acid are methods that have been used to enhance the passivity of titanium. The improved corrosion resistance of the heat-treated and boiling-water-treated materials is at-

tributed in the literature to thicker and more crystalline oxides.⁸⁻¹¹ Trepanier¹² showed nitric acid passivation to improve the corrosion resistance of a titanium-nickel alloy. The authors attributed the improvement to the acid's removing the native oxide, which was said to be highly defective, and growing in its place a more uniform oxide.¹² Wallinder¹³ and Noh¹⁴ showed improved corrosion properties for stainless steel passivated in nitric acid. These studies showed the effects of nitric acid to be a function of time of immersion, acid concentration, and temperature. The main reason given for the improvement was an increase in the chromium content in the surface oxide.^{13, 14}

However, Callen¹⁵ and Lowenberg¹⁶ have shown nitric acid passivation of the alloy Ti-6Al-4V to increase the dissolution of titanium, aluminum, and vanadium ions compared with non passivated Ti-6Al-4V. The same effect was not exhibited by commercially pure titanium (cpTi) samples. The authors attributed the increase to thinner oxides and the presence of aluminum in the surface oxide of the alloy. On the basis of the results of their studies, the authors questioned the efficacy of nitric acid treatment as a passivation method for titanium alloys.^{15, 16}

The importance of the Callen¹⁵ and Lowenberg¹⁶ studies lies in the fact that medical device manufacturers currently use nitric acid treatments to clean and passivate titanium and titanium alloy implants as part of the manufacturing process. In fact, an American Society for Testing and Materials (ASTM) standard exists for the nitric acid passivation of metallic surgical implants, ASTM F86.¹⁷ The standard was originally developed for stainless steels and cobalt-chromium alloy but was later expanded to include titanium and titanium alloys.

It is important to note that ASTM F86 specifies ranges of values for the different passivation parameters. The specified concentration range is 20-40 percent by volume (vol%), and specified for at least 30 min at room temperature and at least 20 min at 49-60°C. Thus, in light of the results of Wallinder¹³ and Noh¹⁴, which showed oxide and corrosion properties to vary over a range of passivation parameters, one may wonder what happens to titanium and titanium alloys over a range of parameter values.

Comparisons of studies on the use of nitric acid for treating titanium are difficult because of the variety of passivation parameters used. Ong¹⁸ reported immersing cpTi in 40 vol% nitric acid for 30 min, while Kilpadi¹⁹ immersed cpTi in 30 vol% for 20 min. Callen¹⁵ and Lowenberg¹⁶ reported using 34 vol% nitric acid for 1 h under ultrasonication to passivate both cpTi and Ti-6Al-4V specimens.

The use of ultrasonication by Callen¹⁵ and Lowenberg¹⁶ raises yet another parameter to consider when assessing the effects of passivation. Whillock²⁰ showed that cavitation, the formation and collapse of voids that is caused by the propagation of an ultrasonic wave through a liquid, results in very high pressures and temperatures in the vicinity of the collapsing void. The locally high temperatures and pressures can affect the chemical reactions during passivation; in addition, high-velocity liquid jets that result from the collapse of the void can be directed at the surface and can mechanically damage the surface (i.e., cause cavitation erosion).²⁰

Another parameter that may be relevant, especially for the passivation of medical implants, is the presence of titanium ions in the nitric acid solution. Robin^{21, 22} found that the corrosion rate of titanium was diminished in nitric acid when there were additional titanium ions in the solution. Further investigations showed that there existed a threshold

titanium concentration necessary to inhibit corrosion and that the threshold was sensitive to the concentration of nitric acid and the titanium material being passivated.²² This finding is relevant to the medical device industry in that, typically, large nitric acid baths are used to passivate batches of implants and multiple batches are processed with the same nitric acid bath. Consequently, one would expect an increase in the amount of titanium ions in the nitric acid bath over the course of the processing, which may result in differently passivated surfaces for the implants of different batches.

Thus, the overall goal of the research for this dissertation was to determine the effects of various passivation techniques and of changes in the parameters within specific passivation treatments. In the first study, titanium and titanium alloys passivated with nitric acid and with heat treatment were compared with non passivated titanium and titanium alloys. In the second and third studies, the focus was on the nitric acid passivation process. The second study investigated the effects of time of passivation and the concentration and temperature of the nitric acid. The third study examined the effects of ultrasonication and the presence of additional titanium ions in the nitric acid solution on the passivated samples.

The effects of the various passivation treatments were determined by characterizing the surface oxide properties, corrosion properties, and biological responses of the treated titanium and titanium alloys. Scanning electron microscopy (SEM) was used to document the surface morphology. Corrosion and oxide properties were determined with electrochemical impedance spectroscopy (EIS) and potentiodynamic polarization tests. The surface oxide chemistry was determined with X-ray photoelectron spectroscopy (XPS). Last, the biological response of SaOS-2 osteoblast-like cells to the materials pas-

sivated in various ways was measured using hexosaminidase assay to determine cell attachment and proliferation.

Clinical Relevance

Titanium derives its biocompatibility properties from the presence of a tenacious passive oxide layer on the surface^{5, 7}. To improve the mechanical and wear properties of the relatively weak and soft unalloyed cpTi, titanium alloys, such as Ti-6Al-4V have been used for implant applications. In addition, more recently, beta-titanium alloys have been investigated for biomaterial applications because of their greater strength and their lower elastic modulus, which more closely matches that of bone and thus helps reduce stress shielding in bone implant applications.²³

However, the presence of alloying elements in the surface oxide is of a concern from a biological perspective because some of the constituent ions have been reported to have toxic effects on cells.²⁴⁻²⁷ In addition, for bone implant applications, aluminum and vanadium ions have been reported to hinder apatite formation, which could result in an unsuccessful outcome.²⁸ This concern is exacerbated by reports from Callen¹⁵ and others^{15, 16} that nitric acid passivation, a standard process used in implant manufacturing, actually increases the release of constituent ions. Thus, the focus of this research was to investigate the parameters used in the passivation of titanium and titanium alloys to attempt to gain a better understanding of the passivation effects and to use that understanding to help improve the protective properties of the implant surface.

Dissertation Organization

The dissertation, “Effects of Passivation on Surface Properties of Titanium and Titanium Alloys”, is organized in preprint style. The main body of the dissertation consists of three manuscripts. The first manuscript has been published, and the last two manuscripts are in preparation for submission. The preliminary pages of the dissertation consist of the table of contents, lists of tables and figures found in the manuscripts, the overall abstract for the manuscripts, and this general introduction. Included in the general introduction are the hypotheses for the dissertation. A summary discussion covering all the manuscripts follows the three manuscripts and includes a discussion of each hypothesis. After the summary discussion, recommendations are made for future studies. Finally, references for the dissertation introduction and summary discussion are listed.

Hypotheses

Hypothesis 1:

Heat treatment (350°C for 1 h in air) and nitric acid passivation (40 vol% nitric acid at room temperature for 30 min) will improve the corrosion properties of cpTi, Ti-6Al-4V, and beta-titanium, Ti-15Mo-2.8Nb-0.2Si (Timetal[®] 21SRx).

Hypothesis 2:

Heat treatment (350°C for 1 h in air) and nitric acid passivation (40 vol% nitric acid at room temperature for 30 min) will increase the oxide thickness of cpTi, Ti-6Al-4V, and beta-titanium, Ti-15Mo-2.8Nb-0.2Si (Timetal[®] 21SRx).

Hypothesis 3:

The surface oxides of cpTi, Ti-6Al-4V, and Ti-15Mo-2.8Nb-0.2Si (Timetal[®] 21SRx) materials undergoing similar surface treatments will have similar thicknesses but different chemistries.

Hypothesis 4:

Increasing the time of passivation used in the nitric acid passivation process will improve the protective properties of the surface oxides and the corrosion resistance of cpTi, Ti-6Al-4V, and Ti-15Mo.

Hypothesis 5:

Increasing the nitric acid concentration used in the nitric acid passivation process will improve the protective properties of the surface oxides and the corrosion resistance of cpTi, Ti-6Al-4V, and Ti-15Mo.

Hypothesis 6:

Increasing the nitric acid temperature used in the nitric acid passivation process will improve the protective properties of the surface oxides and the corrosion resistance of cpTi, Ti-6Al-4V, and Ti-15Mo.

Hypothesis 7:

Nitric acid passivation using ultrasonication will decrease the protective properties of the surface oxides of cpTi, Ti-6Al-4V, and Ti-15Mo and decrease corrosion resistance.

Hypothesis 8:

Nitric acid passivation with the addition of titanium ions will improve the protective properties of the surface oxides of cpTi, Ti-6Al-4V, and Ti-15Mo and increase corrosion resistance.

Hypothesis 9:

The nitric acid treatments for cpTi, Ti-6Al-4V, and Ti-15Mo will not reduce cell attachment and proliferation compared to those properties of non passivated materials.

COMPARATIVE EVALUATIONS OF SURFACE CHARACTERISTICS OF CP
TITANIUM, TI-6AL-4V AND TI-15MO-2.8NB-0.2SI (TIMETAL[®] 21SRX)

by

DON PETERSEN, JACK LEMONS, AND LINDA LUCAS

Journal of ASTM International 2(8):1-15, 2005

Copyright

2005

by

ASTM International

Used by permission

Format adapted for dissertation

ABSTRACT

Commercially pure titanium (cpTi), Ti-6Al-4V (Ti64), and Ti-15Mo-2.8Nb-0.2Si (21SRx), with three unique atomic, alpha, alpha-beta, and beta grain structures, respectively, were subjected to three different surface treatments: cleaning, nitric acid passivation, and heat treatment. Experiments were conducted to determine the effects of the type of material and surface modifications on the substrate microstructure, surface oxide composition and thickness, and resultant corrosion behavior.

Metallography showed the cpTi groups were an equiaxed single alpha phase material, the Ti64 groups a dual-phase alpha-beta material, and the 21SRx groups an equiaxed beta material. The different surface treatments did not alter the substrate microstructures of any groups.

Spectroscopic (AES) results showed typical titanium and titanium alloy spectra with dominant Ti and O peaks for all sample groups, indicative of titanium dioxide. In addition, small Al and Mo peaks were detected throughout the surface oxides of the Ti64 and 21SRx specimens, respectively. AES depth profiling showed no significant difference in the oxide thickness between all the Cleaned and Passivated groups regardless of metal or alloy group. However, all the Heat Treated groups had significantly thicker oxides.

In general, corrosion results showed Passivated and Heat Treated groups to have similar corrosion properties and significantly improved corrosion resistances compared to the Cleaned groups. All impedance spectra fit into the Randles equivalent circuit model, and all sample groups exhibited near ideal capacitive behavior ($\phi \cong 90^\circ$) expected for titanium and its alloys.

INTRODUCTION

Titanium and titanium alloys, such as Ti-6Al-4V, are the most commonly used metallic implant biomaterials. Biocompatibility has often been attributed to excellent corrosion properties.¹⁻³ In addition, titanium and its alloys have relatively high strength and low elastic modulus. A lower implant elastic modulus has been proposed to more evenly disperse mechanical loading throughout the implant interface, which in turn minimizes “stress shielding” of the host bone, resulting in less bone atrophy.^{4,5}

The excellent corrosion and biocompatibility properties of titanium and its alloys are attributed to the formation of a stable, protective oxide film on their surfaces.⁶ The composition and thickness of surface oxides are known to depend on the substrate and the environment in which the oxide is formed.⁷⁻⁹ Oxides that form on mechanically polished or machined specimens are generally classified as native oxides. These oxides form quickly on freshly polished or machined specimens on exposure to air or other environments that contain oxygen (e.g., water or tissue fluids). Native oxides are thin (less than 10 nm thick), amorphous in structure, and composed primarily of titanium and oxygen.^{7,10} However, in the case of alloys, alloy elements such as Al and V have been found within the oxide coating.¹⁰⁻¹³

Materials that are exposed to stronger oxidizing solutions than air or water are said to have undergone passivation. In the case of titanium and its alloys, a commonly used method for passivation is by using a nitric acid solution in accordance to the protocol specified in Standard Practice for Surface Preparation and Marking of Metallic Surgical Implants (ASTM F 86-01). Titanium and titanium alloy specimens that have been passivated using this protocol form thin oxides, much like the native oxides, with

thicknesses of less than 10 nm^{11, 14-17}. The details of the effect of passivation on corrosion properties remain as a topic of research. Generally, improved corrosion properties are believed to result from this process; however, conflicting results have been reported.^{11, 18}

Heat treatment at elevated temperatures in air can also further oxidize titanium and its alloys. Heat treatments have been shown to increase the thickness and crystallinity of the oxide, with the extent of such increases depending on the temperature and duration of the heat treatment.^{19, 20} It is generally thought that thicker oxides, which result from oxidation at elevated temperatures, may improve corrosion properties.²¹⁻²⁵

In a number of different implant systems used in medicine and dentistry, surface treatments have included cleaning, acid passivation, and heat treatment at elevated temperatures. Therefore, on a relative basis one could question what specific treatment offers the optimum biocompatibility characteristics.

It is the goal of this study to compare the effects of nitric acid solution passivation and heat treatment on the resultant surface oxide and corrosion properties of titanium and titanium alloys with different chemical compositions and microstructures. In this study, three materials were included: one with a single-phase alpha (hcp) microstructure, cpTi; one with a mixed alpha-beta (hcp and bcc) microstructure, Ti64; and one with a single-phase beta (bcc) microstructure, 21SRx. The microstructure of each material was documented using standard metallographic techniques. The chemistry and thickness of the surface oxides for each material in three different conditions were determined using Auger electron spectroscopy (AES), and the corrosion properties were determined using DC polarization tests and AC electrochemical impedance spectroscopy (EIS).

Materials and Methods

Materials

Discs, 15 mm in diameter and 3 mm thick, were cut from bar stock from the titanium metals and alloys listed in Table 1 using a diamond saw. The discs were subsequently mounted in polymethylmethacrylate and wet ground with silicon carbide paper to a 600-grit finish, and then polished using alumina powder slurry to a 0.3 μm finish.

TABLE 1
List of Titanium and Titanium Alloys Used in This Study

Metal or alloy	ASTM specification	Abbreviation
cp Titanium	F 67 grade 4	CpTi
Ti-6Al-4V	F 136	Ti64
Ti-15Mo-2.8Nb-0.2Si	21SRx

Surface treatments

The discs from each of the three metal groups were then divided into three experimental sample groups, which are listed in Table 2.

Cleaned discs (C) were obtained by ultrasonically cleaning the discs for 10 min in each of the following solutions: distilled water, benzene, acetone, and ethanol. The discs were thoroughly rinsed with distilled water between solvents. Passivated discs (P) were obtained by cleaning discs as above (C) and then passivating the discs for 30 min in 40 % nitric acid (ASTM F 86-01). Finally, the Heat Treated discs (HT) were obtained by taking discs that had been cleaned and passivated (C + P) and heat treating them at 350°C for 1 h in air, followed by air cooling.

TABLE 2
Surface Treatments Used in This Study

Surface treatment	Description
Cleaned (C)	Cleaned ultrasonically in a series of solvents
Passivated (P)	C + passivated in 40 % nitric acid for 30 min
Heat Treated (HT)	C + P + heat treated at 350°C in air for 1 h

Microstructure

Polished samples were etched using Kroll Etchant (2%HF-4%HNO₃) to reveal microstructures, and optical microscopy, and imaging camera equipment was used to examine and document the microstructures.

Auger electron spectroscopy (AES)

An AES system (JOEL, JAMP-30 Auger Microprobe) was used to evaluate the chemical composition of the prepared surfaces. Parameters used in the analysis included a 30-degree take-off angle, 10 keV accelerating electron beam, and 3.0×10^{-7} A probe current. Derivative spectra were used to analyze the elemental composition, with spectra being taken both before (pre-sputter) and after (post-sputter) Argon (Ar) ion sputtering. Continuous depth profiling was performed using Ar ions with a potential of 3 keV and emission current of 30 mA. The sputter rate of 0.2 nm/s was determined by sputtering through a standard 100 nm thick Ta₂O₅ film. The oxide thickness was determined by multiplying the sputter rate of 0.2 nm/s by the time it took the oxygen Auger signal to reach one-half its maximum intensity.

Potentiodynamic polarization corrosion tests

Electrochemical potentiodynamic polarization testing was conducted using equipment (Model 273 Potentiostat/Galvanostat, EG&G PAR) and a corrosion cell standardized to ASTM G5. The polarization scan was conducted from 150 mV more active than open circuit potential to 1000 mV using a scan rate of 0.17 mV/s. A platinum counter electrode and standard calomel reference electrode were used in this study. The electrolyte solution was isotonic saline solution adjusted to pH 7.4 ± 0.1 . Tafel extrapolation and Stern-Geary fits (SoftCorr III, EG&G PAR) were used to obtain the corrosion potential (E_{corr}) and the corrosion rate (I_{corr}) at the maximum corrosion potential. The passive current density (I_{pass}) was obtained by using a straight-line extrapolation to intersect the current density axis.

Electrochemical impedance spectroscopy (EIS)

Electrochemical impedance spectroscopic analyses were conducted using equipment (Model 6310 Impedance Analyzer, EG&G PAR) and a corrosion cell standardized to ASTM G 106. A platinum counter electrode and standard calomel reference electrode were used in this study. A sinusoidal waveform with a frequency sweep from an initial value of 100 kHz to a final value of 10 MHz, with a magnitude of 10 mV, was used. The electrolyte solution was isotonic saline solution adjusted to a pH of 7.4 ± 0.1 . A Randles equivalent circuit was fit to the impedance spectra (Model 398 Impedance Software EG&G PAR) and its circuit element values calculated. A linear relationship between the oxide film and the calculated capacitance is of the form:

$$C = \epsilon_0 \epsilon_r A / d \quad (1)$$

where

C = calculated double layer capacitance

A = nominal surface area of the specimen

d = thickness of the oxide film

ϵ_0 = permittivity of free space

ϵ_r = specific permittivity of the oxide film (~100)

This formula was used to obtain relative differences in the oxide film thickness between the various sample groups. A certain magnitude of error is to be expected for this fit and analysis because the high corrosion resistance of titanium and its alloys in the test electrolyte precludes obtaining a Nyquist semicircle. Thus, the results obtained provide only qualitative information, not quantitative information.

Statistics

Duncan's Multiple Range Test ($\alpha = 0.05$) was used to test for significant statistical differences, if any, in mean oxide thickness values and the corrosion parameters, E_{corr} , I_{corr} , and I_{pass} .

RESULTS

Microstructures

Representative photomicrographs show the microstructures of cpTi, Ti64, and 21SRx (Figs. 1-3). The cpTi grain structure was an equiaxed alpha phase, Figure 1. The Cleaned, Passivated, and Heat Treated conditions showed similar microstructures. The Ti64, Figure 2, was an alpha-beta microstructure with grains of alpha (light) and inter-

granular beta phase (mottled or outlined). No differences in microstructure morphology or grain size were found for the Cleaned, Passivated, and Heat Treated Ti64 groups. The microstructure of the 21SRx showed large equiaxed beta grains on a relative basis, Figure 3. The larger beta phase for the 21SRx indicates that the bar stock from which the samples were made had been annealed. As with cpTi and Ti64, the Cleaned, Passivated, and Heat Treated 21SRx groups showed no differences in microstructure.

AES–Surface oxide elemental composition

Pre-sputter AES spectra for all sample groups showed dominant Ti and O peaks and smaller C, Ca, P, and Si peaks. Minor Al and Mo peaks were detected throughout the surface oxides of the Ti64 and 21SRx specimens, respectively. Post-sputter spectra obtained after depth profiling showed dominant Ti peaks with much smaller O peaks and the disappearance of the C, Ca, and Si peaks that were observed in the pre-sputter spectra. In the case of the alloys, Ti64 and 21SRx, post-sputter spectra showed larger and more defined Al and Mo peaks, respectively. Figure 4 shows a representative post-sputter spectra for a Passivated 21SRx sample.

AES–Surface oxide thickness

The average oxide thicknesses as determined by AES continuous depth profiling are shown in Table 3.

All Cleaned and Passivated groups showed no significant differences (Duncan's Multiple Range Test, $\alpha = 0.05$) in oxide thickness. The Heat Treated group oxides were

significantly thicker than the Cleaned and Passivated groups, and within the Heat Treated groups, cpTi and Ti64 specimens had significantly thicker oxides than 21SRx specimens.

TABLE 3
Average Oxide Thickness (nm), $n = 2$

Surface Treatment	CpTi	Ti64	21SRx
Cleaned	3.0 ± 0.3^a	5.0 ± 0.3^a	4.3 ± 0.6^a
Passivated	4.4 ± 0.6^a	5.4 ± 0.3^a	5.0 ± 0.3^a
Heat Treated	16.8 ± 2.8^c	14.8 ± 0.3^c	8.8 ± 0.0^b

Results with different alphabetical superscripts denote statistically significant differences (Duncan's Multiple Range Test, $\alpha = 0.05$).

DC corrosion tests

The polarization corrosion curves were typical for titanium and titanium alloys, showing active and passive regions. Polarization curves for cpTi, Ti64, and 21SRx exhibited minimal differences in the locations or shapes of the curves within each specific surface treatment. However, differences were seen between surface treatment groups. Figures 5-7 show representative curves for the three surface treatments for each metal or alloy group. These figures illustrate graphically the effect of the surface treatments on each metal and alloy group. For all of the material groups, the Passivated and Heat Treated curves are shifted up and to the left relative to the Cleaned curves. This is indicative of increased corrosion resistance, with a shift up indicating an increase in E_{corr} values (becoming more noble) and the shift to the left indicating smaller I_{corr} values (decreased corrosion current density). The curves for the Cleaned specimen groups showed passive regions in which the current densities were voltage-independent, whereas the Passivated and Heat Treated groups showed voltage-dependent passive regions.

Like the polarization curves, the Ecorr curve results were similar for all three material groups within the same treatment group but different between the treatment groups. The Cleaned and Heat Treated Ecorr curves showed gradual increases in potential over time, while the Passivated curves were relatively stable, as there was little to no change in the open circuit potential over the 1-h period.

The average Ecorr, Icorr, and Ipass values for tested specimens are shown in Tables 4-6, respectively.

TABLE 4
Average Ecorr Results (mV) $n = 3$

Surface Treatment	cpTi Ecorr (mV)	Ti64 Ecorr (mV)	21SRx Ecorr (mV)
Cleaned	-259 ± 24^a	-235 ± 14^a	-250 ± 16^a
Passivated	-89 ± 14^b	-89 ± 40^b	-154 ± 49^b
Heat Treated	-123 ± 50^b	-9 ± 34^c	-115 ± 71^b

Results with different alphabetical superscripts denote statistically significant differences (Duncan's Multiple Range Test, $\alpha = 0.05$).

TABLE 5
Average Icorr Results (nA/cm²) $n = 3$

Surface Treatment	cpTi Icorr (nA/cm ²)	Ti64 Icorr (nA/cm ²)	21SRx Icorr (nA/cm ²)
Cleaned	47 ± 2^{ab}	45 ± 14^b	61 ± 18^a
Passivated	6 ± 1^c	11 ± 3^c	13 ± 5^c
Heat Treated	5 ± 3^c	2 ± 1^c	12 ± 11^c

Results with different alphabetical superscripts denote statistically significant differences (Duncan's Multiple Range Test, $\alpha = 0.05$).

The Ecorr and Icorr results from the polarization tests showed no significant differences between the metallic groups within any of the surface treatments, except for

TABLE 6
Average I_{pass} Results (nA/cm^2) $n = 3$

Surface Treatment	cpTi I_{pass} (nA/cm^2)	Ti64 I_{pass} (nA/cm^2)	21SRx I_{pass} (nA/cm^2)
Cleaned	863 ± 119^{ab}	1101 ± 275^a	927 ± 63^{ab}
Passivated	541 ± 35^c	685 ± 94^a	859 ± 56^{ab}
Heat Treated	286 ± 251^d	9 ± 5^c	42 ± 9^c

Results with different alphabetical superscripts denote statistically significant differences (Duncan's Multiple Range Test, $\alpha = 0.05$).

Cleaned Ti64, which had a significantly lower I_{corr} than Cleaned 21SRx alloy, and Heat Treated Ti64, which had a significantly lower E_{corr} than Heat Treated cpTi and 21SRx. The surface treatment groups, however, showed significant differences in E_{corr} and I_{corr} . The Cleaned specimens had significantly higher I_{corr} and less noble E_{corr} values than the Passivated and Heat Treated groups. There was no significant difference in E_{corr} and I_{corr} for the Passivated and Heat Treated groups, except for the previously mentioned E_{corr} results for Heat Treated Ti64. The same general trends were shown for the I_{pass} results. The Cleaned specimen groups had the higher passive current densities, followed by the Passivated and then the Heat Treated groups. Significant differences were found only for the Heat Treated groups, with lower passive current densities than the Cleaned and Passivated groups.

Electrochemical impedance spectroscopy (EIS)

All impedance spectra fit into the Randles equivalent circuit model. All sample groups exhibited ideal capacitive behavior ($\phi \cong 90^\circ$) expected for titanium and its alloys. The oxide thicknesses obtained for the various sample groups using EIS followed the same rank and file order as that obtained using AES.

DISCUSSION

Microstructure

The microstructural analyses showed the three titanium materials to have three distinct grain structures, equiaxed alpha for all the cpTi groups, duplex alpha-beta for all the Ti64 groups, and equiaxed beta for all the 21SRx groups (Figs. 1-3). The analyses also showed that the substrate microstructure of each of the materials in the cleaned condition was not altered by the surface treatments used in this study, namely, nitric acid passivation and elevated temperature heat treatment (350°C for 1 h). The fact that the treatments did not alter the microstructures of the substrate materials was expected since nitric acid passivation is simply a chemical treatment of the surface, and the 350°C temperature used for the heat treatment is not sufficient to alter the grain structure of the titanium materials used in this study.

AES – Surface oxide chemistry

The AES results on the surface oxide chemistry from this study agree with results found in the literature for similar materials and surface treatments. For example, small peaks for carbon (C), calcium (Ca), phosphorus (P), and silicon (Si) were found for all the pre-sputter spectra, but disappeared after the Ar sputter, which suggests that these elements were part of a carbaceous surface environment-dependent layer, which is routinely found on surfaces analyzed by AES⁷. The carbaceous layer present on the surfaces was most likely due to adsorption of hydrocarbons from the cleaning solvents or air⁷. The other elements, Ca, P, and Si, were most likely the result of the grinding and

polishing procedures¹⁰. As expected, both pre-sputter and post-sputter spectra showed large Ti and O peaks for all materials and surface treatments analyzed in this study. The Ti (LMV) peak at ~420 eV demonstrated a shape that corresponds closely to that of TiO₂.²⁶

Spectra for the Ti64 alloy samples in the Cleaned, Passivated, and Heat Treated conditions were similar and showed peaks for Al but not V. Others have shown the presence of aluminum within the surface oxide. Vanadium, the other alloying element in Ti64, was not detected in any of the Ti64 alloy surfaces in this study. Other researchers have found vanadium within the surface oxide of Ti64 alloys for anodically prepared specimens¹⁰ or when using X-ray photo spectroscopy (XPS)^{10, 11, 15}. One reason for not detecting vanadium in this study may be that the detection of vanadium in titanium alloys is difficult with AES since the vanadium AES peaks overlap those of titanium and oxygen.²⁶

The AES spectra for the Passivated 21SRx is shown in Figure 4. Like the spectra for cpTi and Ti64, the 21SRx spectra show large, dominant titanium and oxygen peaks. All the 21SRx spectra also show small Mo peaks but no Nb. The presence of Mo in surface oxides of various Ti-Mo alloys has been reported using AES by other researchers.^{13, 27} Although no Nb peaks are shown in any of the Ti-15Mo-2.8Nb-0.2Si alloy samples, the presence of Nb cannot be completely ruled out since Nb peaks overlap Mo peaks.

Analysis of the AES spectra for nitrogen was not possible in this study because the only available nitrogen AES peak overlaps one of the Ti peaks.²⁶ Thus, any differences in nitrogen content of the material surfaces in this study could not be determined.

AES–Oxide thickness

Oxide thicknesses for the different samples in this study were measured directly using AES depth profiling techniques. In addition, EIS analysis was used to measure the oxide thicknesses indirectly. AES and EIS analysis results were in basic agreement. Cleaned and Passivated groups for each of the materials in this study had similar oxide thicknesses ranging from 3.0-5.4 nm, with no significant differences between any of these groups. These results are in agreement with results from many other studies for similar materials and treatments.^{6, 10, 11, 14} These results, however, contradict Callen et al., who reported that the oxide thickness for nitric acid passivated Ti64 material was less than that of the non-passivated Ti64.¹¹ Possible explanations include differences in sample preparation and analytical techniques used to measure oxide thickness. Another possibility is the concentration and nature of the nitric acid passivation used to treat the samples. Callen ultrasonicated the samples in a 34 % nitric acid solution, while in this study the samples were passivated statically in a 40 % nitric acid solution. During ultrasonication, high pressures and temperatures due to cavitations can occur near a metal surface. This, in turn, can affect chemical reactions and introduce a number of microstructural changes in the surface layers of the metal oxide.²⁸ Hence, nitric acid passivation done in conjunction with ultrasonication could alter the oxidation process during passivation and thus explain the thinner oxide results of the ultrasonically passivated samples found by Callen.

The heat treat regime used in this study was chosen so as to obtain relatively thin oxides, but ones that were significantly thicker than the native and passivated oxides. The 350°C-1 h regime was successful in doing this as Auger and EIS analysis showed that the

1-h, 350°C heat treatment significantly increased the thickness of the surface oxides of all three materials, compared to all the Cleaned and Passivated materials. Heat Treated cpTi and Ti64 had oxide thicknesses of 16.8 nm and 14.8 nm, respectively, which were not significantly different, while Heat Treated 21SRx had an average oxide thickness of 8.8 nm, which was significantly thinner than those of the Heat Treated cpTi and Ti64. The increased oxide thickness for the heat treatment regime used in this study agrees well with results reported in the literature.^{19, 29, 30} In addition, all the Heat Treated materials were golden in coloration after the heat treatment, which has been reported in the literature to signify an oxide thickness of 10-25 nm,²⁹ which agrees with the thickness results in this study.

The thinner oxide of the 21SRx Heat Treated group was attributed to the larger grain sizes of the alloy due to annealing (Fig. 3). Oxide growth in thermal treatments is controlled in large part by mass diffusion through the grain boundaries.³¹ Thus, mass transport is greater in the fine-grained structures of the cpTi and Ti64 materials than in the larger-grained 21SRx, which leads to the thicker oxides for the fine-grained structured materials, cpTi and Ti64, compared to the larger-grained 21SRx.

DC corrosion

In general, the corrosion results showed no significant differences between cpTi, T64 and 21SRx within specific treatment groups of this study. There were, however, significant differences between the treatment groups, with the Cleaned groups showing significantly less corrosion resistance than the Passivated and Heat Treated groups; the latter two, in general, did not show any significant differences.

However, the differences or lack of differences in corrosion resistance cannot be attributed simply to the thickness of the oxide layers. No significant differences in oxide thicknesses were found for the Cleaned and Passivated groups, yet the Passivated groups were significantly more corrosion resistant. On the other hand, the Heat Treated groups had significantly thicker oxides than the Passivated groups and yet, in general, showed no significant differences in corrosion resistance. These results suggest that other characteristics or properties of the oxide layers besides oxide thickness determine the corrosion properties of these materials.

One possible oxide property that may affect the corrosion properties is the presence and amount of sub-oxides in the oxides. Titanium sub-oxides such as TiO and Ti₂O₃ have been reported to be present in addition to stoichiometric TiO₂ on titanium surfaces.^{10, 14, 20, 26, 32} Lausmaa²⁶ and Ong¹⁴ reported the presence of sub-oxides in the oxide film for cpTi. Ask¹⁰ reported sub-oxides of Ti₂O₃ and TiO for Ti64, while Milosev³² reported oxide percentages of 40 % for TiO₂, 30 % for Ti₂O₃, and 4 % for TiO on Ti64. In addition, in a more recent study, Lee³³ quantitated the amount of titanium sub-oxides on Ti64 that had been surface treated in similar fashions as was done in this study. The XPS results showed the weight% of sub-oxides for “cleaned” Ti64 to be 19.5 wt%, while Ti64 that had been passivated in a 34 % nitric acid solution had 14.8 wt% of sub-oxides, and Ti64 that had been heat treated at 400°C for 1 h had 8.6 wt% of sub-oxides. Thus, these results show that nitric acid passivation and heat treatment decreased the amount of sub-oxides compared to the cleaned condition. This could explain the improved corrosion resistance for the Passivated and Heat Treated groups compared to the Cleaned groups in

our study. However, more in-depth studies of the role(s) of oxide atomic structure are needed to draw conclusions about these relationships.

Another possible reason for the improved corrosion resistance of the Passivated groups compared to the Cleaned groups, despite the result that they had similar oxide thicknesses, might be the structure of the oxides. Nitric acid passivated specimens may remove the plastically deformed native oxide of the Cleaned specimens and grow in its place a more uniform oxide.³⁴ Since the nitric acid passivation process involves the simultaneous dissolution and formation of the existing oxide, preferential dissolution of surface defects would be expected, with concurrent formation of a less defective (i.e., more uniform) oxide.

Still another reason for the improvement in corrosion properties for the Passivated and Heat Treated groups may be enrichment of nitrogen in the near-surface region of the surface oxide due to the passivation in nitric acid. Schmidt³⁵ reported that ion-implanted nitrogen acts as a diffusion barrier by reducing the number of interstitial sites for migration of oxygen. Unfortunately, as discussed earlier, because the AES peak for titanium overlaps the nitrogen peak, changes in nitrogen content could not be determined.

Although the Heat Treated groups had increased oxide thicknesses, the Ecorr and Icorr results for these groups were not significantly different from those for the nitric acid Passivated groups. One possible explanation again may be the relative structure of the oxide. Blackwood³⁶ and others³⁷ have shown that the oxide layer on titanium and titanium alloys typically consists of three layers: an outer TiO₂ layer, an intermediate Ti₂O₃ layer, and an inner TiO layer that is in contact with the titanium or alloy substrate. In addition, Pouilleau³⁸ showed that a heat treatment similar to that done in this study

resulted in a thin outer TiO_2 layer and a thicker intermediate Ti_2O_3 layer. Thus, the short and relatively low heat treatment temperature did not allow the formation of a thicker, more stable stoichiometric TiO_2 layer. The effect of the thinner TiO_2 layer on corrosion properties was shown after Pouilleau's oxide stabilization procedure of boiling in water for 15 min, which did not increase the overall thickness of the oxide layer but did increase the thickness of the outer TiO_2 layer, while decreasing the thickness of the intermediate Ti_2O_3 region. The stabilized specimens showed improved corrosion resistance, thus pointing to the importance of the different oxide structures. Hence, the result that the Heat Treated groups had a thicker oxide but not improved E_{corr} and I_{corr} results compared to the Passivated groups may be due to the circumstance that the heat treatment used in this study was not of sufficient duration and temperature for a thick outer TiO_2 layer to form.

However, it should be noted that the I_{pass} results for the Heat Treated groups were significantly lower than those for the Passivated groups. I_{pass} , by definition, is the current density of the sample when it is in the passive region of the polarization curve. The lower I_{pass} results for the Heat Treated groups may be due to the possible transformation of the intermediate Ti_2O_3 sub-oxide layer into the more stable TiO_2 due to the application of the voltage during the polarization experiment. An increase in the amount of the more stable TiO_2 would result in a decrease in current density compared to the thinner Passivated groups.

Another result from the corrosion studies that provides information on the state of the oxides present on the samples is the shape of the E_{corr} curves. E_{corr} curves measure the open circuit potential over time. According to Abd El Kader,³⁹ shifts in the open

circuit potential to more positive values over time denote oxide thickening and repair, shifts to more negative values indicate oxide breakdown or dissolution, and a constant voltage over time indicates that the oxides were stable. In this study, all the Ecorr curves for the Cleaned and Heat Treated groups had voltages becoming slightly more positive with time, indicating that the oxide films were thickening and becoming repaired. On the other hand, all the Passivated groups had Ecorr curves exhibiting relatively constant voltages over time, indicating stable oxide films. Thus, nitric acid passivation appears to have stabilized the oxide in terms of its behavior in the saline solution, while Cleaned and Heat Treated materials had oxides that continued to passivate in the saline solutions, as indicated by the increasing open circuit potential.

CONCLUSIONS

The results of this study showed similar excellent corrosion properties for cpTi, Ti-6Al-4V (Ti64), and Ti-15Mo-2.8Nb-0.2Si (21SRx) materials despite differences in the chemistry of the surface oxides of these materials. Thus, surface oxide composition did not affect the corrosion properties of cpTi, Ti64 and 21SRx.

Surface treatments, such as passivation in nitric acid solution and heat treatment, did affect the corrosion properties by increasing the corrosion resistance of these surface-treated materials. However, these differences in corrosion properties cannot be attributed simply to changes in oxide thickness. Other oxide properties must play a role in the corrosion properties of these materials. Additional studies on the role(s) of atomic structure versus surface properties are indicated.

References

1. Fraker AC, Corrosion of metallic implants and prosthetic devices. In: Metals handbook, Metals Park, OH: ASM International;1987 p. 1324-1335.
2. Zitter H, Plenk H, Jr., The electrochemical behavior of metallic implant materials as an indicator of their biocompatibility. *J Biomed Mater Res* 1987; 21(7):881-96.
3. Williams DF, Titanium and titanium alloys. In: *Biocompatibility of Clinical Implant Materials*, D.F. Williams, Editor. 1981, CRC Press: Boca Raton, Florida. p. Ch. 2.
4. Turner TM, Sumner DR, Urban RM, Igloria R, Galante JO, Maintenance of proximal cortical bone with use of a less stiff femoral component in hemiarthroplasty of the hip without cement. An investigation in a canine model at six months and two years. *J Bone Joint Surg Am* 1997; 79(9):1381-90.
5. Woo SL, Lothringer KS, Akeson WH, Coutts RD, Woo YK, Simon BR, Gomez MA, Less rigid internal fixation plates: Historical perspectives and new concepts. *J Orthop Res* 1984; 1(4):431-49.
6. Lausmaa J, Mattsson L, Rolander U, Kasemo B, Chemical composition and morphology of titanium surface oxides. *Materials Research Society Symposia Proceedings* 1986; 55:351.
7. Lausmaa J, Kasemo B, Mattsson H, Odelius H, Multi-technique surface characterization of oxide films on electropolished and anodically oxidized titanium. *Applied Surface Science* 1990; 45(3):189.
8. Hiromoto S, Hanawa T, Asami K, Composition of surface oxide film of titanium with culturing murine fibroblasts 1929. 2004; 25(6):979.
9. Lausmaa J, Kasemo B. Surface oxides on titanium implants - spectroscopic studies of their composition and thickness, and implications for the biocompatibility of titanium. 1984. Boston, MA, USA Washington, DC, USA: Materials Research Soc, Pittsburgh, PA, USA Soc for Biomaterials, San Antonio, TX, USA.
10. Ask M, Lausmaa J, Kasemo B, Preparation and surface spectroscopic characterization of oxide films on ti6al4v. *Applied Surface Science* 1989; 35(3):283.
11. Callen BW, Lowenberg BF, Lugowski S, Sodhi RNS, Davies JE, Nitric acid passivation of ti6al4v reduces thickness of surface oxide layer and increases trace element release. *Journal of Biomedical Materials Research* 1995; 29(3):279.

12. Lausmaa J, Ask M, Rolander U, Kasemo B, Bjursten LM, Ericson LE, Thomsen P, Surface preparation and spectroscopic analysis of titanium implant materials. *Surface and Interface Analysis* 1990; 16(1-12):571.
13. Laser D, Marcus HL, Auger electron spectroscopy depth profile of thin oxide on a ti-mo alloy. *Journal Electrochemical Society* 1980; 127(3):763-765.
14. Ong JL, Lucas LC, Raikar GN, Gregory JC, Electrochemical corrosion analyses and characterization of surface-modified titanium. *Applied Surface Science* 1993; 72(1):7.
15. Sodhi RN, Weninger A, Davies JE, X-ray photoelectron spectroscopic comparison of sputtered ti, ti6al4v, and passivated bulk metals for use in cell culture techniques. *Journal of Vacuum Science Technology* 1991; A9(3):1329-1333.
16. Smith DC, Pilliar RM, Chernenky R, Dental implant materials. I. Some effects of preparative procedures on surface topography. *Journal of Biomedical Materials Research* 1991; 25(9):1045.
17. Smith DC, Pilliar RM, Metson JB, McIntyre NS, Dental implant materials. II. Preparative procedures and surface spectroscopic studies. *Journal of Biomedical Materials Research* 1991; 25(9):1069.
18. Lowenberg BF, Lugowski S, Chipman M, Davies JE, ASTM-F86 passivation increases trace element release from Ti6Al4V into culture medium. *Journal of Materials Science: Materials in Medicine* 1994; 5(6-7):467.
19. Kilpadi DV, Raikar GN, Liu J, Lemons JE, Vohra Y, Gregory JC, Effect of surface treatment on unalloyed titanium implants: Spectroscopic analyses. *Journal of Biomedical Materials Research* 1998; 40(4):128.
20. Lee TM, Chang E, Yang CY, Surface characteristics of Ti6Al4V alloy: Effect of materials, passivation and autoclaving. *Journal of Materials Science: Materials in Medicine* 1998; 9(8):439.
21. Browne M, Gregson PJ, West RH, Characterization of titanium alloy implant surfaces with improved dissolution resistance. *Journal of Materials Science: Materials in Medicine* 1996; 7(6):323.
22. Garcia-Alonso MC, Saldana L, Valles G, Gonzalez-Carrasco JL, Gonzalez-Cabrero J, Martinez ME, Gil-Garay E, Munuera L, In vitro corrosion behaviour and osteoblast response of thermally oxidised Ti6Al4V alloy. *Biomaterials* 2003; 24(1):19.

23. Kilpadi DV, Lemons JE. Effect of surface and heat treatments on corrosion of unalloyed titanium implants. 1997. Shreveport, LA, USA: IEEE, Piscataway, NJ, USA.
24. Lee TM, Chang E, Yang CY, Effect of passivation on the dissolution behavior of ti6al4v and vacuum-brazed ti6al4v in hank's ethylene diamine tetra-acetic acid solution part i ion release. *Journal of Materials Science: Materials in Medicine* 1999; 10(9):541.
25. Park YJ, Shin MS, Yang HS, Ong JL, Rawls HR. Effect of heat treatment on microstructural and electrochemical properties of titanium and Ti alloy. 1998. San Antonio, TX, USA: IEEE, Piscataway, NJ, USA.
26. Lausmaa J, Kasemo B, Mattsson H, Surface spectroscopic characterization of titanium implant materials. *Applied Surface Science* 1990; 44(2):133.
27. Kim YJ, Oriani RA, Effect of the microstructure of Ti-5Mo on the anodic dissolution in H₂SO₄. *Corrosion* 1987; 43(4):418.
28. Whillock GOH, Harvey BF, Preliminary investigation of the ultrasonically enhanced corrosion of stainless steel in the nitric acid/chloride system. *Ultrasonics Sonochemistry* 1996; 3(2):111-118.
29. Velten D, Biehl V, Aubertin F, Valeske B, Possart W, Breme J, Preparation of TiO₂ layers on cp-Ti and Ti6Al4V by thermal and anodic oxidation and by sol-gel coating techniques and their characterization. *J Biomed Mater Res* 2002; 59(1):18-28.
30. Chang E, Lee TM, Effect of surface chemistries and characteristics of Ti6Al4v on the Ca and P adsorption and ion dissolution in hank's ethylene diamine tetra-acetic acid solution. *Biomaterials* 2002; 23(14):2917.
31. Leyens C, Peters M, Kaysser WA, Influence of microstructure on oxidation behaviour of near-alpha titanium alloys. *Materials Science and Technology* 1996; 12:213-218.
32. Milosev I, Metikos-Hukovic M, Strehblow HH, Passive film on orthopaedic TiAlV alloy formed in physiological solution investigated by x-ray photoelectron spectroscopy. *Biomaterials* 2000; 21(20):2103.
33. Lee TM, Chang E, Yang CY, Comparison of the corrosion behaviour and surface characteristics of vacuum-brazed and heat-treated ti6al4v alloy. *Journal of Materials Science: Materials in Medicine* 1998; 9(8):429.

34. Trepanier C, Tabrizian M, Yahia LH, Bilodeau L, Piron DL, Effect of modification of oxide layer on NiTi stent corrosion resistance. *Journal of Biomedical Materials Research* 1998; 43(4):433.
35. Schmidt M, Stechemesser G, Witte J, Soltani-Farshi M, Depth distributions and anodic polarization behaviour of ion implanted ti6al4v. *Corrosion Science* 1998; 40:1533.
36. Blackwood DJ, Greef R, Peter LM, Ellipsometric study of the growth and open-circuit dissolution of the anodic oxide film on titanium. *Electrochimica Acta* 1989; 34(6):875.
37. Pan J, Thierry D, Leygraf C, Electrochemical impedance spectroscopy study of the passive oxide film on titanium for implant application. *Electrochimica Acta* 1996; 41(7-8):1143.
38. Pouilleau J, Devilliers D, Garrido F, Durand-Vidal S, Mahe E, Structure and composition of passive titanium oxide films. *Materials Science & Engineering B: Solid-State Materials for Advanced Technology* 1997; B47(3):235.
39. Abd El Kader JM, Abd El Wahab FM, El Shayeb HA, Khedr MGA, Oxide film thickening on titanium in aqueous solutions in relation to anion type and concentration. *Brit Corr J* 1981; 16:111.

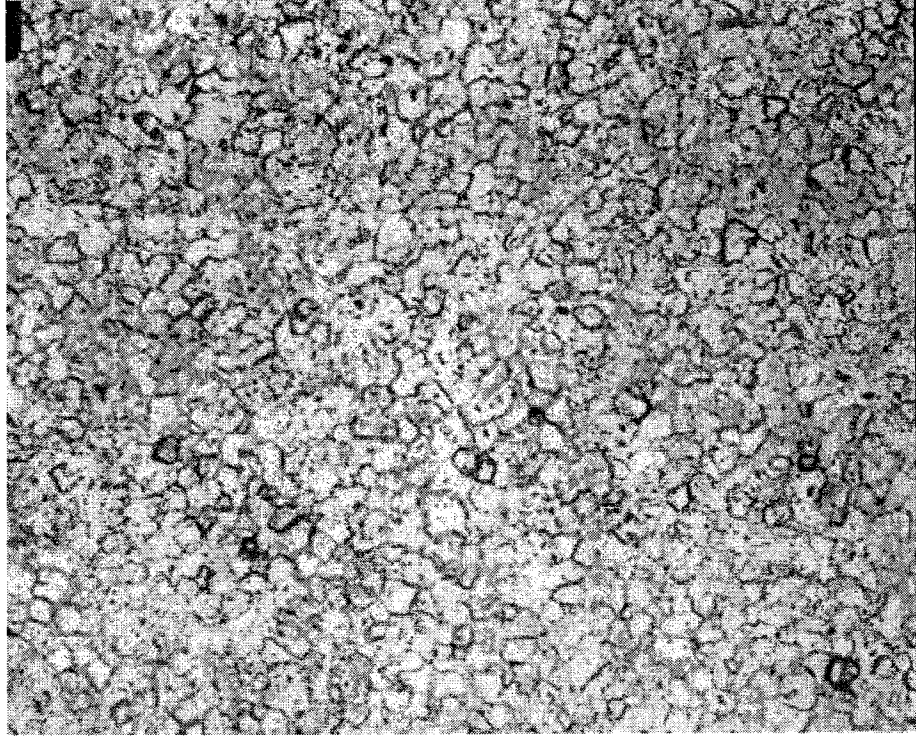


Figure 1. Representative microstructure for cpTi showing equiaxed alpha grains (original magnification x200).

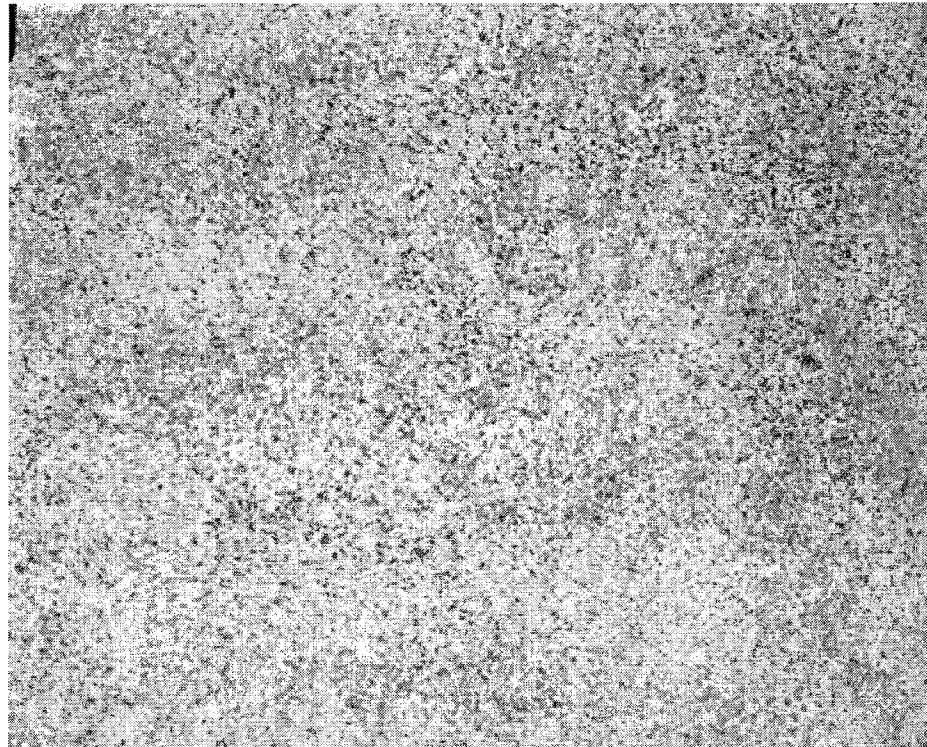


Figure 2. Representative microstructure for Ti64 showing dual phase alpha-beta grains. Alpha regions are light and intergranular beta regions are dark (original magnification x200)

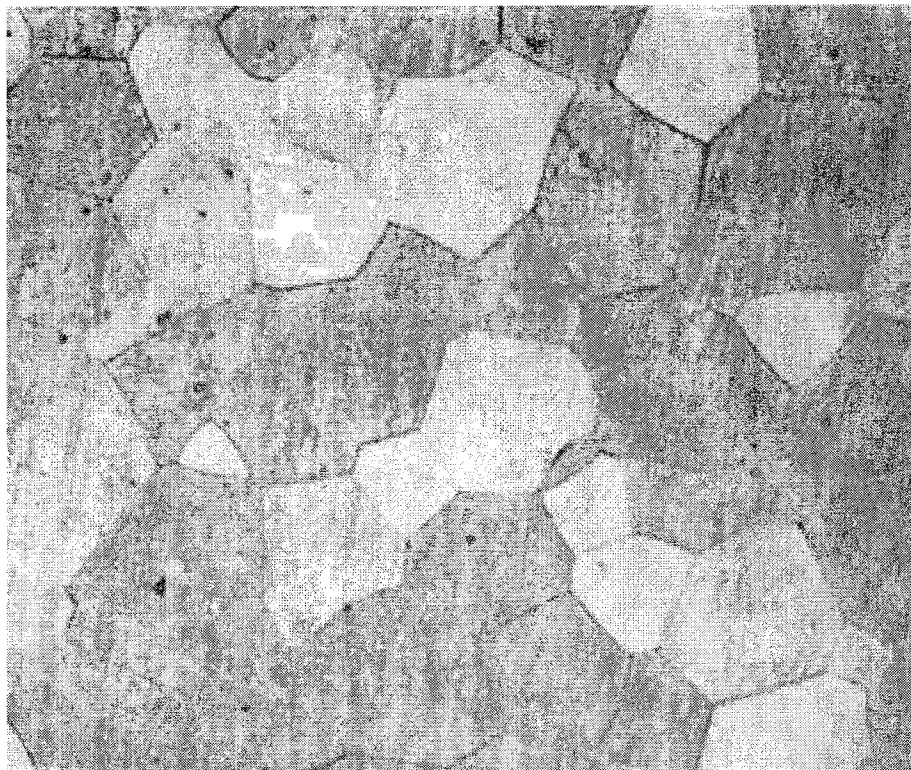


Figure 3. Representative microstructure for 21SRx showing equiaxed beta grains. Grains are substantially larger than cpTi and Ti64 grains (original magnification x200).

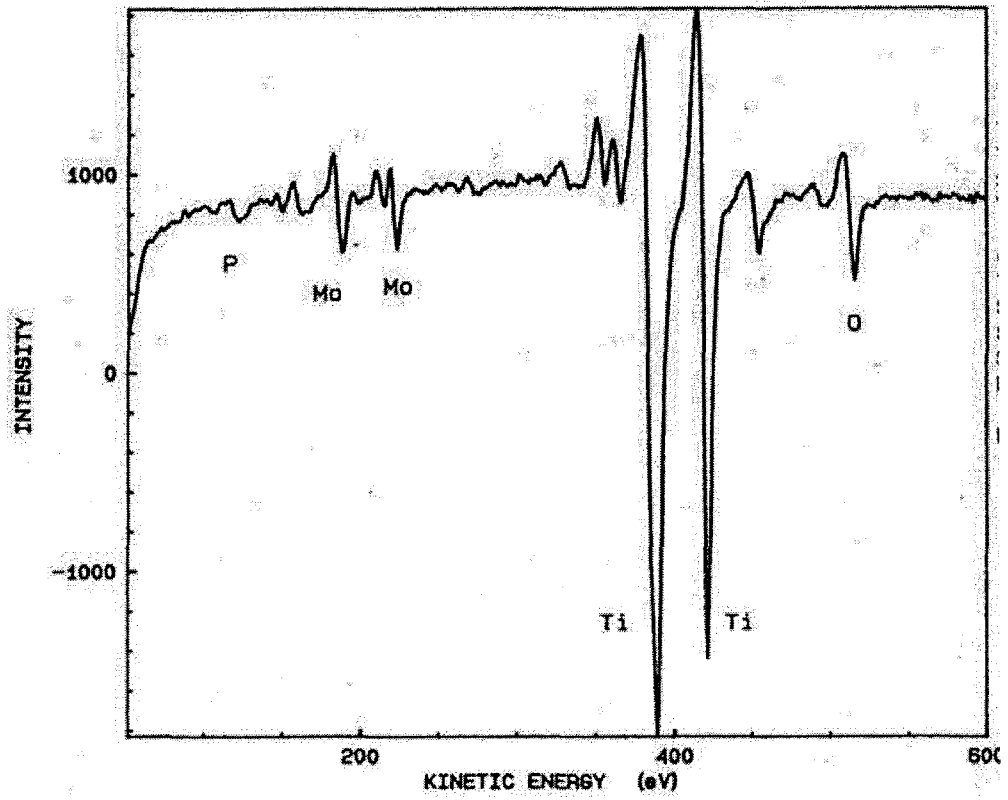


Figure 4. Representative AES spectra of Passivated 21SRx sample after Ar ion sputter.

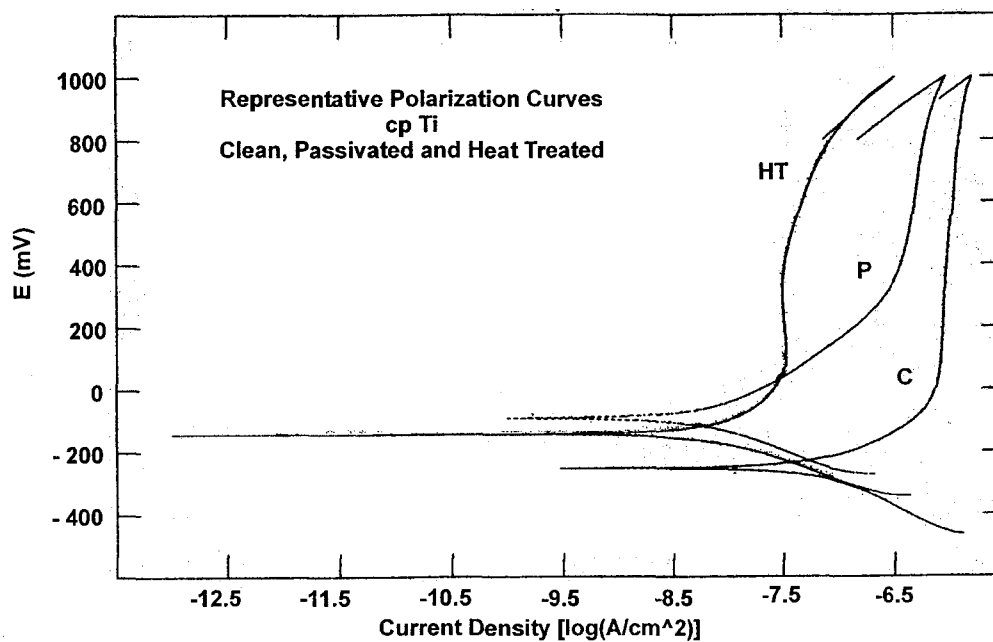


Figure 5. Representative polarization curves for cpTi in the Cleaned, Passivated, and Heat Treated conditions. The upward and leftward shift of the Passivated and Heat Treated curves relative to the Cleaned curve graphically illustrates their increased corrosion resistance. The upward shift indicates a nobler E_{corr} and the leftward shift a decrease in current density (I_{corr}).

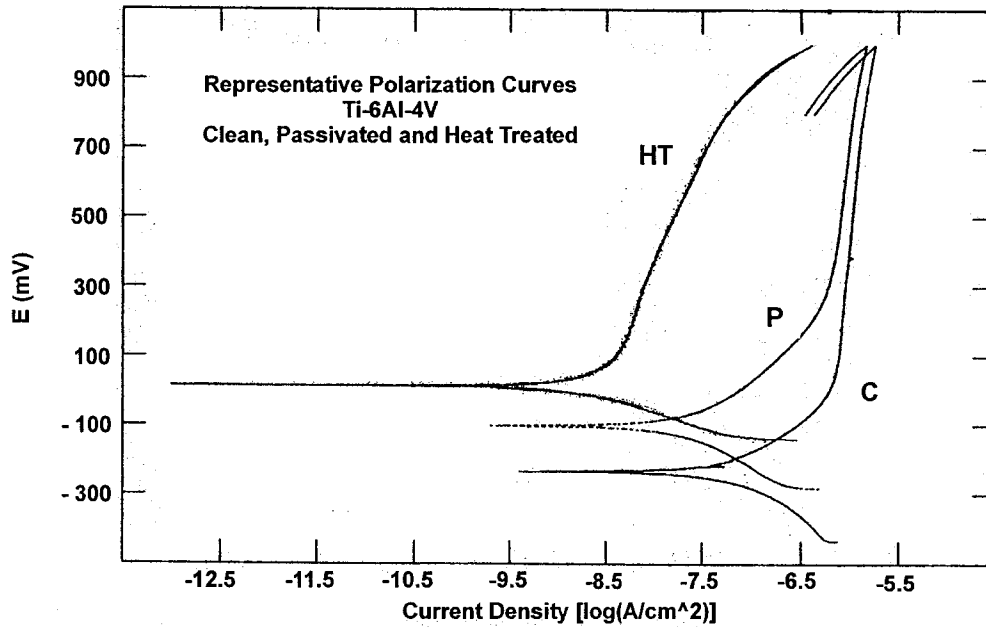


Figure 6. Representative polarization curves for Ti64 in the Cleaned, Passivated, and Heat Treated conditions. As with Figure 5 for cpTi, the upward and leftward shift of the Passivated and Heat Treated curves relative to the Cleaned curve graphically illustrates their increased corrosion resistance. The upward shift indicates a nobler E_{corr} and the leftward shift a decrease in current density (I_{corr}).

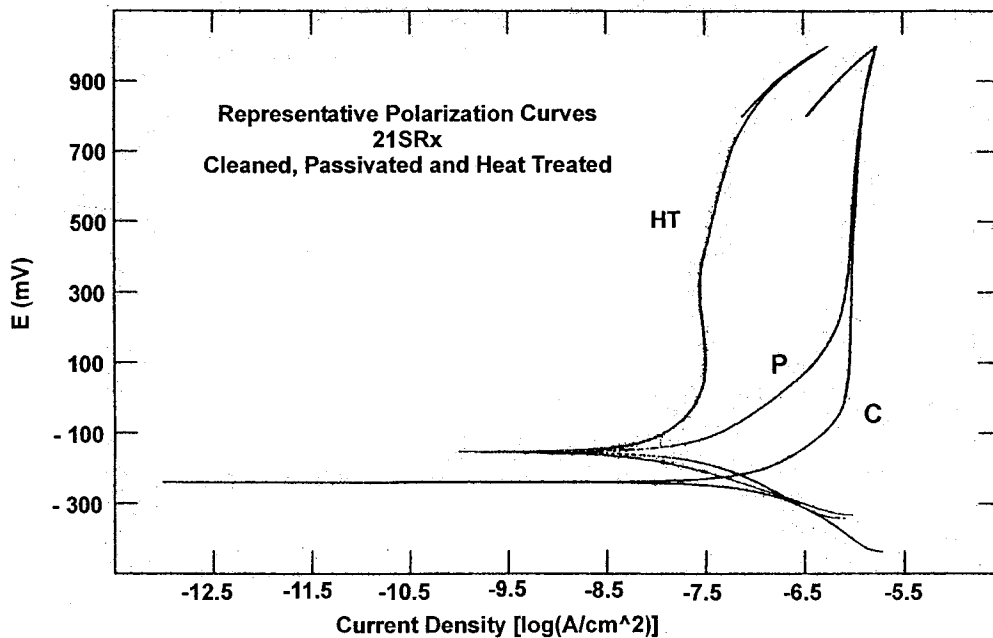


Figure 7. Representative polarization curves for 21SRx in the Cleaned, Passivated, and Heat Treated conditions. Although similar Cleaned and Passivated curves are shown, the quantitative data show the Passivated and Heat Treated groups to be significantly more corrosion resistant than the Cleaned group.

EFFECTS OF NITRIC ACID PASSIVATION PARAMETERS ON TITANIUM
AND TITANIUM ALLOYS RELATED TO CORROSION,
SURFACE CHEMISTRY, AND CELL CULTURE

PART I
EFFECTS OF NITRIC ACID CONCENTRATION, TEMPERATURE, AND TIME

by

DON PETERSEN AND JACK LEMONS

In preparation for *Journal of Biomedical Materials Research*

Format adapted for dissertation

ABSTRACT

Improving functionality and longevity of surgical implants has long been the goal of material scientists. One theoretical way to obtain improvement is by enhancing the surface oxide layer on the implant with passivation in a nitric acid solution. Varying the parameters of nitric acid concentration, temperature, and immersion time can affect the properties of the oxide coating.

Commercially pure titanium (cpTi) and two titanium alloys (Ti-6Al-4V and Ti-15Mo) were used in the study. Corrosion properties of the resultant surfaces were determined by using electrochemical impedance spectroscopy (EIS) and potentiodynamic polarization tests. EIS and X-ray photoelectron spectroscopy (XPS) were used to study surface oxide characteristics and chemistry, respectively. Cell culture tests with osteoblast-like cells (SaOS-2) were used to test any effects on biocompatibility.

Test results showed the three titanium material groups to be affected to varying degrees by the different passivation parameters. In general, improved corrosion properties resulted when higher concentrations and temperatures were used; however, the improvement was time sensitive. Overall, cpTi was the most corrosion resistant, followed by Ti-6Al-4V and then Ti-15Mo. The Ti-15Mo groups were less sensitive to the variations in passivation parameters. Cell culture results showed improvements in cellular responses that tended to follow the corrosion results. Differences in corrosion and biocompatibility properties were related to oxide chemistry and other oxide properties.

INTRODUCTION

A worthy goal for material scientists would be to improve the functionality and longevity of surgical implants by optimizing the surface properties of the implant metals. Modifying the surface chemistry of implant metals is a recognized method of improving their corrosion resistance and longevity.^{1,2} A prominent method of altering the surface chemistry of metals is nitric acid passivation. Commercial metallic implant devices, for example, routinely undergo a nitric acid passivation treatment as part of an American Society for Testing of Materials (ASTM) standard. The ASTM F86 protocol, which specifies cleaning and surface treatment processes for metal implants, was initially established for stainless steels and chrome-cobalt alloys but was later expanded to include titanium and titanium alloys.³

Passivation is the process of exposing metallic materials to an oxidative environment to improve their corrosion properties. The primary effect of the passivation treatment is to form a more effective surface oxide film by changing its composition,⁴ structure,² or thickness⁵ and/or by removing non metallic inclusions.^{6,7} In addition to nitric acid passivation, other passivation treatments used to achieve these goals include other acid treatments, heat treatments, and boiling in water.⁸⁻¹⁰

In the case of nitric acid passivation, the effectiveness of the passivation treatment has been shown to depend on the concentration and temperature of the nitric acid, as well as on the time of immersion. Wallinder⁷, in his paper on passivation of stainless steel, showed increased corrosion resistance with higher nitric acid concentrations and temperatures, as well as with longer passivation times. The improvements in corrosion resistance were attributed to increased chromium content in the surface oxide and increased thick-

ness of the surface oxide⁷. In another study, Noh⁶ found that increasing nitric acid concentrations up to 25 % improved the pitting potentials of stainless steel, whereas concentrations greater than 25 % produced less favorable pitting potentials. Like Wallender, Noh attributed the improved corrosion properties to the increased chromium content of the oxide, which peaked in the 25 % nitric acid treatment samples.⁶

The effect of nitric acid passivation also has been studied for titanium and titanium alloys. Work in the authors' laboratory has shown improved corrosion resistance for commercially pure titanium (cpTi), Ti-6Al-4V, and Ti-15Mo-2.8Nb-0.2Si that had been passivated with nitric acid¹¹. Trepanier also showed improvement in corrosion resistance for nitric-acid-passivated NiTi alloys.¹² Ong showed no differences in corrosion properties for non passivated and nitric-acid-passivated cpTi.¹ However, some studies have shown nitric acid passivation to be detrimental to corrosion properties. Callen¹³ and Lowenberg¹⁴ have shown nitric-acid-passivated Ti-6Al-4V to have an increased release of the alloy constituent ions compared with non passivated Ti-6Al-4V.

The differences in corrosion properties shown in these studies for nitric-acid-passivated titanium and some of its alloys can be attributed to changes in various surface oxide properties. Trepanier¹² attributed the improved corrosion resistance of NiTi alloy to a more uniform surface oxide, which results when the nitric acid removes the air-formed oxide, which they described as a deformed plastic oxide, and replaces it with a more uniform oxide. Kilpadi¹⁵ and others¹⁰ have attributed the corrosion improvement in passivated titanium to the removal of contaminants from the surface oxide.

The presence of alloy constituent ions in the surface oxide of titanium alloys has been documented in numerous studies.^{13, 16-19} Furthermore, it has been shown that nitric

acid passivation of the alloys increases the concentration of the alloy constituents, such as Al and V ions, within the surface oxide.^{9, 13, 17} Variations in alloy constituent concentrations have been cited as reasons for observed differences in corrosion and biological properties^{9, 13}.

The release of the toxic Al and V ions into the host circulation has major clinical implications. High levels of metal ions have been documented in the serum of humans with implants.²⁰ Aluminum ions also tend to accumulate in the brain, causing dementia and Alzheimer's disease.²¹ In general, all these toxic ions cause DNA damage to blood cells, mesenchymal bone marrow cells, fibroblasts, osteoblasts, and lymphocytes.²²⁻²⁴ In addition, Ti, Al, and V ions have been shown to inhibit apatite formation *in vitro*²⁵, which is of importance in bone implants.

The types of alloy constituent ions have been shown to affect how the alloy responds to nitric acid passivation and the resultant oxide and corrosion properties.^{11-13, 26} Thus, different titanium materials respond differently to similar nitric acid passivation treatments.

In addition to Ti-6Al-4V, other titanium alloys are of interest as implant materials. More recently, beta titanium alloys have been investigated.^{27, 28} The advantages of beta titanium alloys cited in the literature include lower elastic modulus and improved corrosion resistance.^{28, 29} One such beta alloy is Ti-15Mo. This alloy, compared with Ti-6Al-4V, has been shown to improve corrosion resistance and have a lower modulus of elasticity.²⁹ However, because of the relative novelty of the beta titanium alloys as an implant material, few studies on the effects of nitric acid passivation on these alloys have been done.

The effects of the various parameters of nitric acid passivation on cpTi, Ti-6Al-4V, and Ti-15Mo were documented in this work by using various analytical techniques. Corrosion properties were determined with electrochemical impedance spectroscopy (EIS) and potentiodynamic polarization tests. EIS is a powerful technique that can yield information on the corrosion resistance of the material, as well as on properties of the surface oxide. Modeling of EIS spectra with an equivalent electrical circuit (EEC) was used to obtain EIS parameters, which were related to specific circuit elements and could be quantified for statistical comparisons. Potentiodynamic polarization testing was used to obtain the corrosion potential (E_{corr}), corrosion current density (I_{corr}), and passive current density (I_{pass}). The surface oxide chemistry was determined with X-ray photoelectron spectroscopy (XPS). In addition to the elemental composition of the surface oxide, XPS results also included depth profiling and high-resolution scans, which yielded information on the stoichiometry of the oxide. Last, the biological response of SaOS-2 osteoblast-like cells to the materials passivated in various ways was measured using hexosaminidase assay to determine cell attachment and proliferation.

Although many studies on the effects of nitric acid passivation on titanium and titanium alloys have been done, these studies used a range of values for the different passivation parameters. The nitric acid passivation protocols used in the studies show variations in the acid concentration, time of immersion, and acid temperature. These differences may account for much of the inconsistency and contradiction in the results reported by these studies and thereby make it difficult to draw useful conclusions from the existing literature. Thus, the purpose of this paper is to gain a better understanding of nitric acid passivation as it relates to titanium and titanium alloys, specifically to deter-

mine the effects of passivation parameters such as nitric acid concentration, temperature, and time of immersion on the corrosion properties, surface oxide, and biological response of the materials.

MATERIALS AND METHODS

Materials

Three groups of titanium metal and alloys were used for this study. Metallic discs were machined from bar stock of cpTi (ASTM F67), Ti-6Al-4V (ASTM F136), and Ti-15Mo. The disks were 12.7 mm and 6 mm in diameter and 2-3 mm thick. All disks were ground with a series of SiC grit papers to a final 600-grit finish. The disks were cleaned by rinsing with distilled water, followed by 15-min ultrasonic baths in acetone, distilled water, reagent alcohol, and, finally, distilled water. Samples were then air dried and stored in a desiccator until further surface treatments were performed. Disk samples in this condition were designated as clean samples.

Nitric acid passivation treatments

Titanium and titanium alloy disk samples were passivated in nitric acid using various combinations of passivation parameters. In this study, the effects of nitric acid concentration, temperature, and time of immersion were studied. Table 1 shows the different values used for these three passivation parameters. Two nitric acid concentrations (10% and 40 percent by volume), two temperatures (20°C and 50°C), and three immersion times (15 min, 1 h, and 2 h) were used. All groups were immersed statically (i.e., without ultrasonication). A complete study group matrix using all possible combina-

tions of these parameters was prepared. Thus, the first test series consisted of 12 test groups for each material.

All nitric acid solutions were made with ACS grade nitric acid and distilled water. All nitric acid concentrations reported here are volume percentages. Temperature-controlled water baths were used for passivation treatments done at 50°C. After passivation treatments, all samples were rinsed with distilled water, ultrasonicated for 5 min in distilled water, air dried, and then stored in a desiccator until testing.

TABLE 1
Passivation Parameters Used for Nitric Acid Passivation Treatments

Nitric Acid Concentration	Nitric Acid Temperature	Nitric Acid Immersion Time
10 vol%	20°C	15 min
40 vol%	50°C	1 h
		2 h

Electrochemical impedance spectroscopy

EIS testing was conducted by using a three-electrode electrochemical cell with graphite rod counter electrodes and a saturated calomel electrode as reference. All potentials reported in this study are relative to standard calomel electrode. The equipment included an impedance response detector (Model 5210 Lock-In Amplifier, EG&G Princeton Applied Research) in combination with a potentiostat/galvanostat system (Model 263A Potentiostat/Galvanostat, EG&G Princeton Applied Research). EIS spectra were obtained at the open-circuit potential. The electrolyte solution was Hanks' Balanced Salt Solution (HBSS) adjusted to pH 7.4 ± 0.1 . Nitrogen gas was used to deaerate the HBSS for 30 min prior to testing and during all testing. All tests were conducted at 37°C.

The magnitude of the applied sinusoidal waveform was 10 mV, and the frequency range was 100 kHz to 10 mHz. Computer software was used to collect (PowerSUITE, Princeton Applied Research) and analyze (ZSimpWin, Princeton Applied Research) the EIS data. The impedance behavior of the samples was expressed in Nyquist and Bode plots. All impedance data were fitted to appropriate equivalent circuits using computer software (ZSimpWin). Triplicate tests were done for all study groups.

Potentiodynamic polarization testing

Direct-current potentiodynamic polarization testing was performed immediately after EIS testing. After EIS testing, the entire corrosion cell was transferred and connected to another potentiostat/galvanostat system (Model 273 Potentiostat/Galvanostat, EG&G Princeton Applied Research), which was used to conduct electrochemical potentiodynamic polarization testing. The polarization scan was from 150 mV more active than open-circuit potential to 1200 mV using a scan rate of 1.0 mV/s. As with the EIS tests, nitrogen gas was used to deaerate the HBSS and tests were conducted at 37°C. Tafel extrapolation and Stern-Geary fits (SoftCorr III, EG&G Princeton Applied Research) were used to obtain the E_{corr} and the I_{corr} at the maximum corrosion potential. The I_{pass} was recorded at a potential of 800 mV. This potential was chosen because it was located within the passive region for all the samples tested. Triplicate tests were done for all study groups.

X-ray photoelectron spectroscopy (XPS)

Chemical analysis of the surface oxide was done with XPS. A Kratos Axis 165 electron spectrometer using a 165-mm mean radius concentric hemispherical analyzer operating in fixed analyzer transmission mode at pass energy of 160 eV was used for the XPS analysis. Typical sampling depth of analysis was about 3 nm from the surface. The analyzed area was approximately 0.8 mm x 0.2 mm, and the chamber pressure during XPS was 1×10^{-9} torr. Low-energy electrons from an integral charge neutralizer system in the Axis 165 compensated for sample charging during XPS. The binding energy scale was referenced to the adventitious carbon C 1s at 285.0 eV. For all samples, initial survey spectra were obtained, followed by high-resolution spectra for C 1s, O 1s, N 1s, and Ti 2p. Additional high-resolution spectra obtained were Al 2p and V 2p for the Ti-6Al-4V samples and Mo 3d for the Ti-15Mo samples. In addition, depth profile analysis of the oxide was done with argon ion etching for specified times. Relative atomic concentrations for all identified elements were quantified from the high-resolution spectra data using system software. Finally, a curve-fitting program was used to differentiate and quantitate the different titanium oxide states, as well as metallic titanium.

Cell culture

The following cell culture methods were used to evaluate the biological compatibility of the titanium materials with different nitric acid passivation treatments. Biological response to the different sample groups was determined by using SaOS-2 osteosarcoma cells. SaOS-2 cells were cultured in complete media consisting of McCoy's modified medium, 10% fetal bovine serum (FBS), amphotericin B (500 μ g/500 ml), and gen-

tamicin sulfate (5 mg/500 mL). The cells were incubated in humidified 5% CO₂ air atmosphere at 37°C, nurtured every 2-3 days until confluence, and then split at a ratio of 1:4. The cells were detached in the media flasks by incubating with trypsin-EDTA at 37°C, and the reaction was stopped by adding complete media to the flask.

Cell attachment and proliferation assays

For the experiments, sample disks were placed tightly into the wells of 96-well tissue culture plates. Disk samples were sterilized prior to testing by soaking in 100% ethanol for 1 h, followed by repeated washing (3x) with sterile filtered phosphate-buffered saline (PBS; 0.2 µm filtered) and overnight incubation with sterile PBS (37°C, 5% CO₂). Cell suspensions were prepared and cells were seeded onto disks at a density of 2×10^4 cells per well. After seeding of the wells, the culture plates were incubated for 1 h, 4 h, and 24 h in complete media for attachment assays and for 1 day, 3 days, and 7 days for proliferation assays. After incubation, the disks were washed with PBS two times to remove non adherent cells. Adherent cells were quantified by using the hexosaminidase assay.³⁰ Blank wells were used as controls. Three samples from each group were used in quadruplicate experiments.

RESULTS

EIS results

EIS Nyquist and Bode plots

EIS spectra in the form of Nyquist and Bode plots were analyzed to qualitatively determine differences in the impedance and capacitive behavior of the samples due to the

different passivation parameters. Nyquist plots plot the imaginary impedance component versus the real impedance component; for thin passive oxides, these plots will display incomplete semicircles, which are indicative of capacitive behavior. The diameter of the semicircles gives the impedance of the system, with larger diameters indicating higher impedance. Bode plots express the impedance behavior of the samples by plotting both the log of the impedance ($\log|Z|$) and the phase angle (θ) against the log of the frequency ($\log f$). For Bode plots, capacitive behavior is denoted by a phase angle that closely approaches -90° and a linear variation of the impedance ($\log|Z|$) and frequency ($\log f$) with a slope close to -1. Thus, changes in capacitive behavior can be determined with Nyquist plots by comparing the magnitude of the diameter of the semicircles and with Bode plots by comparing the magnitude of the maximum phase angle and the width of the frequency range for which the sample maintains the maximum phase angle. In terms of the corrosion properties of a material, the higher the impedance and the more capacitive the behavior of the sample are, the better the corrosion resistance.

In general, the spectra for all the samples showed features characteristic of a thin passive oxide film on titanium or titanium alloy. The Nyquist plots displayed incomplete capacitive semicircles, while the spectra in the Bode plots exhibited a capacitive behavior over wide frequency ranges. The phase angle plots exhibited only a single maximum value, which indicated that there was only one time constant. This result is consistent with a single-layer oxide. Figures 1-6 show a series of representative Nyquist and Bode plots for cpTi, Ti-6Al-4V, and Ti-15Mo. Plots for each material group contain spectra for the non passivated group (Clean Only) and samples that had been passivated in 40% nitric acid at 20°C for 15 min, 1 h, and 2 h.

Table 2 has a summary of the impedance and capacitive behavior of the samples in relation to the time of passivation, as determined by analyzing the spectra in Nyquist and Bode plots.

TABLE 2
Summary of Effect of Time of Nitric Acid Passivation on Impedance and Capacitive Behavior as Determined by Using Spectra From Nyquist and Bode Plots

Group	Time Responses of Impedance and Capacitive Behavior
10%-20°C	cpTi, Ti-6Al-4V, and Ti-15Mo had similar time response patterns. Initial decrease in impedance and capacitive behavior at 15 min and 1 h compared with time zero, followed by an increase at 2 h. Difference between times was less pronounced for alloys, especially Ti-15Mo.
10%-50°C	cpTi, Ti-6Al-4V, and Ti-15Mo had similar time response patterns. Unlike 10%-20°C, all groups had slight to moderate increases in impedance and capacitive behavior at 15 min and 1 h, followed by a larger increase at 2 h.
40%-20°C	cpTi, Ti-6Al-4V, and Ti-15Mo showed dissimilar time response patterns. cpTi had relatively large increase in impedance and capacitive behavior at 15 min, followed by no change at 1 h and then a large decrease at 2 h. Ti64 had a more moderate increase at 15 min, followed by a relatively large increase at 1 h and then a decrease at 2 h. Ti-15Mo had relatively smaller increases at 15 min and 1 h but, unlike cpTi and Ti64, no decrease at 2 h.
40%-50°C	cpTi, Ti-6Al-4V, and Ti-15Mo had similar time response patterns. Groups showed large increase in impedance and capacitive behavior at 15 min, followed by a more moderate increase at 1 h and then a decrease at 2 h.

In general, the effects of concentration on the spectra were greater than those of temperature were found to be. Increasing nitric acid concentrations from 10% to 40% typically increased the impedance and capacitance behavior of the 20°C samples substan-

tially while resulting in more moderate increases for the 50°C groups. The temperature effects were less consistent, as well as less pronounced, compared with the concentration effects. The alloys, in general, showed less sensitivity than the cpTi groups did to the concentration and temperature of passivation.

Comparisons of Nyquist and Bode plots for the three material groups within the same treatment showed similar plots. An exception was the 40%-20°C-1h groups, which showed the cpTi and Ti64 spectra to have greater impedance and capacitive behavior than the Ti-15Mo group did.

EIS parameters

The electrochemical reactions at the surface interface are analogous to an electronic circuit consisting of a specific combination of resistors and capacitors; thus, the electrochemical system can be described in terms of an EEC. In the EEC, circuit elements such as resistors and capacitors are used to represent electrochemical properties of the metal and the oxide film. In this study, the phase angle plots exhibited a single time constant; thus, the surface oxide was assumed to be a simple one-layer oxide. To model the single-layer oxide, a simple EEC consisting of a resistor (R_s) in series with a resistor (R_p)-capacitor (C) parallel circuit was used. The R_s resistor consists essentially of the experimental-system resistance and models resistance due to the electrolyte, the reference electrode, and the electrical leads present in the system. The R_p resistor in parallel with the capacitor component is used to model the resistance of the surface oxide, while the capacitor models the capacitance of the surface oxide. However, to account for the non

ideal capacitive response of the interface, a constant-phase element (CPE) was used instead of a pure capacitor. The impedance of a constant-phase element is defined as

$$Z(\text{CPE}) = [Q(j\omega)^n]^{-1} \text{ with } -1 \leq n \leq 1,$$

where Q is a constant, ω is the angular frequency, j is $\sqrt{-1}$, and n is the CPE power. A value of $n = 1$ represents an ideal capacitor, and the constant parameter Q represents a pure capacitance. The parameter n is related to the non homogeneity of the surface, such as roughness and structure of the oxide.

Experimental spectra were fitted to the theoretical EEC to obtain quantitative results for the EEC circuit parameters, Q , n , and R_p . The experimental data exhibited good fits to the theoretical EEC; all chi-square values were less than 4×10^{-3} . The EEC circuit parameters, Q , n , and R_p , are given in Tables 3-5 for cpTi, Ti64, and Ti-15Mo, respectively. In addition, the results are shown graphically in Figures 7-9. These graphs plot the means of Q , n , and R_p at the three passivation times (15 min, 1 h, and 2 h), for the four passivation groups (10%-20°C, 10%-50°C, 40%-20°C, and 40%-50°C). In addition, the cleaned groups for cpTi, Ti64, and Ti-15Mo were included in the appropriate plots and represent time zero. These graphs provide a good illustration of the effects of time, concentration, and temperature on the measured EIS parameters.

Effect of time of passivation on EIS parameters Q , n , and R_p

Figures 7-9 show changes in Q , n , and R_p values as a function of passivation time. In general, the cpTi passivated groups showed less change in EIS parameters over time when compared with the two alloy groups. The majority of groups showed Q values

TABLE 3
EIS Parameters Q, n, and Rp Results for cpTi

Treatment Group	Q ($\mu\text{F}/\text{cm}^2$)	n	Rp ($\text{K}\Omega\cdot\text{cm}^2$)
Clean Only	27.6 ± 0.7 ^z	0.927 ± 0.002 ^z	517 ± 101 ^z
10%-20°C-15min	29.3 ± 1.9 ^{aC}	0.922 ± 0.004 ^C	290 ± 22 ^{TCz}
10%-20°C-1h	27.6 ± 1.8 ^{bC}	0.915 ± 0.012 ^C	560 ± 268
10%-20°C-2h	33.3 ± 1.0 ^{abC}	0.927 ± 0.002 ^{TC}	494 ± 99 ^C
10%-50°C-15min	28.7 ± 3.1	0.922 ± 0.019	423 ± 37 ^{aT}
10%-50°C-1h	30.6 ± 1.3 ^z	0.932 ± 0.002 ^C	407 ± 60 ^{bC}
10%-50°C-2h	32.7 ± 1.9 ^z	0.949 ± 0.003 ^{TCz}	606 ± 38 ^{ab}
40%-20°C-15min	25.2 ± 1.2 ^{Cz}	0.938 ± 0.002 ^{TCz}	1276 ± 509 ^{Cz}
40%-20°C-1h	24.2 ± 1.0 ^{TCz}	0.946 ± 0.007 ^{Cz}	846 ± 465
40%-20°C-2h	26.8 ± 1.9 ^C	0.937 ± 0.005 ^C	726 ± 20 ^{Cz}
40%-50°C-15min	28.9 ± 2.1	0.950 ± 0.005 ^{aTz}	747 ± 185
40%-50°C-1h	29.4 ± 0.6 ^{Tz}	0.944 ± 0.003 ^C	1233 ± 157 ^{Cz}
40%-50°C-2h	28.9 ± 3.8	0.938 ± 0.005 ^{aC}	916 ± 264 ^z

The values are mean \pm standard deviation ($n = 3$).

Statistically significant differences are denoted with superscripts, which correspond to specific comparisons.

Results with the same superscripts are significantly different ($p < 0.05$).

z superscript denotes differences between Clean Only result and passivated groups (t-test, $p < 0.05$).

abc superscripts denote differences due to time of passivation only (one-way ANOVA, $p < 0.05$).

T superscripts denote differences due to temperature of passivation only (t-test, $p < 0.05$).

C superscripts denote differences due to nitric acid concentration only (t-test, $p < 0.05$).

increasing with time of passivation, while n and Rp results showed increases and decreases over time. The magnitude of the changes in the Q results over time was greater for the two alloy materials, with Ti-15Mo showing the greatest sensitivity to time. One notable decrease in Q occurred for the Ti-15Mo-40%-50°C-2h group. The Q results for cpTi showed one group to have significant differences, while two of the Ti64 groups and

TABLE 4
EIS Parameters Q, n, and Rp Results for Ti-6Al-4V

Treatment Group	Q ($\mu\text{F}/\text{cm}^2$)	n	Rp ($\text{K}\Omega\cdot\text{cm}^2$)
Clean Only	28.6 ± 2.1 ^z	0.900 ± 0.010 ^z	604 ± 210 ^z
10%-20°C-15min	28.5 ± 2.4	0.913 ± 0.002 ^a	563 ± 225
10%-20°C-1h	30.3 ± 1.7 ^T	0.917 ± 0.005 ^b	316 ± 33 ^T
10%-20°C-2h	30.4 ± 0.7 ^{TC}	0.926 ± 0.004 ^{abCz}	567 ± 90
10%-50°C-15min	33.8 ± 1.7 ^{az}	0.917 ± 0.003 ^{abC}	373 ± 13 ^{aC}
10%-50°C-1h	36.2 ± 1.4 ^{aTz}	0.926 ± 0.004 ^{az}	466 ± 35 ^{bTC}
10%-50°C-2h	39.4 ± 1.1 ^{abTz}	0.925 ± 0.002 ^b	749 ± 144 ^{ab}
40%-20°C-15min	30.3 ± 2.2 ^T	0.920 ± 0.003 ^{aT}	598 ± 11
40%-20°C-1h	31.1 ± 2.2	0.918 ± 0.001 ^b	1020 ± 537
40%-20°C-2h	33.2 ± 1.2 ^{TCz}	0.902 ± 0.006 ^{abC}	673 ± 143
40%-50°C-15min	37.2 ± 2.0 ^{Tz}	0.926 ± 0.002 ^{TCz}	754 ± 154 ^{aC}
40%-50°C-1h	41.4 ± 1.3 ^z	0.938 ± 0.011	1351 ± 536 ^{abCz}
40%-50°C-2h	52.3 ± 1.7 ^T	0.923 ± 0.005	516 ± 55 ^b

The values are mean \pm standard deviation ($n = 3$).

Statistically significant differences are denoted with superscripts, which correspond to specific comparisons.

Results with the same superscripts are significantly different ($p < 0.05$).

z superscript denotes differences between Clean Only result and passivated groups (t-test, $p < 0.05$).

abc superscripts denote differences due to time of passivation only (one-way ANOVA, $p < 0.05$).

T superscripts denote differences due to temperature of passivation only (t-test, $p < 0.05$).

C superscripts denote differences due to nitric acid concentration only (t-test, $p < 0.05$).

all four Ti-15Mo groups had significant differences among the different passivation times.

The results for the n coefficient, unlike the Q results, showed both increases and decreases over time. For the two cpTi groups passivated in 10% nitric acid, n decreased initially and then increased over time; for the two 40% nitric acid groups, n initially

TABLE 5
EIS Parameters Q, n, and Rp Results for Ti-15Mo

Treatment Group	Q ($\mu\text{F}/\text{cm}^2$)	n	Rp ($\text{K}\Omega\cdot\text{cm}^2$)
Clean Only	43.7 ± 3.0^z	0.904 ± 0.008^z	377 ± 39^z
10%-20°C-15min	43.0 ± 1.6^{abTC}	0.912 ± 0.002	368 ± 69
10%-20°C-1h	52.6 ± 4.1^{aTCz}	0.896 ± 0.005^T	323 ± 43
10%-20°C-2h	52.1 ± 1.5^{bTCz}	0.907 ± 0.006	368 ± 28^T
10%-50°C-15min	55.4 ± 5.1^{aTCz}	0.906 ± 0.023	396 ± 65
10%-50°C-1h	75.5 ± 3.0^{bTz}	0.923 ± 0.008^{Tz}	510 ± 126
10%-50°C-2h	86.7 ± 4.8^{cTC}	0.915 ± 0.004^z	606 ± 118^{TCz}
40%-20°C-15min	48.8 ± 2.1^{aTC}	0.909 ± 0.001^a	431 ± 88
40%-20°C-1h	43.1 ± 2.4^{bT}	0.902 ± 0.007^b	409 ± 79
40%-20°C-2h	78.7 ± 1.8^{cTCz}	0.924 ± 0.010^{abz}	574 ± 202
40%-50°C-15min	67.2 ± 4.4^{aTCz}	0.901 ± 0.008	518 ± 136
40%-50°C-1h	76.1 ± 1.6^{bTz}	0.916 ± 0.011	480 ± 239
40%-50°C-2h	50.7 ± 4.0^{cTC}	0.902 ± 0.010	370 ± 37^c

The values are mean \pm standard deviation ($n = 3$).

Statistically significant differences are denoted with superscripts, which correspond to specific comparisons.

Results with the same superscripts are significantly different ($p < 0.05$).

z superscript denotes differences between Clean Only result and passivated groups (t-test, $p < 0.05$).

abc superscripts denote differences due to time of passivation only (one-way ANOVA, $p < 0.05$).

T superscripts denote differences due to temperature of passivation only (t-test, $p < 0.05$).

C superscripts denote differences due to nitric acid concentration only (t-test, $p < 0.05$).

increased and then remained relatively constant. For Ti64, the n values increased up to 1 h, and then the values for the 40% groups decreased at 2 h. The Ti-15Mo groups had little change in the n value at the initial 15-min passivation time; however, then the values for the groups passivated at 50°C increased and decreased at 1 h and 2 h, respectively,

while the 20°C groups did the opposite. Differences in n values were statistically significant in one cpTi group, three Ti64 groups, and one Ti-15Mo group.

The R_p results, like the n results, both increased and decreased over time. In general, all the groups that were passivated in 10% nitric acid and all four Ti-15Mo groups had minimal changes in R_p values over time. The R_p values for the cpTi and Ti64 samples passivated in 40% nitric acid were more sensitive to changes in time. Statistically significant differences were shown for one cpTi group, two Ti64 groups, and one Ti-15Mo group.

Effect of temperature of passivation

Figure 10 shows percentage change of Q , n , and R_p due to increased nitric acid temperature. The positive percentages indicate higher Q , n , and R_p values for the samples passivated at 50°C compared with 20°C. Passivation at the higher temperature resulted in increased Q values in all but a few instances and increased the n and R_p values in the majority of cases. The Q graph shows that temperature effects were more pronounced with Ti-15Mo groups, followed by Ti64 groups, with cpTi showing the smallest effects. In addition, the temperature effects on Q results were greater for the samples passivated in 40% nitric acid and for those with longer passivation times. The n values also tended to increase with temperature increases; however, the pattern for changes was not consistent with regard to material group, concentration, or time. The n values for cpTi groups showed increasing temperature effects with time for the samples passivated in 10% nitric acid but were less sensitive for samples passivated in 40% nitric acid. The temperature effects for Ti64 groups tended to increase with time and with concentration, while the Ti-

15Mo groups showed negative changes at the initial 15-min passivation times and again at 2 h for the samples passivated in 40% nitric acid. The R_p values, like those for Q and n , showed mostly positive changes with increased temperature; however, the magnitude of these changes did not show a consistent pattern among material groups and over time. Samples passivated in 40% nitric acid tended to show smaller temperature effects.

Effect of nitric acid concentration

Figure 11 shows the effects of nitric acid concentration on the values of Q , n , and R_p . The general trend for concentration, like that for temperature, was that an increase in concentration tended to increase the values of the EIS parameters; however, this trend was not as consistent as it was for temperature. Indeed, the concentration effects on the Q results for the cpTi groups showed negative changes for all but one group and were more pronounced for the 10% nitric acid groups and over time, whereas the Ti64 groups all increased and the Ti-15Mo groups showed increases and decreases. The Q values for the Ti64 groups passivated at 50°C nitric acid were more sensitive to concentration, while the Q values for the Ti-15Mo groups tended to show larger concentration effects at the longer passivation times, especially at 2 h. The change in n values tended to increase with increasing nitric acid concentration. The cpTi groups had positive concentration effects for all but the 50°C-2h group, and the Ti64 groups had such effects for all but the 20°C-2h and 50°C-2h groups. The Ti-15Mo groups, however, had negative changes with increases in concentration for all the 50°C groups and the 20°C-15min groups. The changes in R_p values due to nitric acid concentration also trended toward positive percentages, with large increases in R_p with increased concentrations. The changes in the

few groups that did show negative percentages were relatively small in magnitude, and all occurred for the 50°C groups.

Potentiodynamic polarization corrosion testing

The potentiodynamic polarization curves for all groups were characteristic of highly passive systems. The I_{pass} were of the order of 2.0 to 7.5 $\mu\text{A}/\text{cm}^2$. The low passive currents, typical of a passive system, persisted throughout the experiment; all curves exhibited negative hysteresis, indicating no localized corrosion. The E_{corr} , I_{corr} , and I_{pass} corrosion results for the potentiodynamic polarization tests are given in Tables 6-8.

In general, compared with non passivated sample groups, samples that had been passivated showed improved corrosion resistance properties in terms of more noble E_{corr} values and lower I_{corr} and I_{pass} results. Time of passivation tended to exhibit a gradual improvement of the measured corrosion properties over time for the groups passivated in 10% nitric acid, while the 40% nitric acid groups generally showed improved properties up to 1 h and then a deterioration of corrosion properties at 2 h. The 40% nitric acid groups typically had nobler E_{corr} and smaller I_{corr} and I_{pass} than similar groups did that had been passivated with 10% nitric acid. The higher passivation temperature had an effect similar to that of the higher concentration in that the 50°C groups typically had improved corrosion properties when compared with similar 20°C groups.

Comparisons between the similarly treated material groups showed the cpTi groups to have the best corrosion properties, followed by Ti64 and then Ti-15Mo.

TABLE 6
E_{corr}, I_{corr}, and I_{pass} Results for cpTi

Treatment Group	E _{corr} (mV)	I _{corr} (nA/cm ²)	I _{pass} (μA/cm ²)
Clean Only	-223 ± 32 ^z	56 ± 8 ^z	4.60 ± 0.22 ^z
10%-20°C-15min	-159 ± 49	87 ± 16 ^C	4.91 ± 0.41 ^C
10%-20°C-1h	-66 ± 152	83 ± 22 ^C	4.15 ± 0.46
10%-20°C-2h	-286 ± 27 ^{TC}	43 ± 11	4.32 ± 0.21
10%-50°C-15min	-63 ± 0 ^z	44 ± 9	4.13 ± 0.34
10%-50°C-1h	-42 ± 70 ^z	63 ± 39	4.24 ± 0.24 ^C
10%-50°C-2h	-74 ± 9 ^{TCz}	47 ± 8	3.93 ± 0.27 ^{Cz}
40%-20°C-15min	-110 ± 14 ^{Tz}	42 ± 21 ^C	3.99 ± 0.25 ^{Cz}
40%-20°C-1h	-83 ± 40 ^z	26 ± 9 ^{Cz}	3.81 ± 0.24 ^z
40%-20°C-2h	-86 ± 9 ^{TCz}	56 ± 23	3.78 ± 0.27 ^{Tz}
40%-50°C-15min	3 ± 45 ^{Tz}	45 ± 10	3.27 ± 0.56 ^{abz}
40%-50°C-1h	42 ± 0 ^z	33 ± 9 ^z	2.00 ± 0.21 ^{aCz}
40%-50°C-2h	18 ± 30 ^{TCz}	28 ± 15	2.33 ± 0.24 ^{bTCz}

The values are mean ± standard deviation ($n = 3$).

Statistically significant differences are denoted with superscripts, which correspond to specific comparisons.

Results with the same superscripts are significantly different ($p < 0.05$).

z superscript denotes differences between Clean Only result and passivated groups (t-test, $p < 0.05$).

abc superscripts denote differences due to time of passivation only (one-way ANOVA, $p < 0.05$).

T superscripts denote differences due to temperature of passivation only (t-test, $p < 0.05$).

C superscripts denote differences due to nitric acid concentration only (t-test, $p < 0.05$).

XPS results

Surface chemistry

XPS analysis included initial survey spectra followed by high-resolution spectra for Ti 2p, O 1s, C 1s, and N 1s for all three material groups. In addition, the Al 2p and V 2p spectra were obtained for the Ti-6Al-4V groups, and the Mo 3d spectra were obtained for

TABLE 7
E_{corr}, I_{corr}, and I_{pass} Results for Ti-6Al-4V

Treatment Group	E _{corr} (mV)	I _{corr} (nA/cm ²)	I _{pass} (μA/cm ²)
Clean Only	-216 ± 57 ^z	46 ± 11 ^z	4.77 ± 0.41 ^z
10%-20°C-15min	-191 ± 60	63 ± 44	4.52 ± 0.07
10%-20°C-1h	-160 ± 59	80 ± 54	4.83 ± 0.28 ^{aC}
10%-20°C-2h	-181 ± 70	51 ± 18	4.02 ± 0.26 ^{az}
10%-50°C-15min	-143 ± 89	42 ± 9	4.45 ± 0.51
10%-50°C-1h	-63 ± 23 ^z	77 ± 84	4.34 ± 0.25 ^C
10%-50°C-2h	-80 ± 20	164 ± 130	3.81 ± 0.31
40%-20°C-15min	-165 ± 18 ^T	31 ± 4	4.22 ± 0.07 ^a
40%-20°C-1h	-102 ± 8 ^T	27 ± 24	3.96 ± 0.92 ^{aTC}
40%-20°C-2h	-78 ± 6	155 ± 64 ^{Tz}	3.99 ± 0.33 ^z
40%-50°C-15min	-18 ± 39 ^{Tz}	84 ± 84	3.90 ± 0.24 ^a
40%-50°C-1h	-40 ± 34 ^{Tz}	13 ± 8 ^z	2.91 ± 0.14 ^{abTCz}
40%-50°C-2h	-26 ± 48 ^z	42 ± 4 ^T	3.55 ± 0.21 ^{bz}

The values are mean ± standard deviation ($n = 3$).

Statistically significant differences are denoted with superscripts, which correspond to specific comparisons.

Results with the same superscripts are significantly different ($p < 0.05$).

z superscript denotes differences between Clean Only result and passivated groups (t-test, $p < 0.05$).

abc superscripts denote differences due to time of passivation only (one-way ANOVA, $p < 0.05$).

T superscripts denote differences due to temperature of passivation only (t-test, $p < 0.05$).

C superscripts denote differences due to nitric acid concentration only (t-test, $p < 0.05$).

the Ti-15Mo groups. Argon ion sputtering was used to obtain depth profiles for the elemental composition. Analysis of high-resolution spectra yielded elemental composition (atomic %).

Survey spectra confirmed the presence of the constituent elements for each material, as well as carbon and nitrogen, which are ubiquitous surface contaminants.

TABLE 8
Ecorr, Icorr, and Ipass Results for Ti-15Mo

Treatment Group	Ecorr (mV)	Icorr (nA/cm ²)	Ipass (μA/cm ²)
Clean Only	-253 ± 23 ^z	70 ± 33	7.26 ± 0.50
10%-20°C-15min	-291 ± 14 ^T	44 ± 12	6.58 ± 0.73
10%-20°C-1h	-257 ± 41 ^{TC}	62 ± 16	7.68 ± 0.88
10%-20°C-2h	-219 ± 67 ^C	54 ± 31	7.05 ± 0.66 ^C
10%-50°C-15min	-150 ± 17 ^{Tz}	47 ± 20	6.62 ± 0.65
10%-50°C-1h	-152 ± 32 ^{Tz}	33 ± 7	6.36 ± 0.94
10%-50°C-2h	-167 ± 42 ^z	39 ± 6	6.74 ± 0.74
40%-20°C-15min	-205 ± 1 ^T	37 ± 5	7.51 ± 0.61 ^a
40%-20°C-1h	-124 ± 14 ^{TCz}	51 ± 24	6.83 ± 0.63 ^b
40%-20°C-2h	-27 ± 3 ^{CTz}	32 ± 6	4.48 ± 0.44 ^{abTC}
40%-50°C-15min	-130 ± 26 ^{abTz}	45 ± 16	6.67 ± 0.46
40%-50°C-1h	-42 ± 7 ^{aTz}	71 ± 47	5.58 ± 2.13
40%-50°C-2h	-93 ± 26 ^T	48 ± 14	6.96 ± 0.90 ^T

The values are mean ± standard deviation ($n = 3$).

Statistically significant differences are denoted with superscripts, which correspond to specific comparisons.

Results with the same superscripts are significantly different ($p < 0.05$).

z superscript denotes differences between Clean Only result and passivated groups (t-test, $p < 0.05$).

abc superscripts denote differences due to time of passivation only (one-way ANOVA, $p < 0.05$).

T superscripts denote differences due to temperature of passivation only (t-test, $p < 0.05$).

C superscripts denote differences due to nitric acid concentration only (t-test, $p < 0.05$).

All of the survey spectra had dominant titanium and oxygen peaks with a relatively large carbon peak. Smaller peaks for the alloy constituents, Al and V for the Ti64 groups and Mo for the Ti-15Mo groups, were also present.

The surface chemistry throughout the oxide layer was quantified by analyzing the high-resolution spectra taken after argon etching for specific time intervals. Tables 9-11 give the surface composition of the cpTi, Ti64, and Ti-15Mo groups, respectively.

TABLE 9
Surface Composition (at%) by XPS Analysis of Various Passivation Treatment Groups of cpTi After Different Etch Times

Group	CpTi Clean	CpTi 15min	CpTi 1h	CpTi 2h	CpTi 10%	CpTi 50C
Ti 0s	14.8 ± 1.7	10.5 ± 0.4	17 ± 0.1	15.7 ± 0.5	16.3 ± 0.4	20.1 ± 0.3
Ti 15s	--	37.1 ± 4.3	--	34.4 ± 0.5	36.6 ± 0.0	35.1 ± 0.0
Ti 30s	45.0 ± 5.7	46.1 ± 10	41.2 ± 2.1	38.7 ± 4.4	40.9 ± 1.8	40.6 ± 1.1
Ti 60s	--	63.5 ± 15	--	51.8 ± 1.7	55.0 ± 0.4	52.1 ± 0.1
Ti 120s	69.4	78.0 ± 7.2	--	70.6 ± 4.8	74.7 ± 3.1	77.3 ± 1.3
Ti 180s	--	82.4 ± 4.7	--	80.3 ± 5.8	82.6 ± 2.1	82.5 ± 1.2
O 0s	33.6 ± 1.3	36.3 ± .05	40.8 ± 7.3	43.7 ± 4.4	43.0 ± 0.1	48.8 ± 0.1
O 15s	--	57.6 ± 2.3	--	60.6 ± 1.5	59.0 ± 0.8	61.5 ± 0.3
O 30s	52.5 ± 2.2	47.5 ± 10	55.9 ± 1.8	57.1 ± 2.1	55.8 ± 2.2	57.6 ± 2.0
O 60s	--	36.6 ± 15	--	48.2 ± 1.7	45.0 ± 0.4	47.9 ± 0.1
O 120s	30.6	22.0 ± 7.2	--	29.4 ± 4.8	25.3 ± 3.1	22.7 ± 1.3
O 180s	--	17.6 ± 4.7	--	19.7 ± 5.8	17.4 ± 2.1	17.5 ± 1.2
C 0s	46.4 ± 3.9	48.0 ± 0.3	40.2 ± 5.5	37.0 ± 6.8	37.0 ± 0.3	29.0 ± 0.2
C 15s	--	4.6 ± 2.2	--	4.6 ± 1.7	4.3 ± 0.6	3.3 ± 0.3
C 30s	1.3 ± 1.9	5.2 ± 0.4	2.4 ± 0.3	3.9 ± 2.1	3.2 ± 0.4	1.8 ± 0.9
N 0s	5.2 ± 0.9	5.2 ± 0.2	2.0 ± 1.9	3.6 ± 0.1	3.7 ± 0.5	2.2 ± 0.0
N 15s	--	0.7 ± 0.2	--	0.5 ± 0.2	0.2 ± 0.3	0 ± 0.0
N 30s	1.2 ± 1.7	1.3 ± 0.4	0.5 ± 0.7	0.4 ± 0.3	0 ± 0.0	0 ± 0.0

The values are mean ± standard deviation (at%; $n = 2$ specimens per group, except $n = 1$ where result has no standard deviation).

Results from Tables 9-11 show some similar trends in all treatment groups for all three material groups. All groups show the titanium concentration to gradually increase, starting from the outermost region (0-s etch time) and going toward the substrate (180-s etch time), while the amount of oxygen initially increases after the first argon etch (15-s

TABLE 10
Surface Composition (at%) by XPS Analysis of Various Passivation Treatment
Groups of Ti-6Al-4V After Different Etch Times

Group	Ti64 Clean	Ti64 15min	Ti64 1h	Ti64 2h	Ti64 10%	Ti64 50C
Ti – 0s	16.8 ± 0.0	16.1 ± 0.3	15.0 ± 1.4	13.2 ± 1.2	15.4 ± 3.4	15.5 ± 2.1
Ti – 15s	32.8 ± 1.1	30.3 ± 0.7	30.9 ± 0.0	29.7 ± 0.6	31.7 ± 0.2	30.0 ± 1.2
Ti – 30s	35.6 ± 0.8	33.1 ± 0.4	34.7 ± 0.0	33.4 ± 0.3	35.6 ± 1.2	32.9 ± 1.3
Ti – 60s	49.6 ± 0.9	48.3 ± 0.9	45.1 ± 2.3	44.2 ± 3.6	48.6 ± 0.6	41.9 ± 1.4
Ti – 120s	73.5 ± 1.6	71.4 ± 7.0	62.1 ± 4.3	62.2 ± 11.0	65.5 ± 2.2	65.9 ± 0.6
Ti – 180s	77.1 ± 0.8	76.7 ± 3.7	71.7 ± 2.3	69.5 ± 8.2	71.1 ± 2.1	75.8 ± 0.4
O – 0s	48.2 ± 0.9	46.5 ± 0.1	43.2 ± 2.1	42.6 ± 3.9	43.1 ± 2.6	44.2 ± 2.7
O – 15s	58.7 ± 1.0	59.2 ± 0.4	56.5 ± 1.3	59.3 ± 1.9	56.7 ± 0.8	62.1 ± 1.1
O – 30s	54.3 ± 2.3	56.1 ± 1.6	53.9 ± 1.8	56.6 ± 0.2	55.0 ± 2.1	58.7 ± 1.9
O – 60s	41.9 ± 0.2	42.4 ± 0.6	44.8 ± 1.8	48.5 ± 2.7	41.4 ± 1.5	50.9 ± 2.7
O – 120s	15.3 ± 0.4	17.5 ± 2.8	24.3 ± 3.8	24.8 ± 10.0	18.7 ± 1.8	23.8 ± 1.2
O – 180s	8.4 ± 0.7	12.1 ± 4.4	12.6 ± 1.2	16.1 ± 9.6	14.2 ± 0.4	12.7 ± 2.5
Al – 0s	2.8 ± 0.1	2.9 ± 1.3	3.4 ± 0.7	2.8 ± 0.7	2.7 ± 0.5	2.8 ± 1.3
Al – 15s	4.5 ± 0.9	4.3 ± 0.4	5.7 ± 0.7	4.9 ± 0.9	5.7 ± 0.0	4.7 ± 0.3
Al – 30s	4.9 ± 1.4	5.3 ± 0.1	5.5 ± 1.1	5.2 ± 0.8	4.3 ± 0.5	4.8 ± 0.5
Al – 60s	6.0 ± 1.2	7.5 ± 0.3	7.2 ± 1.6	5.2 ± 0.8	8.0 ± 0.8	5.4 ± 0.8
Al – 120s	7.7 ± 0.9	7.9 ± 3.8	10.3 ± 0.2	9.0 ± 1.0	12.0 ± 0.5	7.8 ± 0.4
Al – 180s	10.6 ± 1.2	8.0 ± 0.2	11.6 ± 0.1	10.4 ± 1.2	10.4 ± 0.4	8.1 ± 2.6
V – 0s	0.1 ± 0.1	0.2 ± 0.1	0.6 ± 0.1	0.5 ± 0.0	0.2 ± 0.0	0.4 ± 0.0
V – 15s	0.5 ± 0.3	1.0 ± 0.2	1.1 ± 1.0	0.6 ± 0.2	0.8 ± 0.3	0.5 ± 0.2
V – 30s	1.1 ± 0.5	1.4 ± 0.1	1.6 ± 0.6	1.4 ± 0.2	1.4 ± 1.3	0.9 ± 0.3
V – 60s	2.6 ± 0.1	1.9 ± 0.6	2.9 ± 1.1	2.1 ± 0.0	2.0 ± 1.3	1.9 ± 0.5
V – 120s	3.5 ± 0.3	3.1 ± 0.4	3.3 ± 0.7	4.0 ± 0.0	3.8 ± 0.9	2.5 ± 0.2
V – 180s	4.0 ± 1.0	3.2 ± 0.9	4.1 ± 0.9	4.0 ± 0.3	4.3 ± 1.2	3.4 ± 0.2
C – 0s	28.3 ± 1.5	32.1 ± 1.5	35.6 ± 4.5	39.3 ± 5.0	35.6 ± 5.1	36.4 ± 5.9
C – 15s	3.3 ± 1.4	5.1 ± 0.5	5.0 ± 1.5	5.2 ± 0.6	4.7 ± 1.9	2.3 ± 1.9
C – 30s	3.3 ± 0.6	3.7 ± 1.5	4.2 ± 2.2	3.0 ± 0.6	3.9 ± 0.3	2.7 ± 3.0
N – 0s	3.8 ± 0.8	2.1 ± 0.1	2.3 ± 0.4	1.7 ± 0.6	3.0 ± 1.4	0.8 ± 0.2
N – 15s	0.2 ± 0.2	0 ± 0.0	0.9 ± 0.4	0.3 ± 0.3	0.4 ± 0.5	0.5 ± 0.7
N – 30s	0.7 ± 0.5	0.4 ± 0.6	0.1 ± 0.1	0.4 ± 0.6	0.4 ± 0.2	0 ± 0.0

The values are mean ± standard deviation (at%; $n = 2$ specimens per group).

TABLE 11
Surface Composition (at%) by XPS Analysis of Various Passivation Treatment
Groups of Ti-15Mo after Different Etch Times

Group	Ti-15Mo Clean	Ti-15Mo 15min	Ti-15Mo 1h	Ti-15Mo 2h	Ti-15Mo 10%	Ti-15Mo 50C
Ti – 0s	14.6 ± 0.5	17.0 ± 0.6	14.3 ± 0.4	13.8 ± 2.0	17.2 ± 0.4	18.8 ± 0.5
Ti – 15s	31.8 ± 0.5	28.9 ± 3.4	30.3 ± 0.7	31.2 ± 0.5	34.7 ± 0.7	30.3 ± 1.2
Ti – 30s	35.2 ± 1.3	34.5 ± 6.2	35.8 ± 1.4	35.3 ± 1.5	40.6 ± 0.4	32.8 ± 1.0
Ti – 60s	45.0 ± 2.5	46.1 ± 7.1	42.8 ± 1.0	47.2 ± 2.5	55.5 ± 2.3	42.0 ± 0.6
Ti – 120s	53.1 ± 0.3	63.2 ± 7.1	56.2 ± 0.4	65.0 ± 3.0	69.6 ± 3.6	58.9 ± 1.3
Ti – 180s	59.5 ± 7.1	73.0 ± 9.2	64.6 ± 0.0	75.0 ± 3.8	73.7 ± 2.0	64.4 ± 6.6
O – 0s	43.3 ± 2.5	48.7 ± 3.3	45.4 ± 0.8	46.3 ± 1.3	48.4 ± 0.6	52.2 ± 0.1
O – 15s	54.6 ± 1.3	59.9 ± 1.1	59.6 ± 1.4	59.4 ± 0.0	55.5 ± 1.5	62.0 ± 0.1
O – 30s	51.8 ± 0.2	52.9 ± 0.6	54.5 ± 3.3	56.9 ± 0.1	49.2 ± 2.1	59.2 ± 2.3
O – 60s	49.1 ± 2.8	48.6 ± 8.8	51.4 ± 0.3	46.3 ± 3.3	37.4 ± 2.2	52.4 ± 0.5
O – 120s	38.1 ± 1.3	27.1 ± 8.0	34.9 ± 0.8	24.9 ± 3.1	19.6 ± 3.5	31.9 ± 1.3
O – 180s	29.9 ± 7.4	16.9 ± 9.6	24.6 ± 0.2	14.4 ± 2.2	14.3 ± 1.4	23.2 ± 4.6
Mo – 0s	1.0 ± 0.1	1.5 ± 0.0	1.6 ± 0.2	1.5 ± 0.2	1.4 ± 0.0	1.9 ± 0.0
Mo – 15s	2.5 ± 0.1	2.8 ± 0.3	3.0 ± 0.1	3.3 ± 0.3	3.4 ± 0.1	3.2 ± 0.4
Mo – 30s	3.2 ± 0.1	3.7 ± 0.4	3.7 ± 0.2	3.8 ± 0.4	4.4 ± 0.4	3.6 ± 0.0
Mo – 60s	5.9 ± 0.3	5.2 ± 1.7	5.7 ± 0.7	6.5 ± 0.7	7.1 ± 0.1	5.6 ± 0.1
Mo – 120s	8.8 ± 0.9	9.6 ± 1.0	8.9 ± 0.4	10.1 ± 0.1	10.9 ± 0.1	9.2 ± 0.1
Mo – 180s	10.6 ± 0.3	10.1 ± 0.3	10.8 ± 0.3	10.6 ± 1.6	12.0 ± 0.6	12.4 ± 2.0
C – 0s	36.8 ± 3.5	27.0 ± 1.7	35.1 ± 0.3	35.3 ± 0.7	29.4 ± 0.7	26.7 ± 0.9
C – 15s	10.6 ± 1.5	4.8 ± 0.2	7.1 ± 0.7	5.9 ± 0.6	6.3 ± 2.1	4.3 ± 1.4
C – 30s	9.2 ± 0.3	4.2 ± 0.6	5.9 ± 1.9	3.9 ± 1.9	5.7 ± 1.3	4.3 ± 1.3
N – 0s	4.3 ± 0.4	5.8 ± 5.6	3.7 ± 1.2	3.2 ± 1.6	3.7 ± 0.5	0.3 ± 0.3
N – 15s	0.4 ± 0.6	3.6 ± 4.6	0 ± 0.0	0.1 ± 0.2	0 ± 0.1	0.2 ± 0.0
N – 30s	0.6 ± 0.9	4.7 ± 6.7	0.1 ± 0.2	0 ± 0.0	0 ± 0.0	0 ± 0.0

The values are mean ± standard deviation (at%; $n = 2$ specimens per group).

groups) and then gradually declines for all remaining etch times. The initial increase in oxygen is due to the removal of the contaminant carbon. The results show the carbon levels decreasing substantially with the initial etch. These results are consistent for titanium materials. In addition, for the alloy groups, the alloy constituent elements are

also shown to vary with etch time. In general, the aluminum in the Ti64 groups decreases and then increases with etch time, while vanadium gradually increases. The molybdenum in the Ti-15Mo groups generally increases with etch time. The increase of the metallic elements and corresponding decrease of oxygen with etch time indicate the approach of the metal substrate.

The surface composition was affected to various degrees by the different nitric acid passivation parameters: time, concentration, and temperature. Figure 12 shows a graph of the ratio of the atomic percentage of titanium to that of oxygen (Ti/O ratio) for the cpTi groups. In theory, a Ti/O ratio of 50% corresponds to TiO_2 (i.e., one titanium atom to two oxygen atoms), and deviations from 50% indicate the presence of other titanium states (i.e., suboxides Ti_2O_3 and TiO and/or metallic titanium). The figure shows each of the groups to have initial Ti/O ratios below 50%, followed by just over 50% for 15-s etch times and then gradual increases for subsequent etch times. The 15 min group (40% nitric acid at 20°C for 15 min) exhibits the largest differences between the different treatment groups, with the other treatment groups being fairly equal.

To ascertain the effect of nitric acid passivation on the surface chemistry of the alloy groups, the atomic percentages of the metallic elements were converted to weight percentages (wt%), which were normalized to $\text{Ti} + \text{Al} + \text{V} = 100\%$ and $\text{Ti} + \text{Mo} = 100\%$ for Ti64 and Ti-15Mo, respectively. The results for the Al and V wt% for the Ti64 groups are given in Figure 13, and those for the Mo wt% for the Ti-15Mo groups are given in Figure 14.

The graph in Figure 13 for Al wt% shows the groups to exhibit a maximum Al wt% at the outermost region (0-s etch time), followed by varying rates of decrease going

toward the substrate. The Al wt% tended to increase with time of passivation (Clean vs. 15 min vs. 1 h vs. 2 h) and with nitric acid concentration (10% vs. 1 h [=40%]); however, the samples passivated at a higher temperature (1 h [=20°C] vs. 50°C) had lower Al wt% throughout the oxide layer. Comparison of the Al gradients throughout the surface oxide for the different groups showed the 1h and 50°C groups to have the most consistent gradients; that is, the Al wt% for the 1h group initially declined and then remained relatively constant for the subsequent etch times, while the 50°C group had a constant decrease with each subsequent etch time. The other graph in Figure 13 is for V wt%. In general, the groups had increasing V wt% from the outermost surface (0-s etch time) toward the substrate (180-s etch time). Time of passivation tended to increase the vanadium, as did an increase in the concentration of the nitric acid (10% vs. 1 h [=40%]). Higher passivation temperature groups had lower amounts of vanadium at all etch times.

Figure 14 shows the results for the normalized Mo wt%. All groups exhibited similar trends, which consisted of a gradual increase in Mo wt% going from the outermost oxide (0-s etch time) into the oxide toward the substrate (180-s etch time). Nitric acid passivation increased the Mo wt% in the outermost regions of oxide, and this effect was sensitive to the time of passivation (Clean vs. 15 min vs. 1 h vs. 2 h) and concentration of nitric acid (10% vs. 1 h [=40%]) but not to temperature.

Surface oxide stoichiometry

Analysis of the Ti 2p spectra allowed for the quantification of the different oxidation states present in the oxide, specifically, Ti^{0+} (metallic Ti), Ti^{4+} (TiO_2), Ti^{3+} (Ti_2O_3), and Ti^{2+} (TiO). Figure 15 shows a series of high-resolution Ti 2p spectra for cpTi, Ti-

6Al-4V, and Ti-15Mo samples in the passivated condition (40% nitric acid at 20°C for 1 h). The spectra are consistent with titanium oxide. Common features for all the spectra included the presence of a dominant Ti 2p_{3/2} peak at a binding energy of 459.0 eV and a smaller and broader Ti 2p_{1/2} peak at a binding energy of 464.6 eV. These peaks both correspond to Ti⁴⁺ (TiO₂). All the spectra also usually had a small Ti 2p_{3/2} peak at a binding energy of 453.9 eV, which corresponds to Ti⁰⁺ (metallic Ti). In addition, the peaks in these spectra exhibit shoulders to various extents. These shoulders represent titanium suboxide states (i.e., Ti³⁺ [Ti₂O₃] and Ti²⁺ [TiO]). Subtle differences can be seen for the spectra of the different groups, indicating varying effects of the different passivation treatments.

A curve-fitting program was used on the high-resolution Ti 2p spectra to quantify the four oxidization states present in the surface oxide. These states included Ti⁰⁺ (metallic Ti), Ti²⁺ (TiO), Ti³⁺ (Ti₂O₃), and Ti⁴⁺ (TiO₂). The percentages of the different oxides are shown in Table 12. The results show subtle differences in the percentages of oxide states for the different groups. Passivation time was shown to exhibit similar effects for all three materials, with the increases and decreases in the percentages of the different oxidation states alternating over time. Initially, the results going from the cleaned condition to 15 min of passivation showed that the percentage of TiO₂ increased, while the percentages of suboxides Ti₂O₃ and TiO and metallic Ti decreased. Over the subsequent time period, 15 min to 1 h, the results were opposite, with the percentage of TiO₂ decreasing and the suboxides and metallic Ti increasing. The final passivation period, 1 h to 2 h, saw a reversed pattern again, as TiO₂ increased and the suboxides and metallic Ti decreased.

TABLE 12
Percentage of Oxidation States for cpTi, Ti-6Al-4V, and Ti-15Mo After Different Nitric Acid Passivation Treatments

Group	TiO ₂	Ti ₂ O ₃	TiO	Ti
cpTi-Clean	84	3.1	3.2	9.5
cpTi-15min	89.1 ± 2.3	3.0 ± 2.8	6.2 ± 0.6	6.2 ± 0.6
cpTi-1h	80.3 ± 0.8	6.9 ± 1.1	9.2 ± 0.7	9.2 ± 0.7
cpTi-2h	88.5 ± 4.9	3.1 ± 3.6	7.3 ± 0.3	7.3 ± 0.3
cpTi-50°C	81.9 ± 1.6	6.4 ± 0.8	8.3 ± 0.7	9.7 ± 1.2
cpTi-10%	83.5 ± 0.4	4.8 ± 0.1	9.7 ± 1.2	8.3 ± 0.7
Ti64-Clean	79.1 ± 1.1	6.2 ± 0.4	2.9 ± 0.2	12.0 ± 0.5
Ti64-15min	82.0 ± 7.7	6.3 ± 5.7	2.1	9.4 ± 1.6
Ti64-1h	78.9 ± 1.4	7.1 ± 0.6	1.6 ± 0.8	11.0 ± 0.1
Ti64-2h	81.3	6.0	2.0 ± 0.6	9.4
Ti64-50°C	83.3 ± 3.5	5.2 ± 4.2	0.6 ± 0.6	12.9
Ti64-10%	83.5 ± 0.4	10.0	3.7 ± 0.5	8.
Ti-15Mo-Clean	81.0 ± 2.9	6.5 ± 1.6	4.6 ± 0.5	8.1 ± 0.9
Ti-15Mo-15min	93.6	2.1	2.1	2.3
Ti-15Mo-1h	92.3 ± 3.7	1.4 ± 1.1	1.6 ± 0.8	4.6 ± 1.7
Ti-15Mo-2h	90.5 ± 0.7	4.1 ± 0.4	2.0 ± 0.6	3.5 ± 1.8
Ti-15Mo-50°C	91.6 ± 2.3	5.9 ± 1.1	0.6 ± 0.6	2.0 ± 0.6
Ti-15Mo-10%	78.1 ± 0.6	8.4 ± 0.1	3.7 ± 0.5	9.9 ± 0.1

The values are mean ± standard deviation (at%; n = 2 specimens, except n = 1 where no standard deviation is shown).

The effects of passivation temperature are seen by comparing the 1h (=20°C) and 50°C groups for each material. The results for the cpTi and Ti64 materials show the 50°C groups to have a slightly greater percentage of TiO₂ and Ti and smaller percentages of suboxides, Ti₂O₃ and TiO. The Ti-15Mo groups showed the 50°C group to have slightly less TiO₂, Ti, and TiO but relatively more Ti₂O₃.

Last, the effect of the passivation concentration is shown by comparing the 10% nitric acid groups and the 1h (40 % nitric acid) groups for each material. For cpTi, the 40% nitric acid groups had higher percentages of TiO₂ and metallic Ti and lower overall suboxide percentages when compared with the 10 % nitric acid groups. The Ti64 and Ti-

15Mo groups showed similar concentration effects, with the 40 % nitric acid groups having higher percentages of TiO₂ and smaller percentages of suboxides and metallic Ti when compared with 10 % nitric acid treatments. The Ti-15Mo groups showed the largest differences.

Cell culture results

Hexosaminidase activity of the SaOS-2 cells was determined after 1 h, 4 h, 24 h, 3 days, and 7 days of incubation with the experimental samples. Quantification of the hexosaminidase activity was used to characterize the cell numbers at the different time periods to assess cellular attachment and proliferation. Proliferation is taken in this study as the percentage difference between the most recent result and the former result and is calculated as the most recent result less the former result, divided by the former result; an example is $(100*[4\text{ h} - 1\text{ h}]/1\text{ h})\%$. All the cell culture results are presented in bar graph form with standard deviation bars and are given as percentage of control, where the control was blank tissue culture wells.

The results for cells attached at 1, 4, and 24 h are shown in Figure 16. In general, comparisons of the passivation treatment groups within each material group showed increases in cell numbers with longer passivation times (15 min < 1 h < 2 h), higher temperatures (1 h [20°C] < 50°C), and lower concentration (1 h [40 %] < 10 %). For the 1-h attachment time, all the nitric-acid-passivated Ti-15Mo groups had statistically significantly higher cell numbers than the non passivated Ti-15Mo group (Clean) did. In addition, comparisons of the material groups within the passivation treatment groups showed all the passivated Ti-15Mo groups to have significantly higher cell numbers than

similarly treated cpTi groups did and higher numbers than the 15min, 1h, and 10% Ti-6Al-4V treatment groups did.

The graph with the 4-h attachment results shows trends similar to those seen in the 1-h attachment graph. Greater cell numbers are shown for groups with longer passivation times, higher temperature, and lower concentration, and some of the differences were statistically significant. As with the 1-h attachment results, material comparisons within treatment groups showed the Ti-15Mo groups to have higher cell numbers than the cpTi and Ti-6Al-4V groups. These differences were statistically significant for the 15min and 10% passivation treatment groups had. The final graph in Figure 16 shows the cell numbers at 24 h, which shows trends similar to those seen for the 1-h and 4-h attachment time points, with a few of the differences being statistically significant.

The results for the cell numbers at the longer time periods of 3 and 7 days are shown in Figure 17. In contrast to the results at the earlier time points, the 3- and 7-day graphs show cpTi to have slightly greater numbers for the different treatment groups when compared with Ti64 and Ti-15Mo. The time, concentration, and temperature effects of passivation are less pronounced at the longer times. However, both alloy groups that were passivated at 50°C did show significantly lower cell numbers than the cpTi-50C group did at day 7.

The proliferation results for the cells are shown in Figures 18 and 19. Figure 18 shows cell proliferation for the first two time intervals, 1 to 4 h and 4 to 24 h. Comparison of the different passivation treatment groups showed no statistically significant differences within each material group. However, each of the cpTi treatment groups did have greater proliferation than both similarly treated alloys had, with the difference being

statistically significant in all but one case (cpTi-15min compared with Ti-6Al-4V-15min) for the 1- to 4-h time interval.

The graphs in Figure 19 show proliferation results at the 1- to 3-day and 3- to 7-day intervals. In general, comparisons between passivation treatment groups and material groups showed similar proliferation results for both time intervals. The only differences that were statistically significant were for the cpTi-2h and cpTi-10% groups compared with the Ti-15Mo-2h and Ti-15Mo-10% groups during the 1- to 3-day interval.

DISCUSSION

The ASTM F86 protocol specifies the use of nitric acid to clean and passivate metallic implants, including titanium and titanium alloys. Passivation is the phenomenon by which an active metallic surface is made less active, or more corrosion resistant. During nitric acid passivation, simultaneous oxidation and dissolution chemical reactions are taking place at the oxide surface. However, since nitric acid is an oxidizing acid, the favored reaction is the oxidation reaction; thus, oxide formation occurs.

Improvements in corrosion properties due to nitric acid passivation have been attributed to an enhanced surface oxide layer.^{11, 12} However, some studies have shown passivation to increase the dissolution of the constituent ions from the Ti-6Al-4V alloy and to thin the oxide layer.^{13, 14} Other investigators have shown that varying the parameters of passivation affects other oxide properties.^{6, 7} The goal of this study was to determine the effects of different nitric acid passivation parameters—namely, time, concentration, and temperature—on the corrosion and surface oxide properties of cpTi, Ti-6Al-4V, and Ti-15Mo.

In general, all the parameters, separately and in key combinations, as well as the type of material group, affected the surface properties of the materials studied. Thus, the discussion will focus on the effects of each of the individual parameters, as well as the effect of the titanium or titanium alloy, on the corrosion resistance, surface chemistry, and biological response of the materials.

Effect of time of passivation

Changes in the surface properties after the various passivation times were documented in an effort to gain insights into how the passive oxide layer changes over time. Previous studies by Wallinder⁷ and Noh⁶ have shown longer passivation times to improve the corrosion properties of stainless steels; however, such studies for titanium or titanium alloys are limited.

In the present study, the time response was shown to be dependent on the nitric acid concentration, temperature, and material type. The 10 % and 40 % nitric-acid-passivated groups showed dissimilar time response patterns. For the most part, the 10 % groups showed results consistent with oxide degradation and/or dissolution at the initial 15-min and 1-h time periods, followed by the formation of a more protective oxide at the 2-h times; the 40% groups showed initial improvements in oxide layers up to the 1-h time point, followed by degradation of the oxide properties after 2-h of passivation.

Dissolving or degrading oxides were characterized by EIS spectra that showed lower impedance and more capacitive behavior, while the presence of a more protective oxide was indicated by spectra with higher impedance and less capacitive behavior.

In addition, the EIS parameters, Q , n , and R_p , were used to characterize the properties of the surface oxide. From the CPE or near-ideal capacitance value, Q , the thickness of the surface oxide can be estimated using the parallel-plate capacitor formula:

$$Q = \epsilon\epsilon_0 A/d_{ox} \quad (1)$$

where ϵ is the dielectric constant of the oxide, ϵ_0 is the permittivity of vacuum ($8.85 \times 10^{-8} \mu\text{F/cm}$), A is the effective surface area, and d_{ox} is the thickness of the surface oxide. Therefore, since Q varies inversely with d_{ox} , an increase in Q indicates a decrease in the thickness of the surface oxide or dissolution of the oxide, while a decrease in Q suggests an increase in the surface oxide or net oxide formation. However, care must be taken in making conclusions about oxide thickness based solely on the inverse relationship with Q , since equation (1) also shows that the dielectric constant and effective surface area are directly related to the oxide thickness. This issue will be discussed in more detail later in the paper.

As mentioned previously, the physical meaning of the n value has been related to the surface roughness³¹, the presence of a porous corrosion product layer³², or the homogeneity of the surface oxide³³, with higher n values indicating a smoother, more uniform surface oxide and less presence of a porous overlayer of oxide. Finally, the R_p value represents the resistance of the oxide, with higher values of R_p implying improved corrosion resistance.

For both the 10 % and 40 % groups, slightly larger Q values were shown after each subsequent passivation time, suggesting that the surface oxides were continually thinning over time. However, the n and R_p values did not show a consistent trend for the three materials or concentrations. The 10 % groups tended to have n and R_p values that

decreased up to 1 h, which is consistent with oxide degradation, followed by increases after 2-h; the 40 % groups had initial improvements up to 1 h, followed by decreases. Higher temperatures (50°C) tended to exaggerate the time response trends.

The degradation or improvements in the oxide properties shown over time by the EIS results were generally reflected in the corrosion results. The 10 % groups tended to show increased corrosion at 15-min and 1-h, followed by decreased corrosion at 2-h; while the 40 % groups tended show improved corrosion properties up to 1-h, followed by less corrosion resistance at 2-h.

Changes in the surface oxide properties due to time of passivation might be explained by changes in the surface chemistry. The XPS results showed the 10 %-20°C-1h groups to have increases in the atomic percentages of the suboxides Ti_2O_3 and TiO and in metallic Ti when compared with the non passivated (Clean) groups. Increases in suboxide amounts have been linked in the literature with decreased corrosion resistance,³⁴ while increases in metallic Ti have been interpreted as indicative of a thinner oxide.^{13, 17, 34} XPS results for the 40 %-20°C groups, for the most part, did not show consistent trends in changes in suboxide amounts or metallic Ti over the experimental passivation times.

The depth profile XPS results, specifically the amount and distribution of alloying elements within the oxide, might also help explain the differences shown over time. Alloying elements within the oxide have been reported in the literature for Ti-6Al-4V^{13, 17, 34, 35} and Ti-15Mo.¹⁹ For Ti-6Al-4V, many of these studies have reported enrichment of Al within the oxide layer.^{13, 17, 34} Aluminum enrichment in the oxides can be attributed to the fact that aluminum oxide has a highly negative free energy of formation (higher than that of titanium oxide) so there is a greater driving force for the formation of aluminum

oxide.⁹ The results for V are more mixed, with some studies reporting the presence of V^{13, 16, 36} and others showing no V.^{17, 34, 35} In the present study, Al and V were shown in the surface oxide of all Ti-6Al-4V groups, and Mo was present in all the Ti-15Mo oxides. The normalized Al concentrations, in fact, were greater than the substrate concentrations were, indicating that the oxides were enriched with Al. In contrast to the Al concentrations, the normalized V and Mo concentrations in the oxides were typically less than the substrate concentrations were. As will be explained later, the presence of alloy elements can introduce point defects in the oxide because of size mismatches between the ionic radii of incorporated alloy elements.

It seems apparent that these alloy elements within the oxide layer diminish the oxide protective properties. However, the distribution of alloy elements within the oxide may be more important, in terms of protective properties, than their simple presence is. Sharper and more irregular gradients of alloying elements would be expected to result in an oxide that is less protective than an oxide with a more constant and regular gradient would be. For example, Figures 13 and 14 show that both 10 %-20°C-1h groups, which the EIS and corrosion results showed to have a less protective oxide, had more irregular distributions of the alloy elements as a function of etch time when compared with the non passivated (Clean) groups.

The changes in alloy gradients for the 40 % groups over time also reflected the EIS and corrosion results for those groups. The V and, especially, the Al gradients became less sharp and more constant at the 15-min and 1-h passivation times but then became more irregular at 2-h. Again, this pattern is consistent with the EIS and corrosion results, which showed improved oxide properties up to 1-h of passivation, followed by

degradation in oxide properties and increase in corrosion after 2-h of passivation. In contrast, the Ti-15Mo groups all showed fairly consistent Mo gradients at all time periods; however, this, too, was consistent with the EIS and corrosion results, since the 40 %-20°C-Ti-15Mo groups did not show the degradation at 2-h that was seen for Ti-6Al-4V.

The results for the EIS parameters n and R_p , with the corresponding alloy gradients, indicate that the groups with the highest n and R_p values also had the more consistent alloy distribution throughout the surface oxide and had the more protective oxide.

The reasons for the changes in alloy gradients for the different passivation times are not clear. The fact that the Al is concentrated in the oxide with nitric acid passivation would suggest that either the Ti is being preferentially dissolved or Al is being preferentially oxidized. Studies have shown that dilute nitric acid concentrations are less oxidizing than higher concentrations are.^{6, 7} Thus, one might hypothesize that, at the shorter times, the chemical reactions at the oxide surface for the 10 % groups are less uniform, leading to a more irregular alloy gradient. For the groups passivated in the higher (40 %) concentration, the oxidation reactions are more prevalent and stronger, leading initially to uniform dissolution and oxidation over the surface and thus a more constant alloy gradient within the oxide. However, after a certain time (i.e., 1-h) an irregular gradient may result because of the formation of a thin, porous oxide overlayer.

Effect of nitric acid concentration

Two concentrations of nitric acid, 10 % and 40 %, were used in the passivation treatments in this study. Wallinder⁷ and Noh⁶, in addition to showing the time effects, have shown that the concentration of nitric acid has a major effect on the corrosion

resistance of stainless steel. Wallinder showed greater concentration effects at shorter passivation times, and Noh demonstrated the existence of an optimum concentration—exceeding it resulted in poorer corrosion properties of the stainless steel.

In the present study, nitric acid concentration was shown to have a significant effect on the surface properties of the titanium and titanium alloys studied. The effect depended on the material being passivated. In general, the samples passivated with 40% nitric acid showed higher R_p values and improved corrosion resistance when compared with similar groups treated with 10 % nitric acid. Similarly, the effects were more pronounced at the shorter passivation times of 15-min and 1-h than at 2-h. However, the nitric acid concentration effects on the Q and n values did not follow a consistent pattern for the different material groups.

For cpTi, the higher nitric acid concentration resulted in significantly lower Q values and higher n values. This indicates a thicker and more homogeneous surface oxide. In contrast, all the 40 %-Ti-6Al-4V groups tended to have slightly higher Q values, with n values also slightly higher, except for the 2-h groups. The Ti-6Al-4V results indicate that the higher concentration of nitric acid tended to thin the oxide but also initially to improve the homogeneity of the oxide. At longer time periods, the higher concentration had an adverse affect, most likely introduced by the formation of a porous oxide layer.

The concentration effects on the Ti-15Mo groups were interesting in that the Q values were shown to be quite sensitive, while the n and R_p values were relatively insensitive to differences in concentration. Changes in these parameters did not show any

consistent trends. The Ti-15Mo results suggest that the oxide thickness but not the oxide homogeneity or resistance varied with concentration.

The concentration differences had minor effects on the Ti and O elemental composition of cpTi and Ti-6Al-4V. However, the Ti-15Mo groups did show concentration effects on the Ti/O ratios. Table 13 shows the Ti/O ratios for the different materials, which had been passivated with 10 % and 40 % nitric acid. As mentioned earlier, a Ti/O ratio of 0.50 indicates TiO₂, while ratios farther away from 0.50 imply the presence of less TiO₂. Higher ratios imply more suboxides or metallic titanium. As Table 13 shows, the 40 %-Ti-15Mo group had a Ti/O ratio closer to the theoretical 0.50, compared with the 10 %-Ti-15Mo group, at each etch time (except at 0-s), thus indicating a greater percentage of TiO₂ for the 40 %-Ti-15Mo groups after each etch time.

The stoichiometry results for Ti-15Mo groups support the Ti/O ratio results, as the 40% groups had less sub-oxides (3.0 % vs. 11.1 %) than the 10 % groups did. The Ti-6Al-4V groups also showed more sub-oxides for the 10 % groups (14.4 %) than for the 40 % groups (10.2 %).

However, as with the effect of time, the most important surface chemistry differences due to concentration may have been the relative amounts and distribution of the alloying elements throughout the oxide layer. Figure 13 shows that the 40%-Ti-6Al-4V groups had a higher percentage of Al and V at each etch time and displayed more constant gradients for both elements throughout the oxide layer when compared with the 10%-Ti-6Al-4V groups. Figure 14 shows similar results for the percentages of Mo throughout the Ti-15Mo groups. These results are consistent with the EIS and corrosion results, which show the 40 % groups to have more protective oxides and less corrosion

than the 10 % groups do.

TABLE 13
Ti/O Ratios for cpTi, Ti-6Al-4V, and Ti-15Mo at Different Etch Times:
Effect of 10% and 40% Nitric Acid Concentration

Etch Time	<u>cpTi</u>	<u>cpTi</u>	<u>Ti-64</u>	<u>Ti-64</u>	<u>Ti-15</u>	<u>Ti-15</u>
	10% HNO ₃	40% HNO ₃	10% HNO ₃	40% HNO ₃	10% HNO ₃	40% HNO ₃
0 s	0.38	0.42	0.36	0.35	0.36	0.31
15 s	0.62	--	0.56	0.55	0.63	0.51
30 s	0.73	0.74	0.65	0.64	0.83	0.66
60 s	1.12	--	1.17	1.01	1.48	0.83
120 s	2.95	--	3.56	2.55	3.55	1.61
180 s	4.75	--	5.01	5.68	5.15	2.63

Effect of nitric acid temperature

The increases in the passivation temperature tended to result in higher Q, n, and Rp values. The increases in Q values showed material sensitivity, with the alloy materials having larger increases and the Ti-15Mo groups showing the greatest percentage changes due to temperature. Corrosion results showed that samples passivated in the higher-temperature nitric acid solutions typically exhibited more noble E_{corr} and lower I_{pass} but mixed I_{corr} results. One notable exception was the 50°C-Ti-15Mo-40 % group that had been passivated for 2-h. When compared with the 20°C-Ti-15Mo-40 % group, this group showed smaller Q, n, and Rp values, with increased corrosion.

The stoichiometry for the three metal groups had similar changes due to the higher passivation temperature. All the changes were slight and showed the 50°C groups to have slightly more TiO₂, slightly less total suboxides, and slightly less metallic Ti than

the 20°C-cpTi group had. These results were consistent with those of other studies found in the literature, which have been attributed to increased oxidation reactions due to the higher temperatures. As a result of the increased oxidation, thicker oxides are formed with more TiO₂ and less sub-oxides.^{13, 36}

As with the time and concentration effects, the passivation temperature was shown to affect the distribution of alloy elements in the oxides of the two alloys. Figure 13 shows that the 50°C-Ti-6Al-4V groups had smaller percentages of Al and V elements throughout the surface oxide layer when compared with the 20°C-Ti-6Al-4V groups.

Another difference between these groups was the distribution of Al elements. The 50°C group showed consistently diminishing Al percentages going from the outermost surface toward the substrate, while the 20°C group had a larger decrease at the outermost region and then a constant percentage throughout the remainder of the analyzed region. The lower concentrations of alloying elements agree with the consistently higher n and R_p results for the 50°C-Ti-6Al-4V groups, which indicate greater oxide homogeneity and less corrosion.

The Ti-15Mo XPS results, like the Ti-6Al-4V results, showed a slightly smaller percentage of Mo at the outermost surface (0-s etch time) for 50°C-Ti-15Mo than for 20°C-Ti-15Mo. The distributions of Mo ions were similar.

Material groups comparison

The results of this study showed different effects within the various passivation parameters for the three materials tested. The EIS results showed all of the Ti-15Mo groups had to have significantly higher Q values than similarly treated cpTi and Ti-6Al-

4V groups and showed the cpTi groups typically to have significantly smaller Q values than the Ti-6Al-4V groups had.

As was mentioned earlier in the Discussion, the Q value can be related to the oxide thickness (d_{ox}) with the parallel-plate capacitor formula, $Q = \epsilon\epsilon_0A/d_{ox}$. In the literature, this equation is commonly used to estimate the oxide thickness, with values for the effective area, A, and dielectric constant, ϵ , being assumed.³⁷ As one can see from the formula, the Q value depends not only on the oxide thickness but also on the effective area and the dielectric constant. Examination of the surfaces showed that the 600-grit polishing procedure resulted in markedly different surface morphologies for the three materials, with the Ti-15Mo surfaces shown to be substantially rougher than those of cpTi and Ti-6Al-4V were. Figure 20 shows SEM micrographs for the different materials. The rougher Ti-15Mo surface morphologies would have greater effective areas and thus higher Q values.

Consequently, the higher Q values do not necessarily imply a thinner surface oxide. The XPS analysis of the oxidation states of the surfaces showed the surfaces of the Ti-15Mo groups to have lower percentages of metallic Ti than the similarly treated cpTi and Ti-6Al-4V groups had. A lower percentage of metallic Ti on the surfaces is usually associated with thicker oxide layers.³⁴

In contrast to the Ti-15Mo groups, the cpTi and Ti-6Al-4V groups exhibited relatively smoother surfaces, which were similar to each other. The fact that cpTi and Ti-6Al-4V had similar surface roughness would indicate similar effective areas. Consequently, the significantly higher Q values for Ti-6Al-4V groups than for cpTi groups, are not the

effect of a rougher surface but rather probably reflect thinner oxide layers for the Ti-6Al-4V groups.

In addition to the effective area, the dielectric constant of the oxide also helps determine the Q value. Typically, for simplicity, a single dielectric constant value is assumed for all groups being compared. However, one must not overlook the possibility that the dielectric constant could be different for the materials because of variations in the chemistries of the oxides or in the effects of different treatments. In fact, the dielectric constant is known to be strongly dependent on the conditions in which the surface oxide is formed.³⁷ Ohtsuka showed that faster film growth rates resulted in higher dielectric constants, an effect that was attributed to greater hydration levels for the oxides.³⁸ Higher hydration levels for faster-forming oxides may also be responsible for the higher Q values seen for the 40 % nitric acid and 50°C treatment groups since higher concentrations and temperatures would be expected to have increased oxide growth rates.

Comparisons of the n values for the similarly treated material groups showed the cpTi groups typically to have higher n values than the Ti-6Al-4V and Ti-15Mo groups did. However, rougher surfaces lower the n values, unlike the Q values, which they increase. Consequently, the lower n values for the Ti-15Mo groups are due in part to the rougher surface.

Lower n values have also been linked to the heterogeneity and defectiveness of the oxide.³⁹ As the results of the present study showed, alloy elements were found throughout the oxides of the alloy materials. The presence of alloy elements can introduce point defects in the oxide because of size mismatches between the ionic radii of

incorporated alloy elements (i.e., Al, V, and Mo) and the “host” element (i.e., Ti).⁴⁰ Table 14 shows the ionic radii of titanium, aluminum, vanadium, and molybdenum.⁴¹

TABLE 14
Ionic Radii of Titanium, Aluminum, Vanadium, and Molybdenum

Element (oxidation state)	Coordination Number	Ionic Radius (Å)
Ti (4+)	6	0.61
Al (3+)	4	0.39
Al (3+)	6	0.54
V (2+)	6	0.79
V (5+)	6	0.54
Mo (3+)	6	0.69
Mo (4+)	6	0.65
Mo (5+)	6	0.61
Mo (6+)	6	0.59

The mismatches between the aluminum and vanadium ionic radii and the titanium ionic radius would be expected to introduce point defects in the oxide. This effect could explain the smaller n values for Ti-6Al-4V. On the other hand, the difference between the molybdenum and titanium ionic radii is not as great, which should lead to fewer point defects in the oxides containing molybdenum. Thus, the increased roughness of the Ti-15Mo groups would appear to be the main reason for the lower n values for Ti-15Mo.

Typically, the oxide resistance (R_p) of cpTi was greater than that of Ti-6Al-4V, which, in turn, was greater than that of Ti-15Mo. The reasons for the differences are most likely similar to those given for differences in the Q and n parameters.

Increases in oxide resistance have been attributed to greater oxide thickness, improvement of the insulating properties through the oxidation of Ti_2O_3 to TiO_2 (i.e., reduction of sub-oxides), smoother surfaces, and the elimination of point defects.⁴² Thus, higher resistance in oxides was typically associated with lower Q values (thicker oxides)

and higher n values (smoother, more homogeneous, and less defective oxides), which can be expected to reduce the corrosion of the material.

In general, the potentiodynamic polarization results showed all the material groups to exhibit excellent corrosion resistance, with cpTi showing the highest corrosion resistance, followed by Ti-6Al-4V and then Ti-15Mo. However, because the corrosion properties are related to the surface area of the sample, the rougher Ti-15Mo surfaces would be expected to have higher corrosion rates due to the larger surface area. The corrosion results did closely follow the EIS results, confirming the complementary nature of these two types of analysis.

Comparisons between the surface chemistries with XPS showed the presence of alloying elements in the surface oxide layers of the alloys. The reduced corrosion resistance of the alloys in comparison with that of the unalloyed cpTi is most likely the result of the presence of alloy elements in the oxide of the alloys. The relative mismatch of the ionic radii of the elements in the alloy oxides leads to increased point defects and lower oxide resistance. A more irregular distribution of the alloy elements, found in some of the alloy groups, also results in a less protective oxide. Thus, the oxide chemistry is shown to be a factor in determining the corrosion properties of the material groups in this study.

Cell culture

SaOS-2 osteoblast-like cells were used to determine the cellular response to the different treatment groups. Hexosaminidase assay was used to quantify the cell numbers at various time points. This assay measures the amount of hexosaminidase enzyme, which has been shown to be directly proportional to the number of attached cells.³⁰ In

addition to cell numbers, cell proliferation between successive time points was quantified.

The largest differences in the cell numbers among the tested groups occurred at the initial time point, 1-h. The passivated Ti-15Mo groups had significantly higher cell numbers than the cpTi and Ti-6Al-4V groups did. The most likely explanation is that the Ti-15Mo samples had a rougher surface than the cpTi and Ti-6Al-4V samples had. Numerous studies have shown that increased surface roughness increases cell attachment.⁴³⁻⁴⁵

A similar trend was shown at 4-h, but the differences were not as pronounced; in addition, the trend was reversed at 24-h, when cpTi groups tended to have the higher cell numbers. At the later time periods, 3- and 7-days, the cell numbers for the groups tended to converge; however, two cpTi groups had significantly higher cell numbers than the Ti-6Al-4V and Ti-15Mo groups did.

Comparisons among passivation treatment groups did not show as many statistically significant differences as the comparisons among material groups did. However, all the passivated Ti-15Mo groups had significantly higher cell numbers than the non-passivated group did at 1-h, indicating that the nitric acid passivation improved the ability of the cells to attach at the initial 1-h time point. The reason for this finding is not clear. The EIS, corrosion, and XPS results for these groups did not show a consistent change in a single variable or a set of variables that would explain this difference. However, although SEM analysis did not show any obvious differences in surface morphology between the passivated and non passivated Ti-15Mo groups, perhaps the nitric acid

treatments hindered cell attachment by removing or altering some irregular surface features.

General trends in comparisons of the treatment groups showed that the cell attachment numbers increased with increased time of passivation and were higher for the 10 % and 50°C treatment groups. Although these differences, for the most part, were not statistically significant, the general trend seemed to follow the Q value, with groups having higher Q values showing increased cell numbers, especially at the initial time periods. As discussed in the previous Materials section, higher Q values could be the result of increased roughness, which helps the initial cellular attachment.^{43, 44}

The proliferation results typically showed the cpTi groups to have higher proliferation rates than similarly treated Ti-6Al-4V had; in turn, the latter groups had higher rates than Ti-15Mo had. The differences were more pronounced at the earlier time intervals. These differences could well be due to the presence of Al, V, and Mo ions, which are known to be toxic, in the surface oxide of the alloys.^{22, 24} However, studies in the literature show conflicting results for the effects of the presence of these alloy elements on the cellular response.^{24, 46-48}

In general, all the materials and treatment groups showed good cellular attachment and cell proliferation over the time frame of this study. However, variation in the long-term effects of the different passivation treatments for the materials is still possible.

CONCLUSIONS

The ASTM standard for passivation of titanium allows for ranges in the nitric acid concentration and in passivation time and temperature. This study showed that the

protective properties of the surface oxide would change significantly when these parameters are varied. The following conclusions were drawn from the results of this study:

1. The protective properties of the oxides of the materials varied as a function of time, and the optimal passivation times were dependent on the nitric acid concentration.
2. The less oxidizing environments with the lower experimental nitric acid concentration (10%) tended to reduce the protective properties of the oxide up to 1-h of passivation time and then resulted in improved protective properties at 2-h.
3. The more oxidizing environments with the higher experimental nitric acid concentration (40 %) immediately resulted in more protective properties lasting up to 1-h but then showed degraded protective properties at 2-h.
4. Increasing the oxidizing environments by passivating the samples at higher nitric acid temperature and/or concentration for 1h resulted in more protective oxides.
5. EIS results were predictive of corrosion properties, and the presence and irregular distribution of alloy elements such as Al, V, and Mo generally resulted in decreased corrosion resistance.
6. All material and treatment groups displayed excellent corrosion properties, with the unalloyed cpTi having the best corrosion properties, followed by Ti-6Al-4V and then Ti-15Mo. The lower corrosion resistance of Ti-15Mo was attributed to an increase in the effective surface area due to a rougher surface topography.
7. Conflicting oxide thickness results, as determined by using EIS and XPS, were explained by differences in the surface roughness of the metals and in the dielectric constant of the oxides.

8. Materials undergoing nitric acid passivation had similar biological responses that were comparable to those of non passivated materials and tissue culture controls. The rougher Ti-15Mo surfaces resulted in higher cell numbers at the initial time period.

The overall results indicated that the optimal combination of parameters for nitric acid passivation of titanium and titanium alloys tested in this study was 40% nitric acid for 1 h at 50°C.

Part II of this study will look at the effects of ultrasonication, surface morphologies, and the presence of titanium ions in the nitric acid solution on passivation.

References

1. Ong JL, Lucas LC, Raikar GN, Gregory JC, Electrochemical corrosion analyses and characterization of surface-modified titanium. *Applied Surface Science* 1993; 72(1):7.
2. Browne M, Gregson PJ, Surface modification of titanium alloy implants. *Biomaterials* 1994; 15(11):894.
3. ASTM F86-91 standard practice for surface preparation and marking of metallic surgical implants. *Annual Book of ASTM Standards* 1995; 13.01:6-7.
4. Kilpadi DV, Lemons JE. Effect of surface and heat treatments on corrosion of unalloyed titanium implants. 1997. Shreveport, LA, USA: IEEE, Piscataway, NJ, USA.
5. Wan GJ, Yang P, Leng YX, Sun H, Chen JY, Wang J, Huang N. Enhanced corrosion resistance of Ti6Al4v with Ti-O film deposited by dc metal vacuum arc deposition. *IEEE International Conference on Plasma Science* 2003; p.419.
6. Noh JS, Laycock NJ, Gao W, Wells DB, Effects of nitric acid passivation on the pitting resistance of 316 stainless steel. *Corr Sci* 2000; 42(12):2069.

7. Wallinder D, Pan J, Leygraf C, Delblanc-Bauer A, EIS and XPS study of surface modification of 316LMV stainless steel after passivation. *Corr Sci* 1999; 41(2):275.
8. Wisbey A, Gregson PJ, Peter LM, Tuke M, Effect of surface treatment on the dissolution of titanium-based implant materials. *Biomaterials* 1991; 12(5):470.
9. Lee TM, Chang E, Yang CY, A comparison of the surface characteristics and ion release of ti6al4v and heat-treated ti6al4v. *J Biomed Mater Res* 2000; 50(4):499-511.
10. Sittig C, Textor M, Spencer ND, Wieland M, Vallotton PH, Surface characterization of implant materials cpTi, Ti-6Al-7Nb and Ti-6Al-4V with different pre-treatments. *J Mater Sci: Mater Med* 1999; 10(1):35.
11. Petersen D, Lemons, J.E. and Lucas, L.C, Comparative evaluations of surface characteristics of cp Titanium, Ti-6Al-4V and Ti-15Mo-2.8Nb-0.2Si (Timetal 21SRX). Titanium, niobium, zirconium and tantalum for medical and surgical applications, ASTM STP. 2005, West Conshohocken: ASTM International.
12. Trepanier C, Tabrizian M, Yahia LH, Bilodeau L, Piron DL. Improvement of the corrosion resistance of niti stents by surface treatments. *Mater Res Soc Symp Proc* 1997; 459:363-368.
13. Callen BW, Lowenberg BF, Lugowski S, Sodhi RNS, Davies JE, Nitric acid passivation of Ti6Al4V reduces thickness of surface oxide layer and increases trace element release. *J Biomed Mater Res* 1995; 29(3):279.
14. Lowenberg BF, Lugowski S, Chipman M, Davies JE, ASTM-F86 passivation increases trace element release from Ti6Al4V into culture medium. *J Mater Sci: Mater Med* 1994; 5(6-7):467.
15. Kilpadi DV, Raikar GN, Liu J, Lemons JE, Vohra Y, Gregory JC, Effect of surface treatment on unalloyed titanium implants: Spectroscopic analyses. *J Biomed Mater Res* 1998; 40(4):128.
16. Ask M, Lausmaa J, Kasemo B, Preparation and surface spectroscopic characterization of oxide films on Ti6Al4V. *Applied Surface Science* 1989; 35(3):283.
17. Sodhi RN, Weninger A, Davies JE, X-ray photoelectron spectroscopic comparison of sputtered Ti, Ti6Al4V, and passivated bulk metals for use in cell culture techniques. *J Vac Sci Tech* 1991; A9(3):1329-1333.
18. Lausmaa J, Ask M, Rolander U, Kasemo B, Bjursten LM, Ericson LE, Thomsen P, Surface preparation and spectroscopic analysis of titanium implant materials. *Surface and Interface Analysis* 1990; 16(1-12):571.

19. Laser D, Marcus HL, Auger electron spectroscopy depth profile of thin oxide on a Ti-Mo alloy. *J Electrochem Soc* 1980; 127(3):763-765.
20. Jacobs JJ, Skipor AK, Black J, Urban R, Galante JO, Release and excretion of metal in patients who have a total hip-replacement component made of titanium-base alloy. *J Bone Joint Surg Am* 1991; 73(10):1475-86.
21. van der Voet GB, Marani E, Tio S, De Wolff FA, Aluminum neurotoxicity, In: *Histo- and cytochemistry as a tool in environmental toxicology*, W. Graumann and J. Drukker, Editors. 1991, Stuttgart. p. 235-242.
22. Thompson GJ, Puleo DA, Ti-6Al-4V ion solution inhibition of osteogenic cell phenotype as a function of differentiation timecourse in vitro. *Biomaterials* 1996; 17(20):1949-54.
23. Wataha JC, Hanks CT, Craig RG, The effect of cell monolayer density on the cytotoxicity of metal ions which are released from dental alloys. *Dent Mater* 1993; 9(3):172-6.
24. Rae T, The toxicity of metals used in orthopaedic prostheses. An experimental study using cultured human synovial fibroblasts. *J Bone Joint Surg Br* 1981; 63-B(3):435-40.
25. Blumenthal NC, Cosma V, Inhibition of apatite formation by titanium and vanadium ions. *J Biomed Mater Res* 1989; 23(A1 SUPPL):13.
26. Chyou SD, Shih HC, X-ray photoelectron spectroscopy and Auger electron spectroscopy studies on the passivation behavior of plasma-nitrided low alloy steel in nitric acid. 1991; A148(2):347.
27. Imam MA, Fraker AC. Titanium alloys as implant materials. *ASTM STP 1272 Medical applications of titanium and its alloys*, ed. S.A. Brown, Lemons, J.E. 1996, West Conshohocken: ASTM. p. 3-16.
28. Long M, Rack HJ, Titanium alloys in total joint replacement - A materials science perspective. *Biomaterials* 1998; 19(18):1621.
29. Zardiackas LD, Mitchell, D.W., Disegi, J.A., Characterization of Ti-15Mo beta titanium alloy for orthopedic implant applications. *ASTM STP 1272 Medical applications of titanium and its alloys*, ed. S.A. Brown, Lemons, J.E. 1996, West Conshohocken: ASTM.
30. Landegren U, Measurement of cell numbers by means of the endogenous enzyme hexosaminidase. Applications to detection of lymphokines and cell surface antigens. *J Immun Methods* 1984; 67:379-388.

31. Rammelt U, Reinhard, G., The influence of surface roughness on the impedance data for iron electrodes in acidic solutions. *Corrosion Science* 1987; 27:373-382.
32. Park JR, MacDonald, D.D., Impedance studies on the growth of porous magnetite films on carbon steels in high temperature aqueous systems. *Corrosion Science* 1983; 23(4):295-315.
33. MacDonald DD, Impedance spectroscopy, ed. W.B. Johnson. 1987, New York: John Wiley. 154-156.
34. Lee TM, Chang E, Yang CY, Surface characteristics of Ti6Al4V alloy: Effect of materials, passivation and autoclaving. *J Mater Sci: Mater Med* 1998; 9(8):439.
35. Smith DC, Pilliar RM, Metson JB, McIntyre NS, Dental implant materials. II. Preparative procedures and surface spectroscopic studies. *J Biomed Mater Res* 1991; 25(9):1069.
36. Milosev I, Metikos-Hukovic M, Strehblow HH, Passive film on orthopaedic TiAlV alloy formed in physiological solution investigated by x-ray photoelectron spectroscopy. *Biomaterials* 2000; 21(20):2103.
37. Pan J, Leygraf C, Thierry D, Ektessabi AM, Corrosion resistance for biomaterial applications of TiO₂ films deposited on titanium and stainless steel by ion-beam-assisted sputtering. *J Biomed Mater Res* 1997; 35(3):309-18.
38. Ohtsuka T, Otsuki, T, The influence of the growth rate on the semiconductive properties of titanium anodic oxide films. *Corr Sci* 1998; 40(6):951-958.
39. Souto RM, Alayali, H, Electrochemical characteristics of steel coated with TiN and TiAlN coatings. *Corr Sci* 2000; 42(12):2201-2211.
40. Metikos-Hukovic M, Kwokal A, Piljac J, The influence of niobium and vanadium on passivity of titanium-based implants in physiological solution. *Biomaterials* 2003; 24(21):3765.
41. CRC handbook of chemistry and physics. 75 ed, ed. D.R. Lide. 1994, Boca Raton: CRC Press.
42. Fonseca C, Barbosa MA, Corrosion behaviour of titanium in biofluids containing H₂O₂ studied by electrochemical impedance spectroscopy. *Corr Sci* 2001; 43(3):547.
43. Ahmad M, Gawronski, D, Blum J., Golderg J, Gronowicz, Differential response of human osteoblast-like cells to commercially pure (cp) titanium grades 1 and 4. *J Biomed Mater Res* 1999; 46:121-131.

44. Feng B, Weng J, Yang BC, Qu SX, Zhang XD, Characterization of surface oxide films on titanium and adhesion of osteoblast. *Biomaterials* 2003; 24(25):4663.
45. Stanford CM, Keller JC, Solursh M, Bone cell expression on titanium surfaces is altered by sterilization treatments. *J Dent Res* 1994; 73(5):1061-71.
46. Lee TM, Chang E, Yang CY, Attachment and proliferation of neonatal rat calvarial osteoblasts on Ti6Al4V: Effect of surface chemistries of the alloy. *Biomaterials* 2004; 25(1):23.
47. Oji MO, Wood, J.V., Downes, S., Effects of surface-treated cpTi and Ti6Al4V alloy on the initial attachment of human osteoblasts. *J Mater Sci: Mater Med* 1999; 10:869-872.
48. Escalas F, Galante J, Rostoker W, Biocompatibility of materials for total joint replacement. *J Biomed Mater Res* 1976; 10(2):175-95.

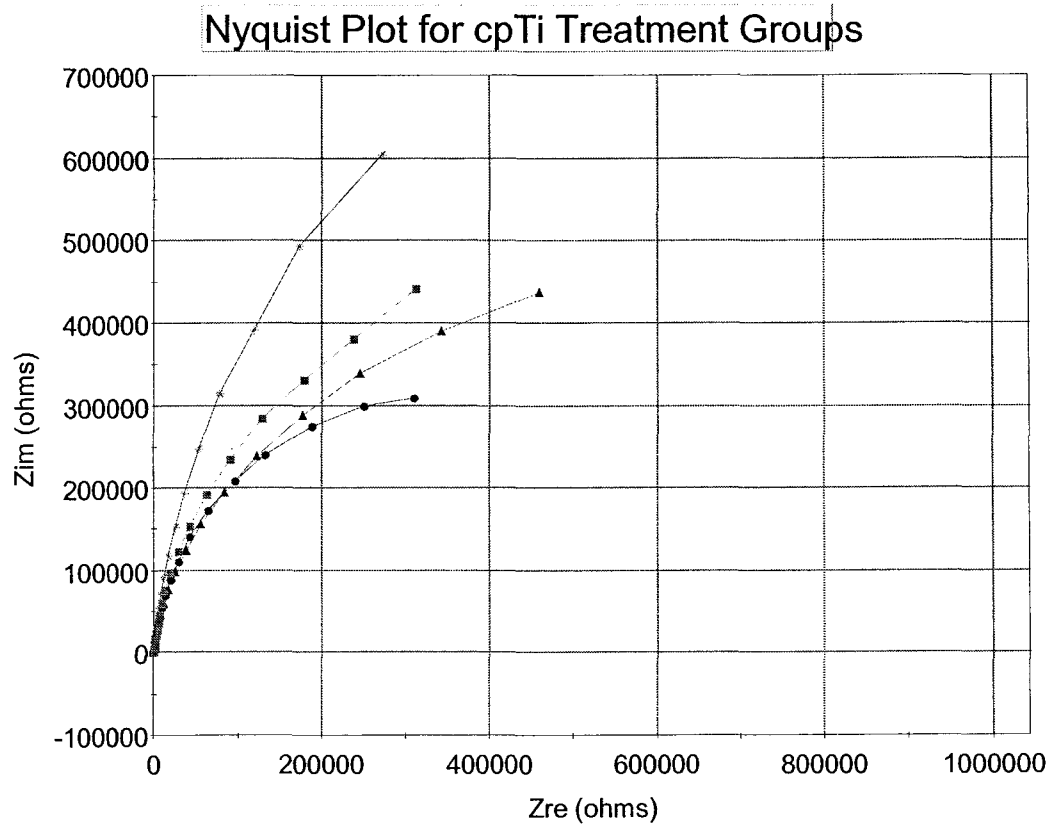


Figure 1. Nyquist plot for cpTi treatment groups. Treatment groups included non-passivated (Clean) and 40%-20°C-15min, -1h, and -2h. Semicircle order from smallest diameter to largest is C < 1 h < 2 h < 15 min.

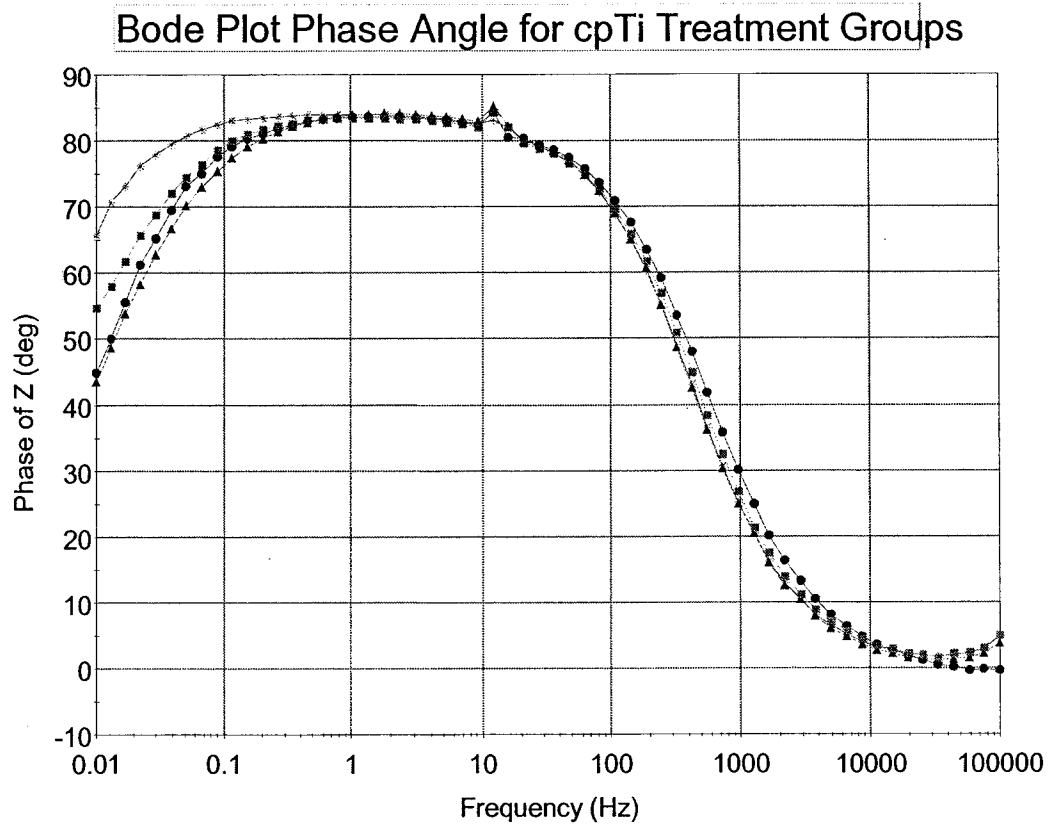


Figure 2. Bode phase angle plot for cpTi treatment groups. Treatment groups included non passivated (Clean) and 40%-20°C-15min, -1h, and -2h. Spectra order from least capacitive to greatest capacitive response is C < 1 h < 2 h < 15 min.

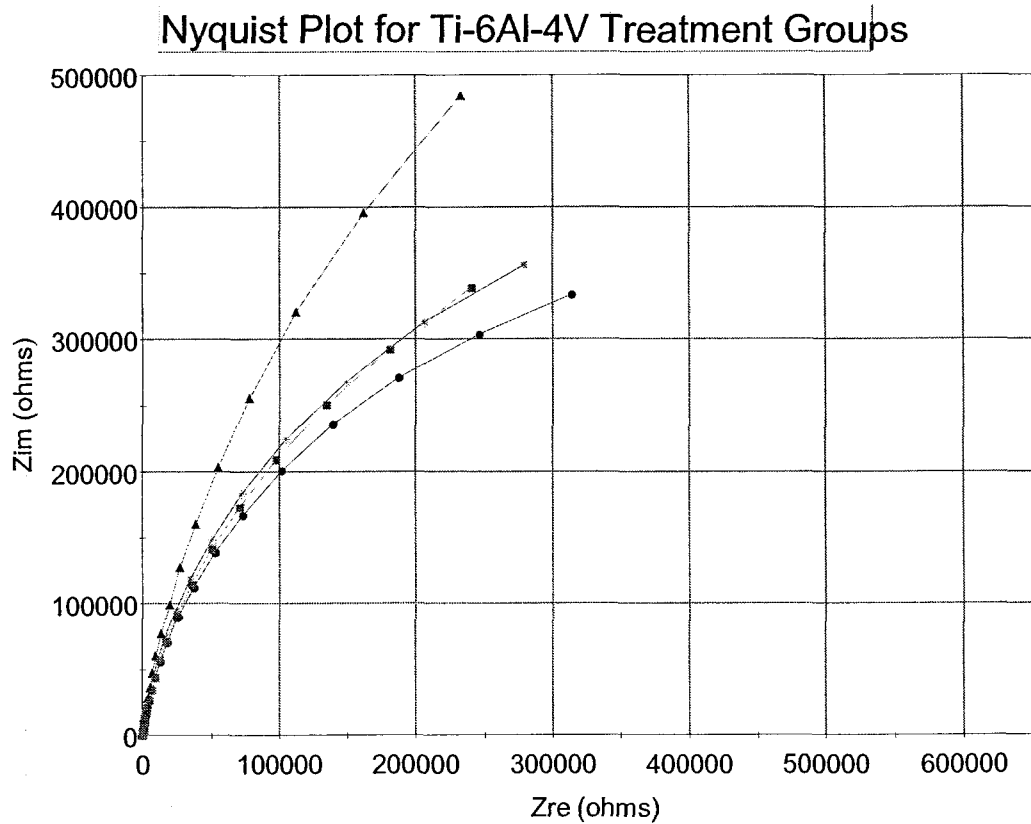


Figure 3. Nyquist plot for Ti-6Al-4V treatment groups. Treatment groups included non-passivated (Clean) and 40%-20°C-15min, -1h, and -2h. Semicircle order from smallest diameter to largest is C < 15 min < 2 h < 1 h.

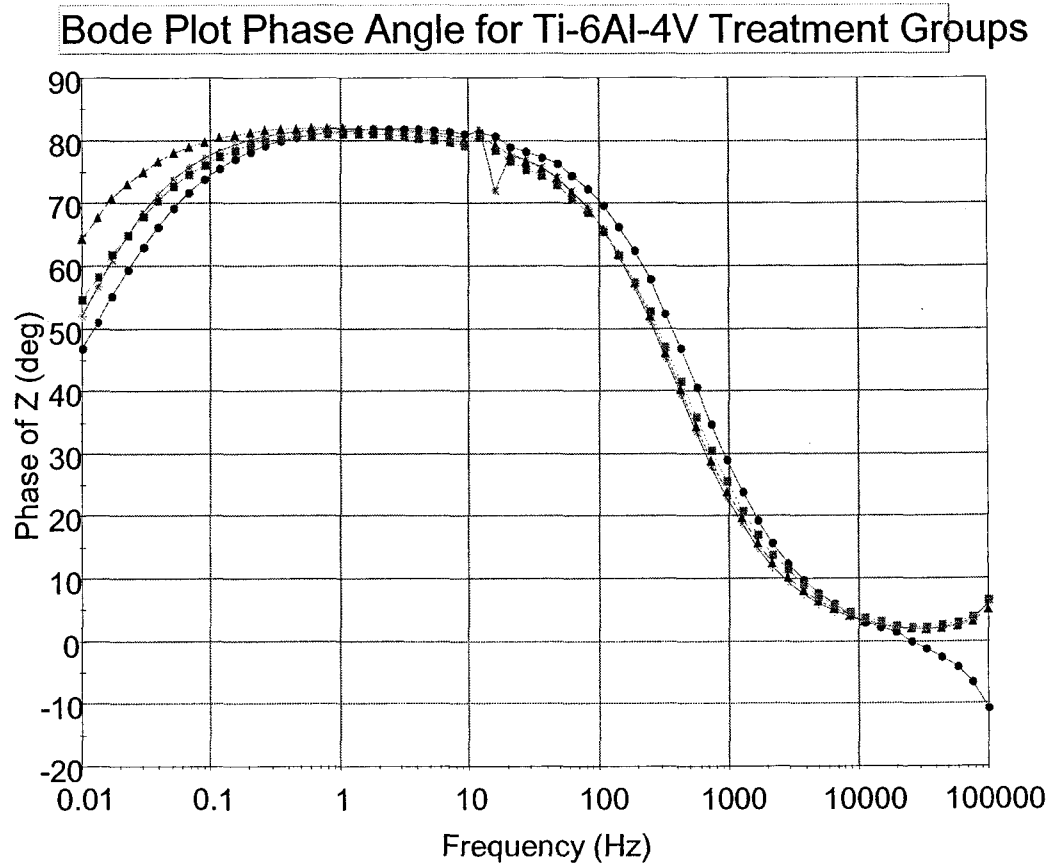


Figure 4. Bode phase angle plot for Ti-6Al-4V treatment groups. Treatment groups included non passivated (Clean) and 40%-20°C-15min, -1h, and -2h. Spectra order from least capacitive to greatest capacitive response is C < 15 min < 2 h < 1 h.

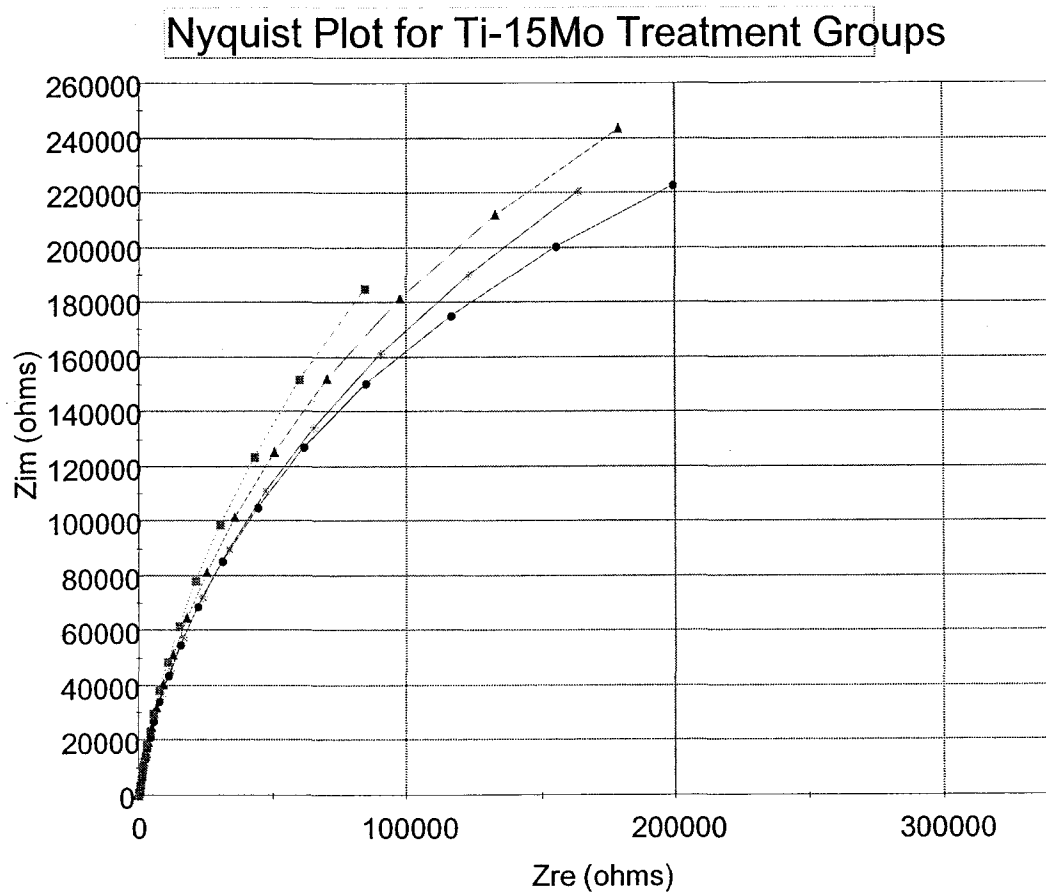


Figure 5. Nyquist plot for Ti-15Mo treatment groups. Treatment groups included non-passivated (Clean) and 40%-20°C-15min, -1h, and -2h. Semicircle order from smallest diameter to largest is C < 15 min < 1 h < 2 h.

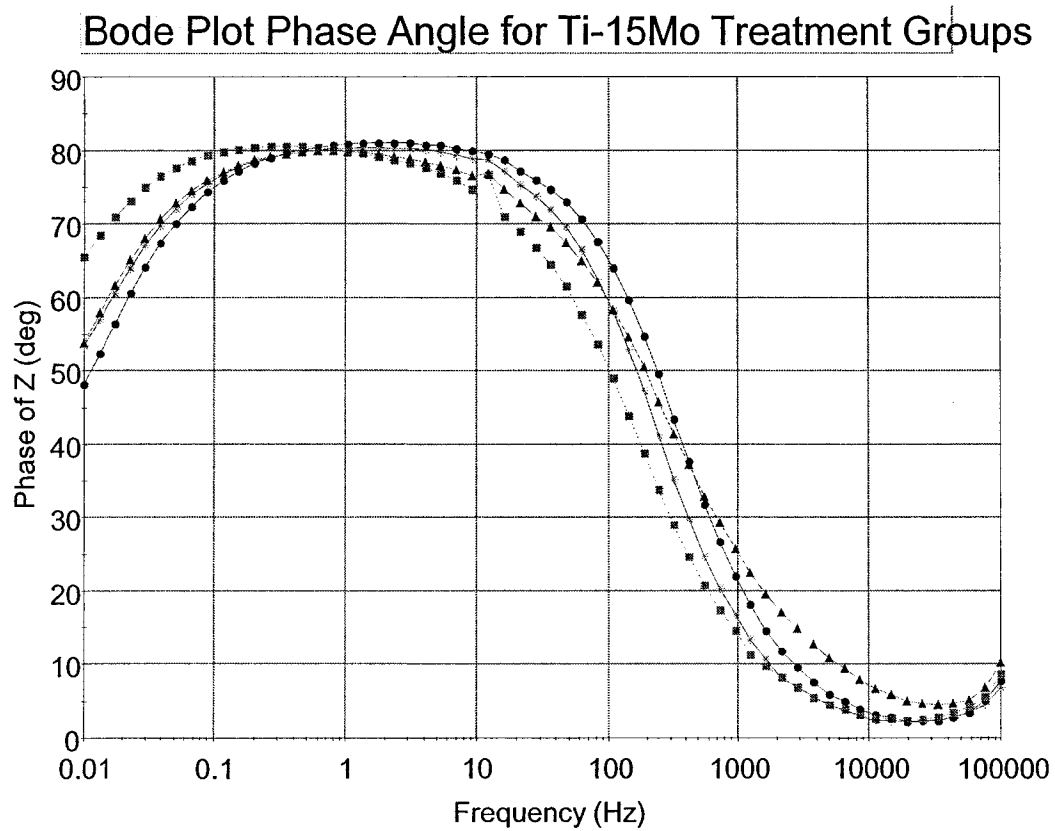


Figure 6. Bode phase angle plot for Ti-15Mo treatment groups. Treatment groups included non passivated (Clean) and 40%-20°C-15min, -1h, and -2h. Spectra order from least capacitive to greatest capacitive response is C < 15 min < 1 h < 2 h.

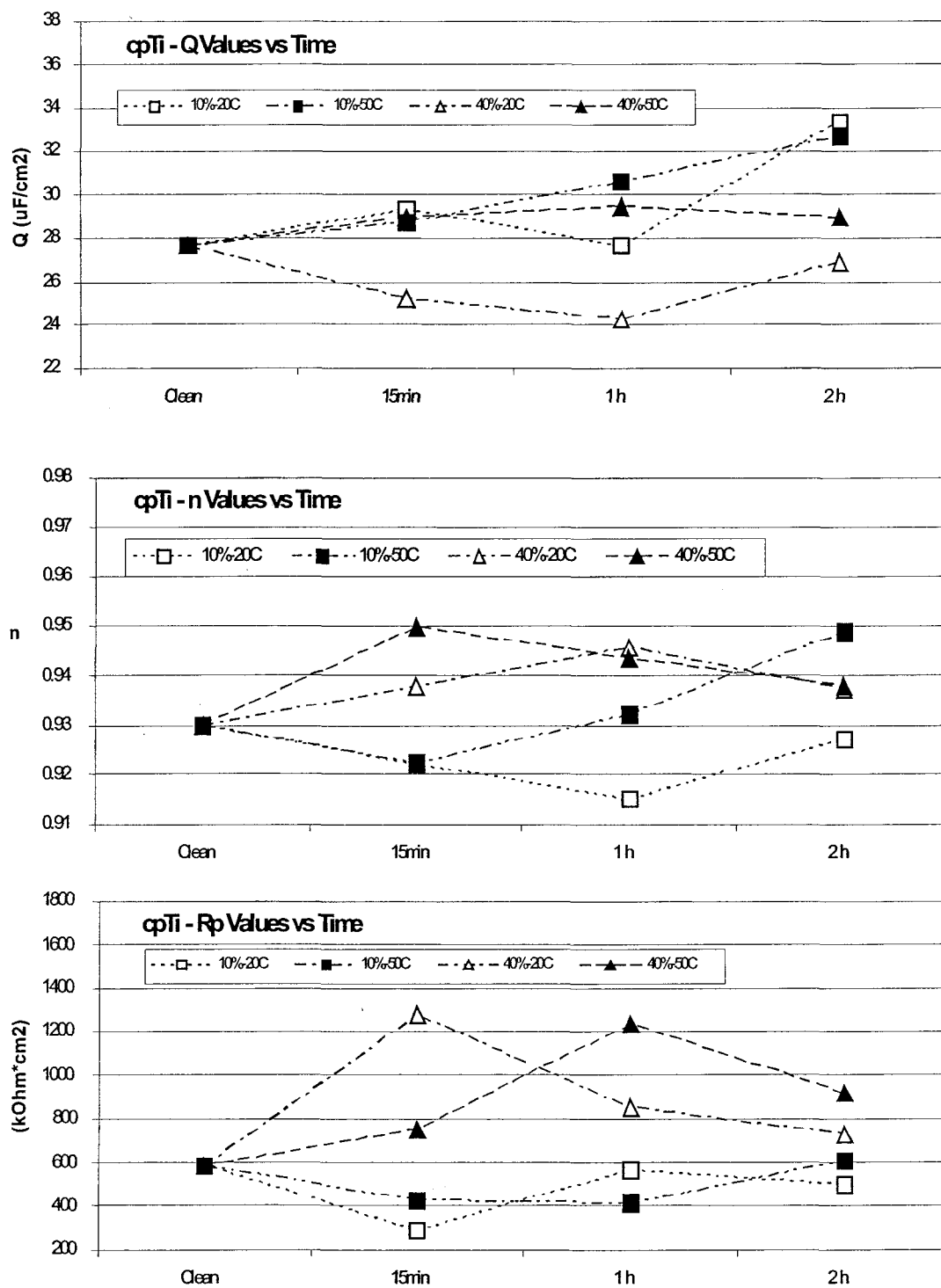


Figure 7. The Q, n, and Rp results for cpTi as a function of passivation time. The groups represent the four concentration and temperature passivation treatments tested in this study. The Clean group was used as the time zero group.

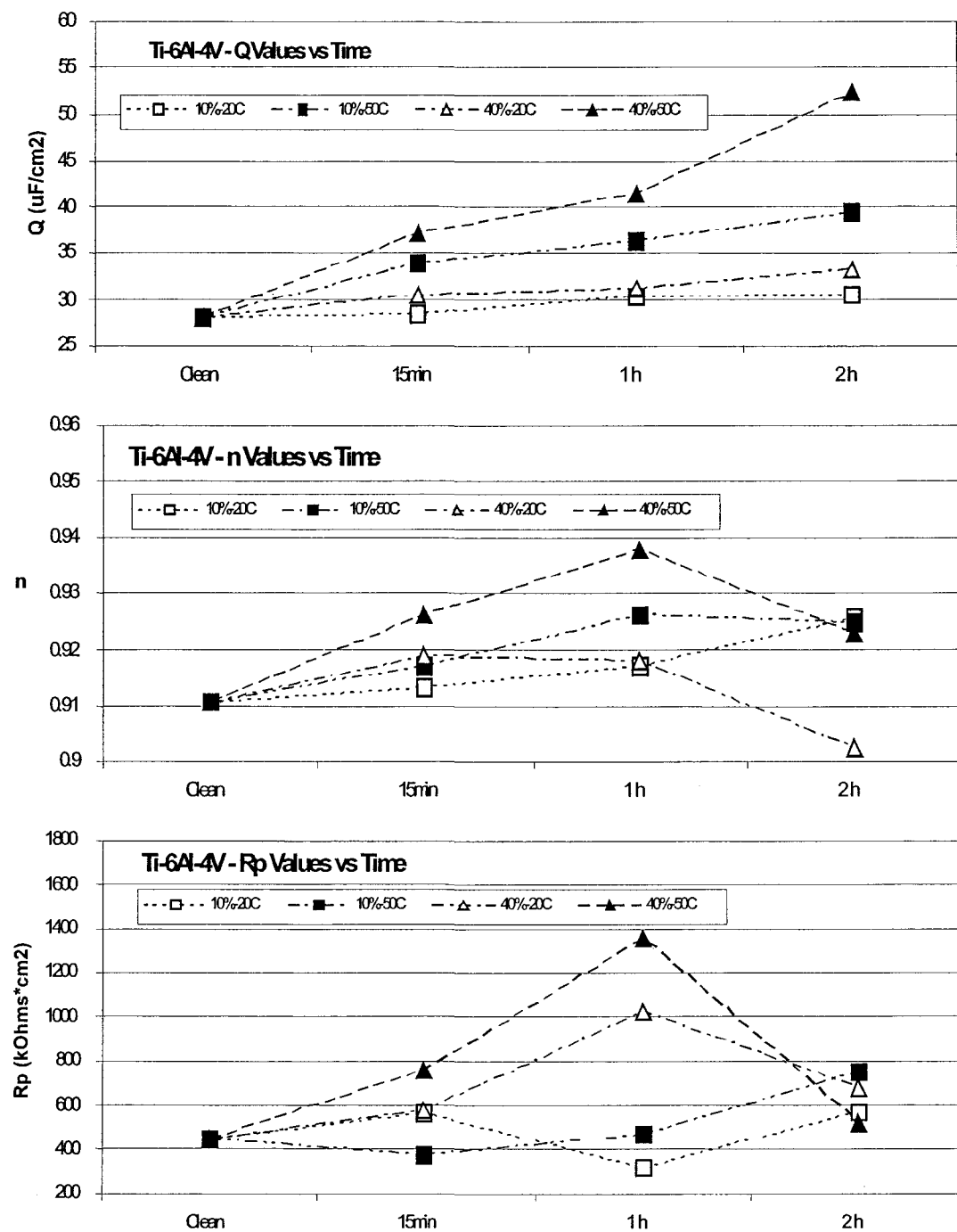


Figure 8. The Q , n , and R_p results for Ti64 as a function of passivation time. The groups represent the four concentration and temperature passivation treatments tested in this study. The Clean group was used as the time zero group.

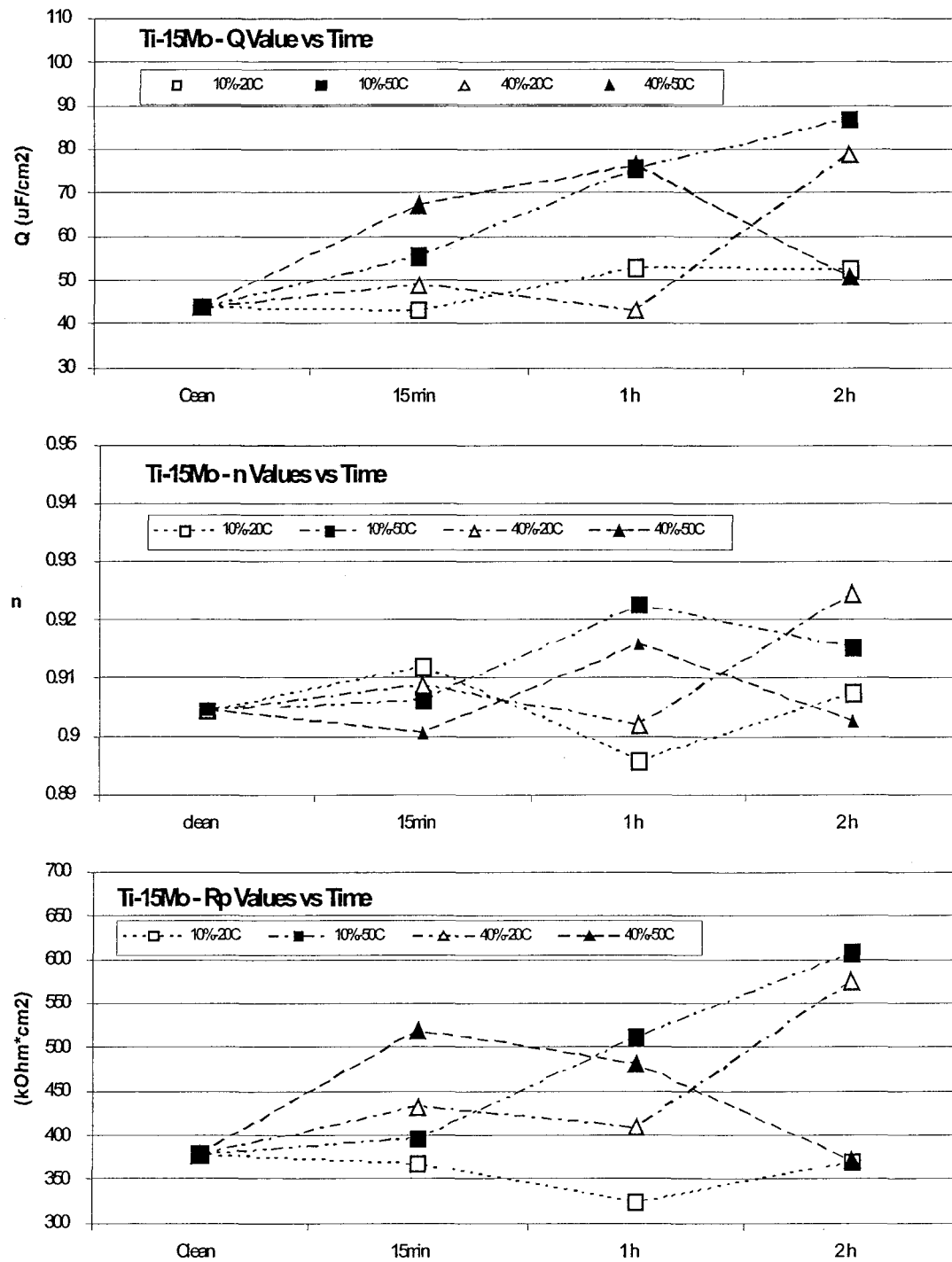


Figure 9. The Q , n , and R_p results for Ti-15Mo as a function of passivation time. The groups represent the four concentration and temperature passivation treatments tested in this study. The Clean group was used as the time zero group.

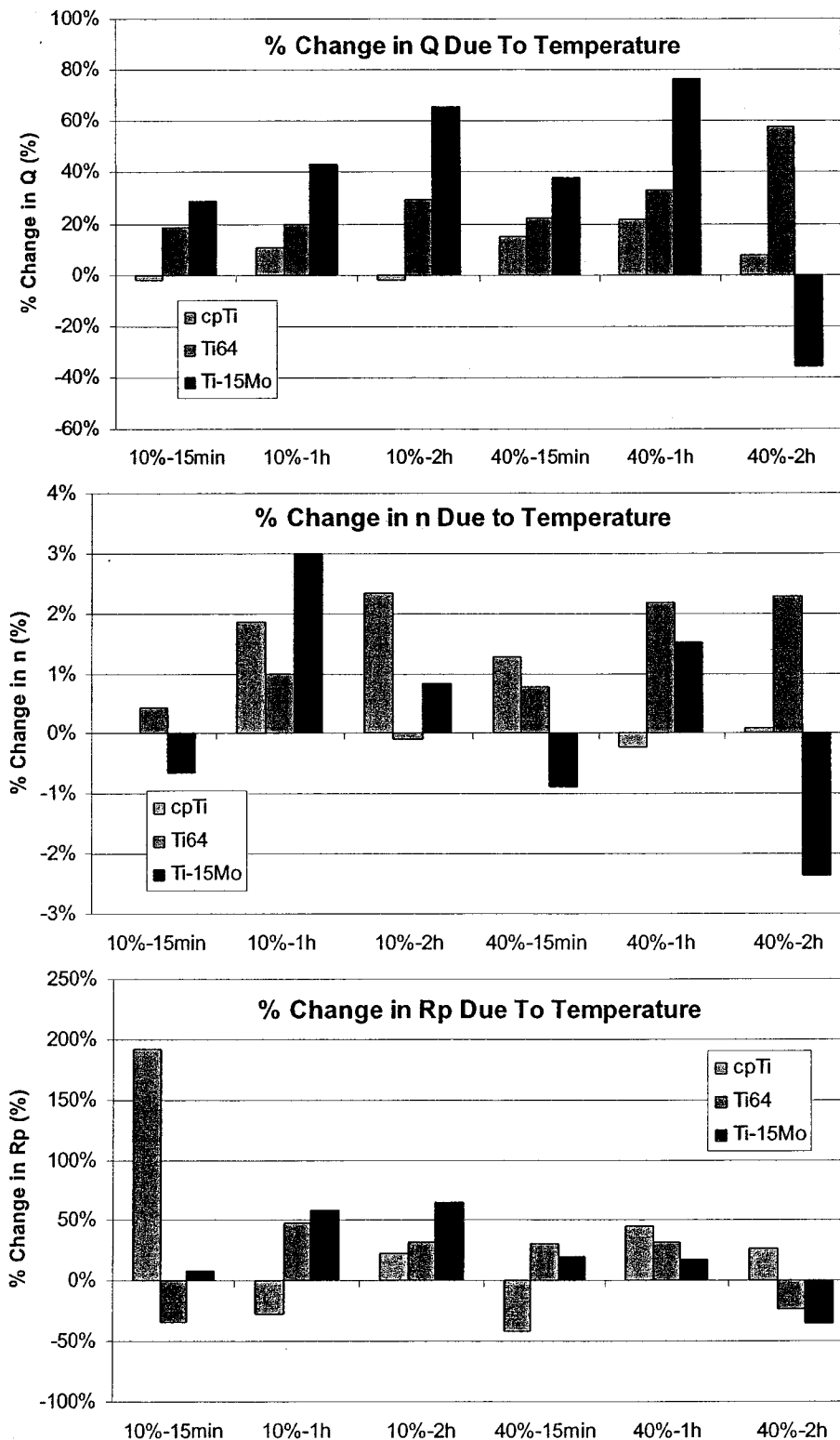


Figure 10. Percentage change between Q, n, and Rp values of groups passivated in 20°C nitric acid and those values of groups passivated in 50°C nitric acid ($n = 3$).

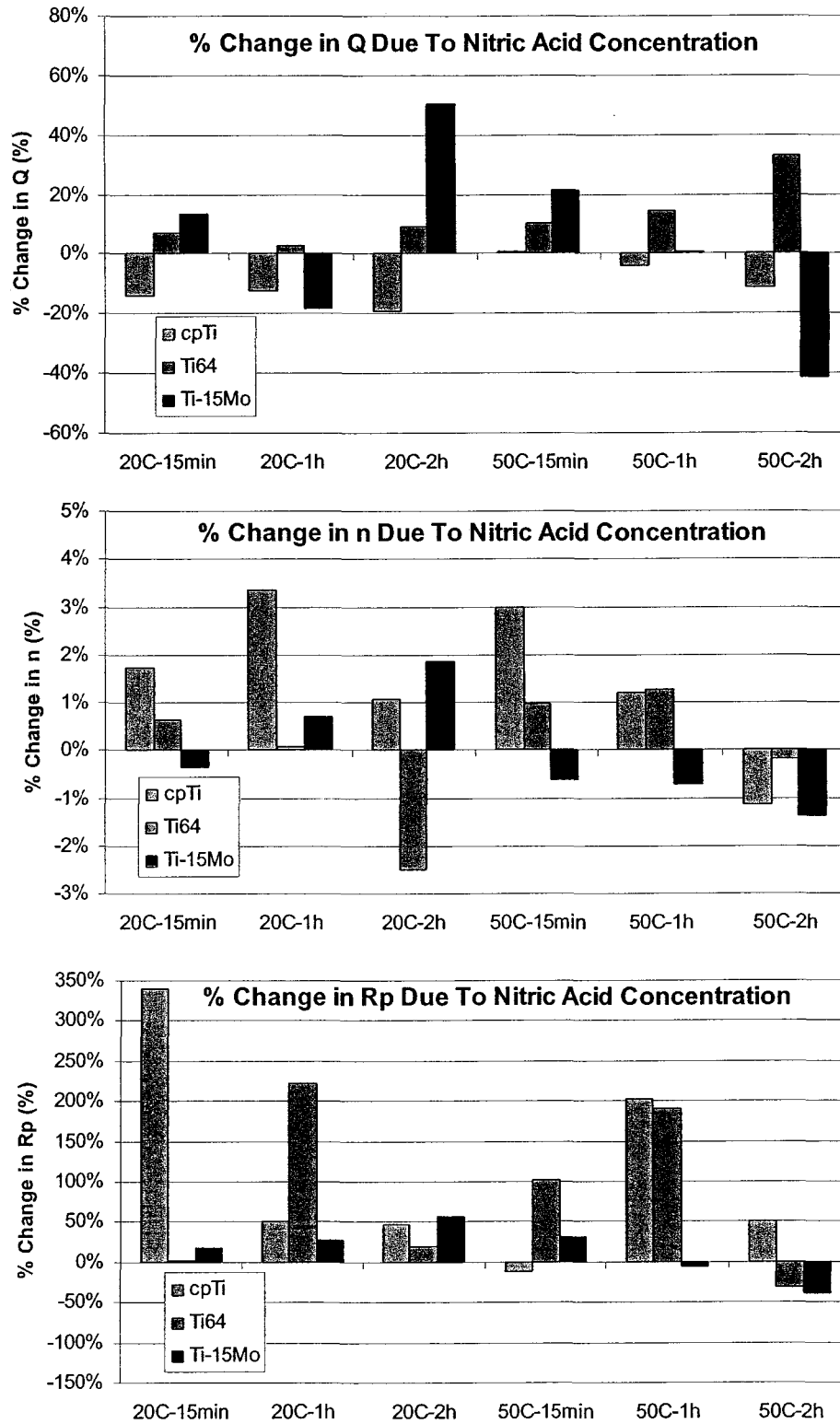


Figure 11. Percentage change between Q , n , and R_p values of groups passivated in 10 % nitric acid and those values of groups passivated in 40 % nitric acid ($n = 3$).

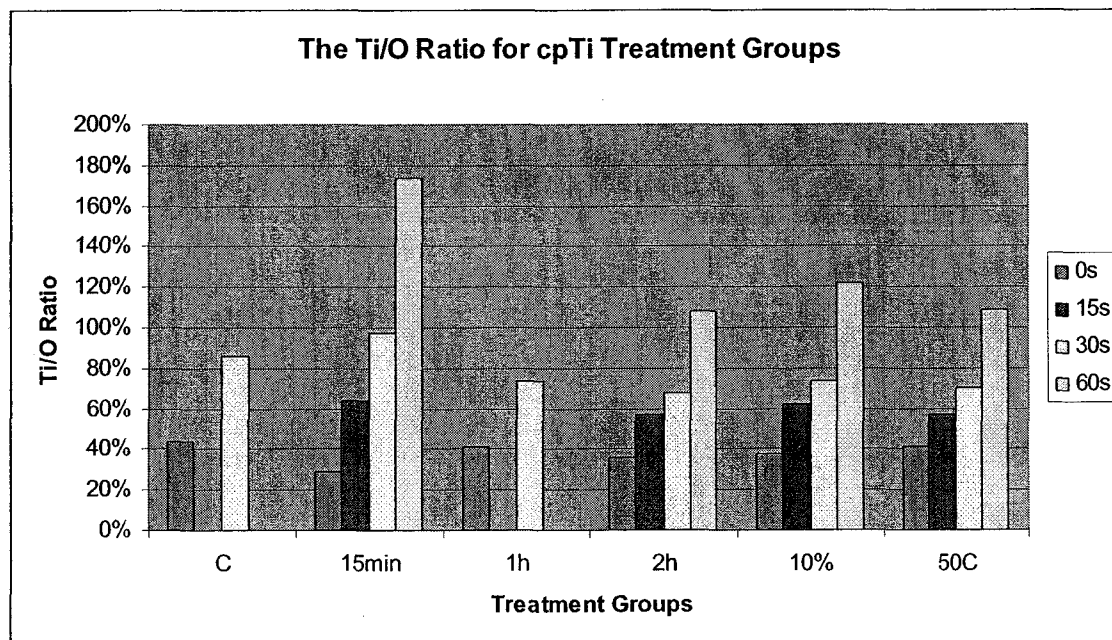


Figure 12. Ti/O ratio results for the different cpTi treatment groups. The graph shows the results for different etch times for each particular treatment group. The Ti/O ratio increases with etch time for all groups. The 15-min group exhibits the largest differences between etch times. C = clean (non passivated), 15-min = 40 % nitric acid at 20°C for 15-min, 1-h = 40 % nitric acid at 20°C for 1-h, 2h = 40 % nitric acid at 20°C for 2-h, 10 % = 10 % nitric acid at 20°C for 1-h, and 50°C = 40% nitric acid at 50°C for 1-h.

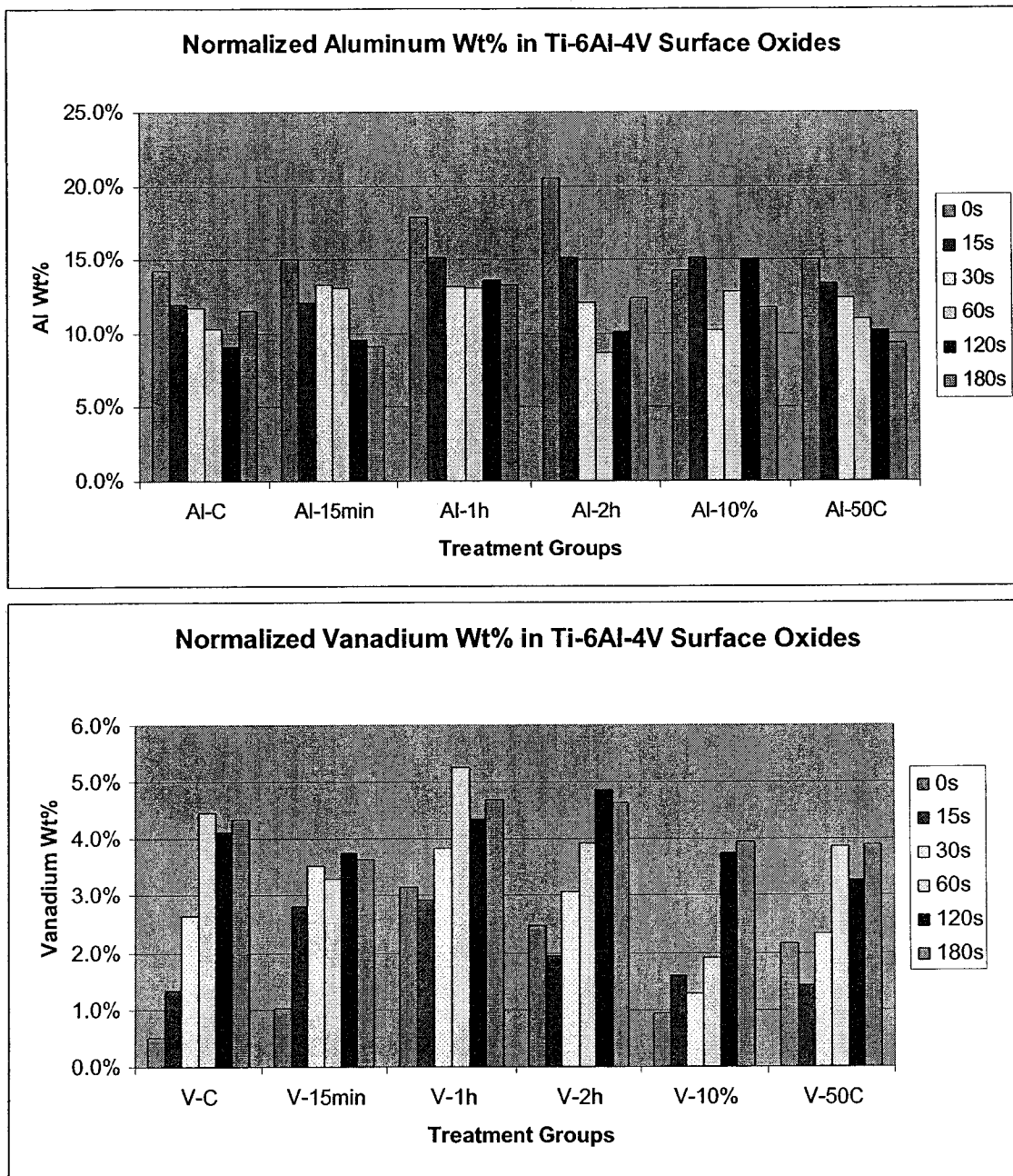


Figure 13. Normalized Al wt% and V wt% results for the different Ti-6Al-4V treatment groups. The graph shows the results for different etch times for each particular treatment group. C = clean (non passivated); 15-min = 40 % nitric acid at 20°C for 15 min, 1-h = 40% nitric acid at 20°C for 1-h, 2-h = 40 % nitric acid at 20°C for 2-h, 10 % = 10 % nitric acid at 20°C for 1-h; and 50°C = 40 % nitric acid at 50°C for 1-h.

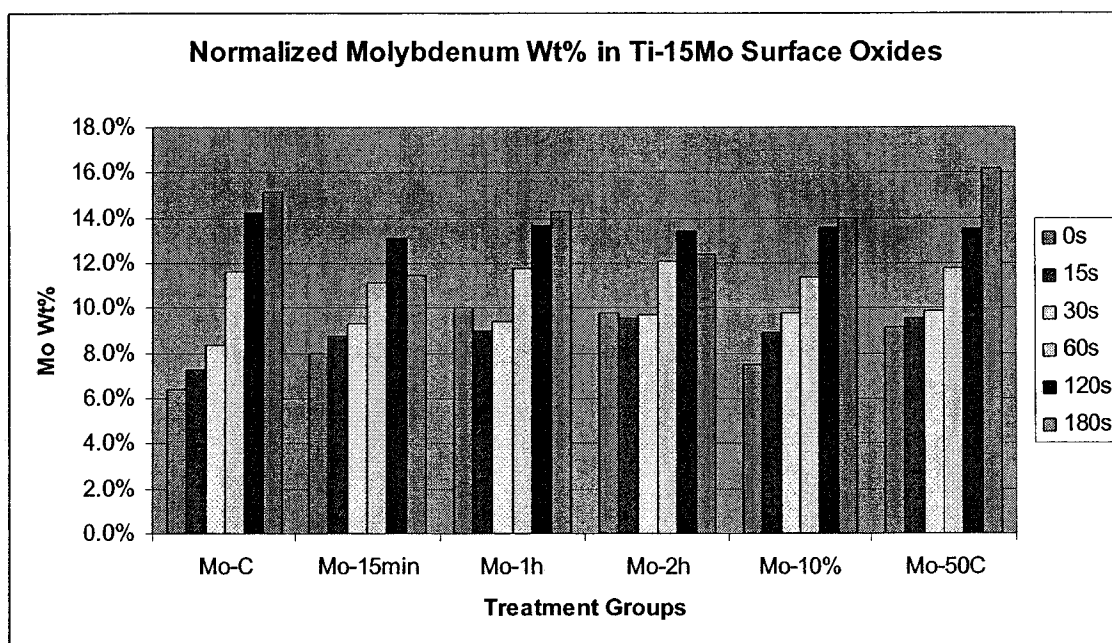


Figure 14. Normalized Mo wt% results for the different Ti-15Mo treatment groups. The graph shows the results for different etch times for each particular treatment group. C = clean (non passivated), 15-min = 40 % nitric acid at 20°C for 15-min, 1-h = 40 % nitric acid at 20°C for 1-h, 2-h = 40 % nitric acid at 20°C for 2-h; 10 % = 10 % nitric acid at 20°C for 1-h, and 50°C = 40 % nitric acid at 50°C for 1-h.

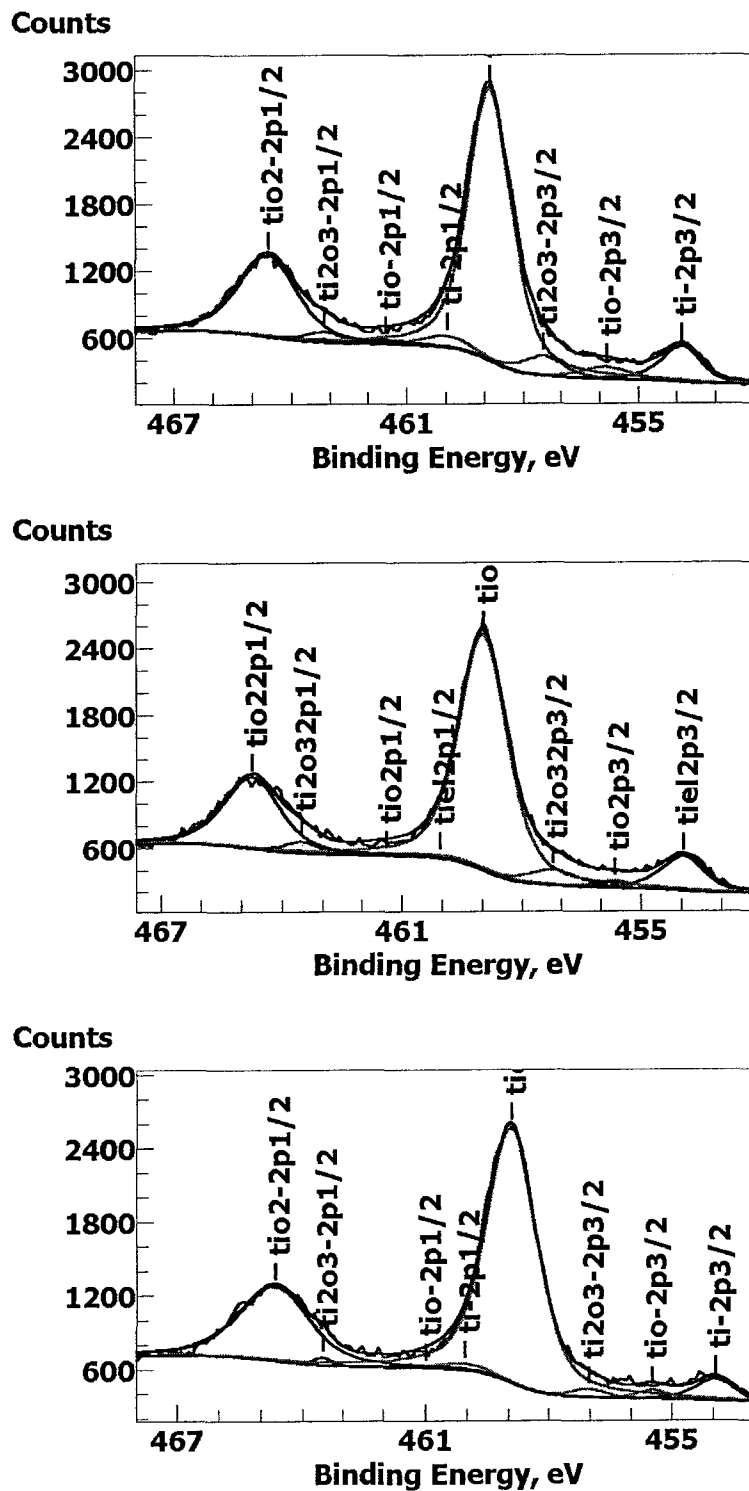


Figure 15. XPS high-resolution Ti 2p spectra for passivated cpTi (top), Ti-6Al-4V (middle), and Ti-15Mo (bottom) samples (40% nitric acid at 20°C for 1 h).

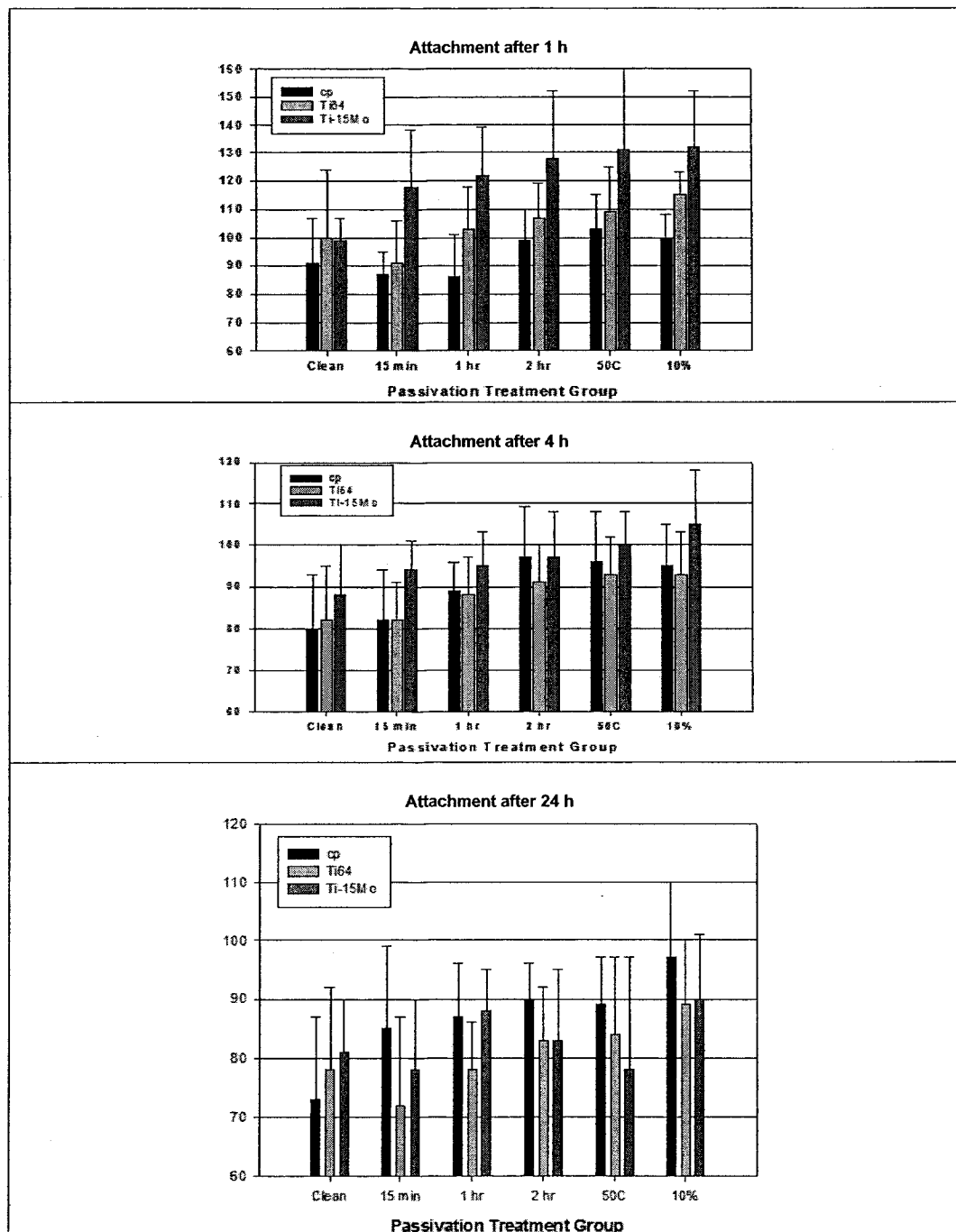


Figure 16. Attachment results after 1, 4, and 24 h of incubation. Results are shown as percentage of control, with the control being results from cells seeded onto blank wells (tissue culture plastic). Passivation treatment groups are as follows: Clean = non-passivated; 15 min, 1 hr, and 2 hr = 40% nitric acid at 20°C for 15 min, 1 h, and 2 h, respectively; 50C = 40% nitric acid at 50°C for 1 h; and 10% = 10% nitric acid at 20°C for 1 h. Bars and error bars represent mean and standard deviation, respectively ($n = 4$).

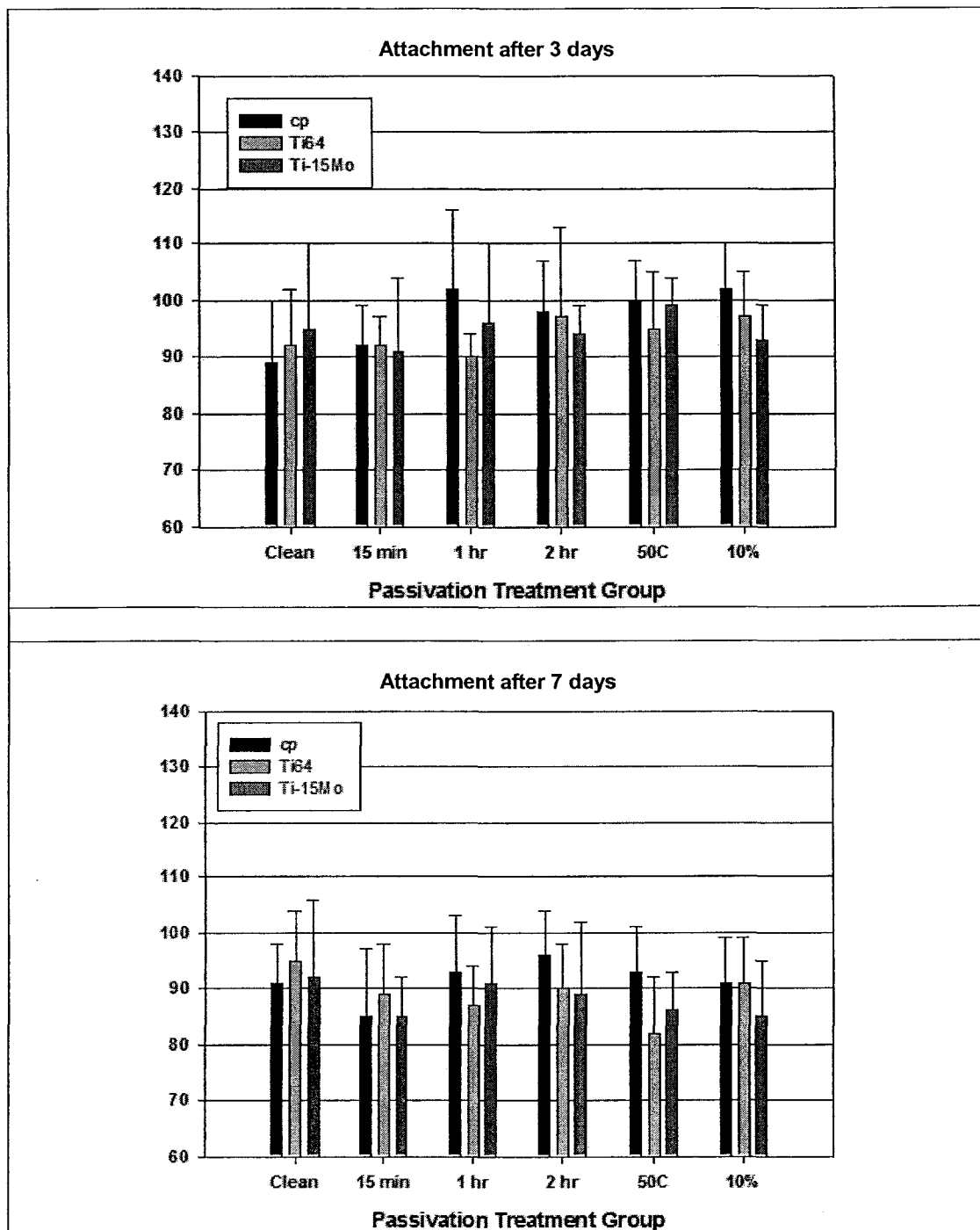


Figure 17. Attachment results after 3 and 7 days of incubation. Results are shown as percentage of control, with the control being results from cells seeded onto blank wells (tissue culture plastic). Passivation treatment groups are as follows: Clean = non-passivated; 15 min, 1 hr, and 2 hr = 40% nitric acid at 20°C for 15 min, 1 h, and 2 h, respectively; 50C = 40% nitric acid at 50°C for 1 h; and 10% = 10% nitric acid at 20°C for 1 h. Bars and error bars represent mean and standard deviation, respectively ($n = 4$).

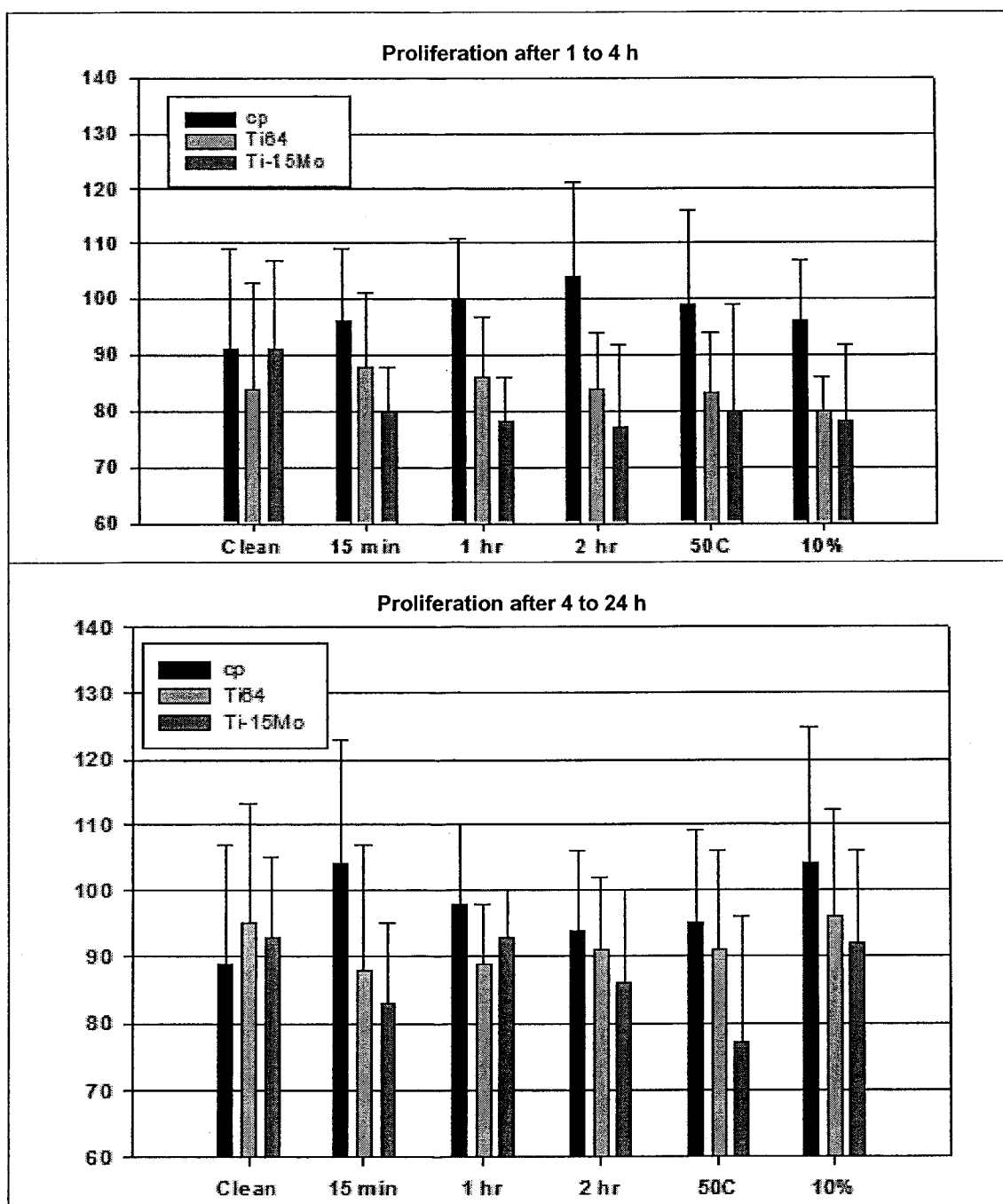


Figure 18. Proliferation results for 1 to 4 h and 4 to 24 h of incubation. Results are shown as percentage of control, with the control being results from cells seeded onto blank wells (tissue culture plastic). Passivation treatment groups are as follows: Clean = non-passivated; 15 min, 1 hr, and 2 hr = 40% nitric acid at 20°C for 15 min, 1 h, and 2 h, respectively; 50C = 40% nitric acid at 50°C for 1 h; and 10% = 10% nitric acid at 20°C for 1 h. Bars and error bars represent mean and standard deviation, respectively ($n =$

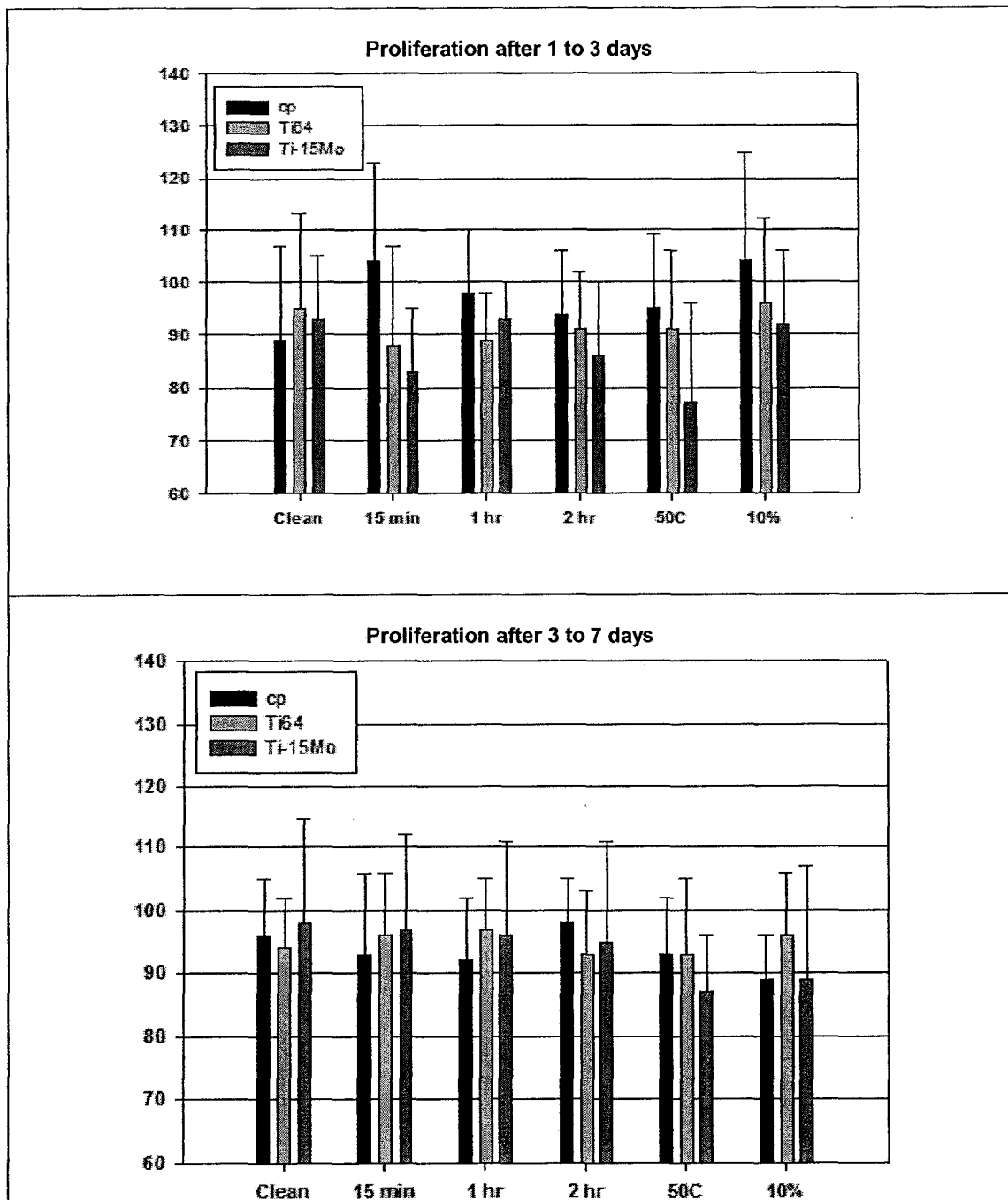


Figure 19. Proliferation results for 1 to 3 days and 3 to 7 days of incubation. Results are shown as percentage of control, with the control being results from cells seeded onto blank wells (tissue culture plastic). Passivation treatment groups are as follows: Clean = non-passivated; 15 min, 1 hr, and 2 hr = 40% nitric acid at 20°C for 15 min, 1 h, and 2 h, respectively; 50C = 40% nitric acid at 50°C for 1 h; and 10% = 10% nitric acid at 20°C for 1 h. Bars and error bars represent mean and standard deviation, respectively ($n = 4$).

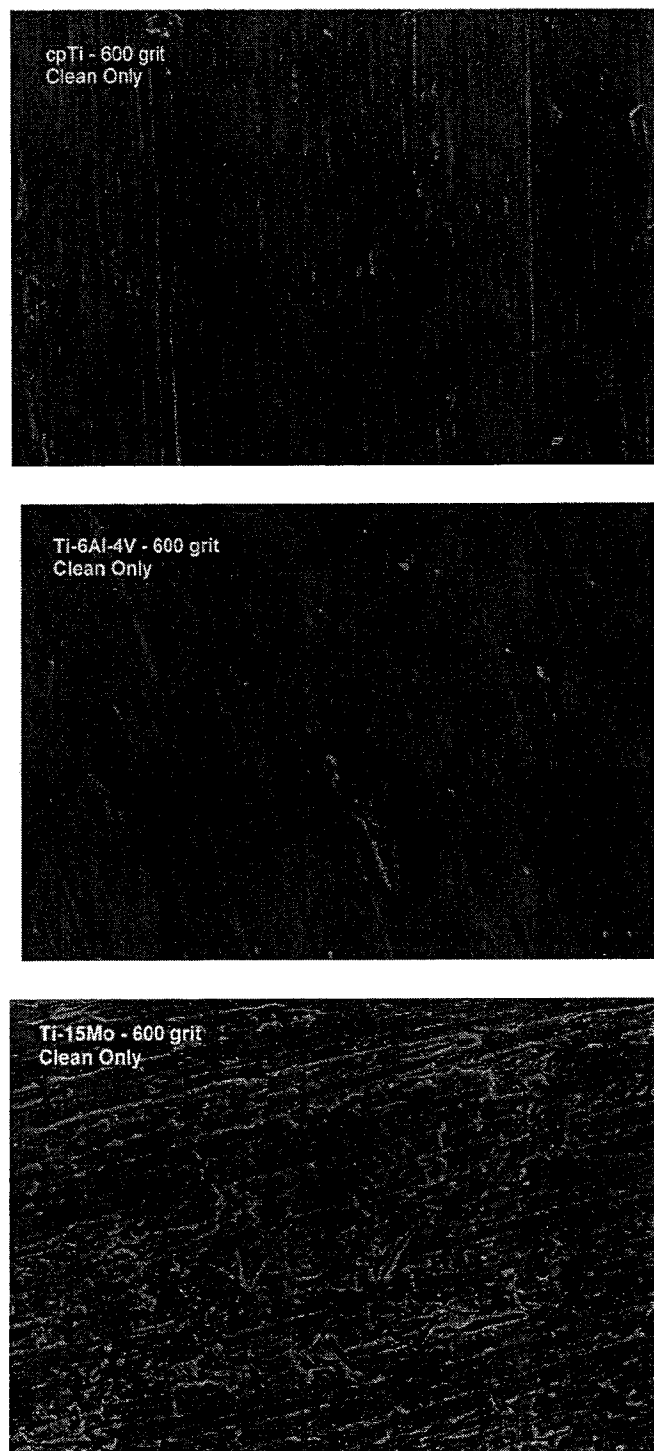


Figure 20. Representative SEM micrographs of cpTi (top), Ti-6Al-4V (middle), and Ti-15Mo (bottom) material with 600-grit finish in the Clean condition (original magnification x1000).

EFFECTS OF NITRIC ACID PASSIVATION PARAMETERS ON TITANIUM
AND TITANIUM ALLOYS RELATED TO CORROSION,
SURFACE CHEMISTRY, AND CELL CULTURE

PART II
EFFECTS OF USING ULTRASONICATION, TITANIUM IONS IN SOLUTION, AND
DIFFERENT SURFACE MORPHOLOGIES

by

DON PETERSEN AND JACK LEMONS

In preparation for *Journal of Biomedical Materials Research*

Format adapted for dissertation

ABSTRACT

Part I of this two-part study found the optimal passivation parameters for titanium and titanium alloys to be 40% nitric acid for 1 h at 50°C. Part II deals with the variables of ultrasonic nitric acid passivation, rougher surface morphologies, and addition of titanium ions to the nitric acid bath.

To facilitate the penetration of nitric acid into small crevices, such as those of beaded implants, some manufacturers use ultrasonic passivation. Adding titanium ions to the nitric acid bath has been shown to affect the surface oxide. This study evaluates these additional parameters' effects on the surface oxide coating.

Commercially pure titanium (cpTi) and two titanium alloys (Ti-6Al-4V and Ti-15Mo) were used in the study. Corrosion properties of the resultant surfaces were determined by using electrochemical impedance spectroscopy (EIS) and potentiodynamic polarization tests. EIS and X-ray photoelectron spectroscopy (XPS) were used to study surface oxide characteristics and chemistry, respectively. Cell culture tests with osteoblast-like cells (SaOS-2) were used to test effects on biocompatibility.

The results showed that, in comparison with static passivation ultrasonic nitric acid passivation resulted in increased capacitance (Q) values and lower Al atomic percentages at the outermost surface of the oxide.

For rougher surfaces, with greater surface areas, electrochemical impedance spectroscopy parameters had higher capacitance values, lower oxide homogeneity values, and lower oxide resistance values, thus accounting for changes seen in corrosion properties. The addition of titanium ions to the nitric acid passivation solutions resulted in minimal

effects on the analyzed surface and corrosion properties, but it did increase the appearance of pit-like features on the surface.

Cell attachment and proliferation results for the different treatment groups were similar and comparable to those of the tissue culture plastic control, indicating good biocompatibility of all the materials regardless of surface treatments.

The presence of molybdenum in Ti-15Mo made it less sensitive to nitric acid passivation in comparison with commercially pure Ti and Ti-6Al-4V.

INTRODUCTION

Nitric acid passivation is a process used to clean metallic implants and improve their corrosion properties.¹ Improvements in the corrosion properties are attributed to an enhanced surface oxide that results from the passivation process.^{2,3} ASTM F 86 is the standard process used today for preparing and cleaning metallic implants.¹

Nitric acid passivation has been shown to improve the corrosion resistance of titanium and titanium alloys in numerous studies.² However, some studies have shown nitric acid passivation of Ti-6Al-4V to increase the release of titanium, aluminum, and vanadium into culture media.⁴⁻⁶ The authors of these studies attributed the increased release of trace elements to a decrease in oxide thickness and an increase in concentration of aluminum ions in the oxide.⁴⁻⁶

The corrosion and dissolution properties of titanium and its alloys can be associated with the composition, thickness, and structure of the surface oxide. The effects of nitric acid passivation on these parameters have been reported previously.⁷⁻¹⁰

The ASTM F86 standard specifies immersion in nitric acid, but many of the nitric acid passivation studies have also used ultrasonication during the passivation process. Ultrasonication is used in the passivation of porously coated implants to eliminate air bubbles and to create a more uniform interaction of the nitric acid with the metal surfaces.⁴ In addition, ultrasonication is known to result in locally high temperatures and pressures on sample surfaces, which can affect chemical reactions. Whillock¹¹ showed that ultrasonication of 304L stainless steel in nitric acid caused earlier passivation in non passive metal and promoted the breakdown of passivity and accelerated corrosion in passive metal. Thus, it seems reasonable to believe that differences in the resultant surface oxide could occur between samples passivated by simple immersion in nitric acid and those treated with ultrasonication in nitric acid.

Another parameter that may affect the nitric acid passivation process is the concentration of titanium ions present in the nitric acid. Studies have shown that an increased concentration of titanium ions in the nitric acid solution reduces the corrosion rate of titanium and titanium alloy samples in nitric acid. The decreased corrosion was attributed to faster growth of the passive oxide and enhanced stability of the passivity of the oxide due to the formation of titanium ions in the nitric acid solutions.¹² However, it is not clear whether the change in the passivation process that led to an improvement in corrosion properties for the material tested in nitric acid will result in a similar improvement when the material is used in an implant application. Furthermore, the effect of increased titanium ions on the passivation process is important when one considers that multiple batches of implants may be treated in a single nitric acid bath. One would expect multiple passivation treatments to increase the amount of titanium ions over time; as a result, the

environment for the first and last batches may be significantly different in terms of the level of titanium ions.

In addition to passivation, the roughness of implant material influences many of the relevant biomaterial properties, including corrosion¹³⁻¹⁶ and biological response.¹⁷⁻²¹ In a previous study by our laboratory²², we found that a similar grinding and polishing procedure (600-grit silicon carbide polish) resulted in markedly different surface morphologies for different materials. Ti-15Mo, a beta titanium alloy, was found to have a much rougher surface after the 600-grit polishing procedure than commercially pure Ti (cpTi) and Ti-6Al-4V had. Results from the study also showed that corrosion, surface oxide, and biological properties were affected by both passivation and roughness, making conclusions about the effects of passivation on the materials more difficult. Thus, in the present study, 60-grit and 600-grit finishes were used to determine how the roughness of the material interacts with the effects of nitric acid passivation on the surface properties.

As in our previous studies²², cpTi and two titanium alloys were used to determine how the presence of the alloying elements might influence the effects of different passivation processes or environments. Alloy elements at the surface of the alloys might be expected to affect how those materials respond to aggressive ultrasonic or concentrated titanium ion environments.

The primary goal of the present study was to determine the effects of ultrasonication and the presence of titanium ions on nitric acid passivation of clinically relevant titanium and titanium alloys, cpTi, Ti-6Al-4V, and Ti-15Mo. An additional goal was to determine how passivation results are affected by the surface roughness of the material.

Surface morphology analysis, corrosion tests, surface chemistry analysis, and *in vitro* cell culture testing were done to achieve the goals of this study. Scanning electron microscopy (SEM) was used to document the surface morphology. Corrosion and oxide properties were determined with electrochemical impedance spectroscopy (EIS) and potentiodynamic polarization tests. The surface oxide chemistry was determined with X-ray photoelectron spectroscopy (XPS). Last, the biological response of SaOS-2 osteoblast-like cells to the materials passivated in various ways was measured using hexosaminidase assay to determine cell attachment and proliferation.

MATERIALS AND METHODS

Materials

The material groups were the same as those used in the Part I paper. These consisted of three groups of titanium metal and alloys, cpTi (ASTM F67), Ti-6Al-4V (ASTM F136), and Ti-15Mo. Metallic disc samples were machined from bar stock of these materials. The disks were 12.7 mm and 6 mm in diameter and 2-3 mm thick. All disks were ground with a series of SiC grit papers to a final grit finish of either 60 grit or 600 grit. The disks were cleaned by rinsing with distilled water, followed by 15-min ultrasonic baths in acetone, distilled water, reagent alcohol, and, finally, distilled water. Samples were then air dried and stored in a desiccator until further surface treatments were performed. Disk samples in this condition were designated as Clean samples.

Nitric acid passivation treatments

In the first test series (reported in Part I), the effects of nitric acid concentration, temperature, and time of immersion were studied. In this second test series, the effects of ultrasonication, the presence of titanium ions, and surface roughness were studied. Table 1 shows the passivating parameters used for this second series. Briefly, two nitric acid concentrations (10 % and 40 % by volume) were again used, but only one immersion time (1-h) and one temperature (20°C) were used. These parameters were used in conjunction with static immersion (Static), ultrasonic immersion (Ultrasonic), or the addition of titanium ions, 160 mg of titanium per liter of solution (160Ti). The nitric acid solutions with 160 mg/L Ti were obtained by preparing a stock titanium solution (10 mg/mL Ti) by dissolving 200 mg of titanium powder in 20 mL of 20% sulfuric acid (H₂SO₄) and subsequently adding 1.6 mL of the stock solution for every 100 mL of nitric acid solution to yield a final nitric acid solution with 160 mg/L Ti.

All nitric acid solutions were made with ACS grade nitric acid and distilled water. All nitric acid concentrations reported here are volume percentages. After passivation treatments, all samples were rinsed with distilled water, ultrasonicated for 5 min in distilled water, air dried, and then stored in a desiccator until testing.

TABLE 1
Passivation Methods and Parameters Used

Group	Nitric Acid Solution (vol%)	Method	Time	Temp.
Static	10% and 40%	Static	1 h	20°C
Ultrasonic	10% and 40%	Ultrasonic	1 h	20°C
160Ti	10% and 40% + 160 mg/L Ti	Static	1 h	20°C
60 grit	40%	Static	1 h	20°C

In the remainder of the paper, the group designations in Table 1 combined with the nitric acid concentrations will be used identify the study groups (e.g., Static-10 % = passivation via static immersion in 10 % nitric acid at 20°C for 1-h). Samples in the Clean condition were used as controls.

Scanning electron microscopy (SEM)

Surface morphology was determined by using SEM analysis. A Philips XL30 scanning electron microscope was used to obtain images at primary beam energies of 15 kV. The SEM images obtained were used to make qualitative surface roughness evaluations.

Electrochemical impedance spectroscopy (EIS)

EIS testing was conducted by using a three-electrode electrochemical cell with graphite rod counter electrodes and a saturated calomel electrode (SCE) as reference. All potentials reported in this study are relative to SCE. The equipment included an impedance response detector (Model 5210 Lock-In Amplifier, EG&G Princeton Applied Research) in combination with a potentiostat/galvanostat system (Model 263A Potentiostat/Galvanostat, EG&G Princeton Applied Research). EIS spectra were obtained at the open-circuit potential. The electrolyte solution was Hanks' Balanced Salt Solution (HBSS) adjusted to $\text{pH } 7.4 \pm 0.1$. Nitrogen gas was used to deaerate the HBSS for 30 min prior to testing and during all testing. All tests were conducted at 37°C. The magnitude of the applied sinusoidal waveform was 10 mV, and the frequency range was 100 kHz to 10 mHz. Computer software was used to collect (PowerSUITE, Princeton Applied Re-

search) and analyze (ZSimpWin, Princeton Applied Research) the EIS data. The impedance behavior of the samples was expressed in Nyquist and Bode plots. All impedance data were fit to appropriate equivalent circuits using computer software (ZSimpWin). Triplicate tests were done for all study groups.

Potentiodynamic polarization testing

Direct-current potentiodynamic polarization testing was performed immediately after EIS testing. After EIS testing, the corrosion cell was transferred and connected to another potentiostat/galvanostat system (Model 273 Potentiostat/Galvanostat, EG&G Princeton Applied Research), which was used to conduct electrochemical potentiodynamic polarization testing. The polarization scan was from 150 mV more active than open-circuit potential to 1200 mV using a scan rate of 1.0 mV/s. As with the EIS tests, nitrogen gas was used to deaerate the HBSS and tests were conducted at 37°C. Tafel extrapolation and Stern-Geary fits (SoftCorr III, EG&G Princeton Applied Research) were used to obtain the corrosion potential (E_{corr}) and the corrosion rate (I_{corr}) at the maximum corrosion potential. The passive current density (I_{pass}) was recorded at a potential of 800 mV. This potential was chosen because it was located within the passive region for all the samples tested. Triplicate tests were done for all study groups.

Activation corrosion testing

Activation corrosion tests were conducted with the same corrosion cell that was used for EIS and potentiodynamic tests: a three-electrode electrochemical cell with graphite rod counter electrodes and a SCE as reference. To achieve sample activation

(i.e., an actively corroding sample) a 3-M sulfuric acid (H_2SO_4) solution at 37°C was used. The corrosion potential was recorded over time with a potentiostat/galvanostat system (Model 273 Potentiostat/Galvanostat, EG&G Princeton Applied Research) until the specimen began to actively corrode. The activation time was taken to be the time at which the corrosion potential had reached the activation potential. Tests were done in triplicate.

X-ray photoelectron spectroscopy (XPS)

Chemical analysis of the surface oxide was done with XPS. A Kratos Axis 165 electron spectrometer using a 165-mm mean radius concentric hemispherical analyzer operating in fixed analyzer transmission mode at pass energy of 160 eV was used for the XPS analysis. Typical sampling depth of analysis was about 3 nm from the surface. The analyzed area was approximately 0.8 mm x 0.2 mm, and the chamber pressure during XPS was 1×10^{-9} torr. Low-energy electrons from an integral charge neutralizer system in the Axis 165 compensated for sample charging during XPS. The binding energy scale was referenced to the adventitious carbon C 1s at 285.0 eV. For all samples, initial survey spectra were obtained, followed by high-resolution spectra for C 1s, O 1s, N 1s, and Ti 2p. Additional high-resolution spectra obtained were Al 2p and V 2p for the Ti-6Al-4V samples and Mo 3d for the Ti-15Mo samples. In addition, depth profile analysis of the oxide was done with argon ion etching for specified times. Relative atomic concentrations for all identified elements were quantified from the high-resolution spectra data using system software. Finally, a curve-fitting program was used to differentiate and quantify the different titanium oxide states, as well as metallic titanium.

Cell culture

The following cell culture methods were used to evaluate the biological compatibility of the titanium materials with different nitric acid passivation treatments. Biological response to the different sample groups was determined by using SaOS-2 osteosarcoma cells. SaOS-2 cells were cultured in complete media consisting of McCoy's modified medium, 10% fetal bovine serum (FBS), amphotericin B (500 µg/500 mL), and gentamicin sulfate (5 mg/500 mL). The cells were incubated in humidified 5% CO₂ air atmosphere at 37°C, nurtured every 2-3 days until confluence, and then split at a ratio of 1:4. The cells were detached in the media flasks by incubating with trypsin-EDTA at 37°C and the reaction stopped by adding complete media to the flask.

Cell attachment and proliferation assays

For the experiments, sample disks were placed tightly into the wells of 96-well tissue culture plates. Disk samples were sterilized prior to testing by soaking in 100% ethanol for 1 h, followed by repeated washing (3x) with sterile filtered phosphate-buffered saline (PBS; 0.2 µm filtered) and overnight incubation with sterile PBS (37°C, 5% CO₂). Cell suspensions were prepared and cells were seeded onto disks at a density of 2×10^4 cells per well. After seeding of the wells, the culture plates were incubated for 1 h, 4 h, and 24 h in complete media for attachment assays and for 1 day, 3 days, and 7 days for proliferation assays. After incubation, the disks were washed with PBS two times to remove non adherent cells. Adherent cells were quantified by using the hexosaminidase assay.²³ Blank wells were used as controls. Three samples from each group were used in quadruplicate experiments.

RESULTS

Scanning electron microscopy (SEM)

SEM images were taken to compare the surface morphologies of the different study groups. Figures 1 to 3 contain representative SEM micrographs of cpTi, Ti-6Al-4V, and Ti-15Mo samples, respectively. Each figure has micrographs of samples with 60- and 600-grit finishes in the Clean condition. Gross qualitative analysis of the surfaces indicates a significant difference in surface morphologies between the 60- and 600-grit finishes for all three material groups. Figures 1 and 2 show the 600-grit surfaces of the cpTi and Ti-6Al-4V materials to be notably smoother and more uniform than the 60-grit surfaces are. Conversely, Figure 3 shows the 600-grit surface of the Ti-15Mo sample to be covered with numerous small, island-like surface features; however the 60-grit surface is shown to have larger but less numerous island-like features.

Comparisons between material groups showed all the 60-grit finishes to be similar, although the grooves for the Ti-6Al-4V material appeared more distinct with fewer “smeared metal” features when compared with the grooves of the cpTi and Ti-15Mo materials.

Comparisons between the treatment groups within each material group showed the groups passivated in the presence of 160 mg Ti/L to exhibit pit-like features. Figure 4 shows SEM micrographs for cpTi and Ti-15Mo materials passivated with the addition of 160 mg Ti/L. SEM analysis of the other treatment groups, including non passivated surfaces, also showed pit-like features; however, the pit-like features were more prevalent and tended to be larger on the 160Ti surfaces. This difference appeared to be more preva-

lent for the cpTi material than for the Ti-6Al-4V and Ti-15Mo materials. Differences between the other treatment groups, excluding the 160Ti groups, were minimal.

EIS results

EIS Nyquist and Bode plots

EIS spectra in the form of Nyquist and Bode plots were analyzed to qualitatively determine differences in the impedance and capacitive behavior of the samples due to the different passivation methodologies. All of the Nyquist plots exhibited incomplete semi-circles, consistent with a highly capacitive surface. The Bode plots also displayed spectra consistent with capacitive behavior. The Bode plots typically had maximum phase angles near -90° , which occurred over a range of frequencies; the impedance plots (log impedance vs. log frequency) showed a linear variation with a slope near -1 over much of the frequency range.

However, differences between some of the spectra were evident. The spectra of some of the Ultrasonic and 160Ti groups exhibited two maximum phase angles, unlike the Static groups, which all showed a single maximum phase angle. Spectra containing two maximum phase angles are indicative of a dual-layer oxide, typically a dense inner oxide covered by a porous outer oxide. Figure 5 shows examples of spectra exhibiting two-phase maximums Ti-6Al-4V groups.

Comparisons of the different treatment groups (Static, Ultrasonic, and 160Ti) within a particular material group showed cpTi and Ti-15Mo treatment groups to have similar trends, with the highest capacitive behavior shown by the 160Ti groups, followed by the Ultrasonic and then the Static groups. The Ti-6Al-4V treatment groups showed a

slightly different ranking, with the Static and Ultrasonic groups having slightly better capacitive behavior than the 160Ti groups had. Comparison by nitric acid concentration showed better capacitive behavior for all the 40 % nitric acid groups than for the 10 % groups. Comparisons of the different material groups within particular treatments generally showed cpTi to have the best capacitive behavior, followed by Ti-6Al-4V and then Ti-15Mo.

Comparisons between the EIS spectra for 60- and 600-grit samples showed the 60-grit spectra for cpTi and Ti-6Al-4V samples to have Nyquist plots with smaller semicircles and Bode plots with diminished capacitive behavior than were found for the spectra of similarly treated 600-grit samples. In contrast, the 60-grit samples for the Ti-15Mo material had larger Nyquist semicircles and Bode plots with extended capacitive regions when compared with the 600-grit samples. All 60-grit spectra showed only one maximum phase angle, indicating a single time constant, except the 60-grit samples for Ti-15Mo, which had some spectra with two maximum phase angles. Passivated 60-grit samples for each material group exhibited spectra consistent with increased impedance and capacitive behavior.

EIS parameters

The electrochemical reactions at the surface interface are analogous to the behavior of an electronic circuit consisting of a specific combination of resistors and capacitors; thus, the electrochemical system can be described in terms of an equivalent electrical circuit (EEC). In the EEC, circuit elements such as resistors and capacitors are used to represent electrochemical properties of the metal and the oxide film. In this study, the

phase angle plots exhibited both one and two time constants; therefore, the surface oxide was assumed to consist of either a single layer or a dual layer. To model the single-layer oxide, a simple EEC consisting of a resistor (R_s) in series with a resistor (R_p)-capacitor (C) parallel circuit was used. The EEC for the dual-layer oxide was the same as for the single-layer oxide but with another resistor (R_{por})-capacitor (C_{por}) parallel circuit placed in series with the original RC parallel circuit. The R_s resistor models experimental-system resistance (i.e., resistance due to the electrolyte, reference electrode, and electrical leads of the system). The R_p resistor models the resistance of the single-layer oxide and the inner oxide of the dual-layer model. The R_{por} resistor represents the resistance of the outer oxide in the dual-layer model. The capacitors, C_p and C_{por} , model the capacitance of the inner and outer surface oxides, respectively. However, to account for the non ideal capacitive response of the interface, a constant-phase element (CPE) was used instead of a pure capacitor. The impedance of a CPE is defined as

$$Z(\text{CPE}) = Q \omega^{-n} \text{ with } -1 \leq n \leq 1,$$

where Q is a constant, ω is the angular frequency, $j = \sqrt{-1}$, and n is the CPE power. A value of $n = 1$ represents an ideal capacitor, and the constant parameter Q represents a pure capacitance. The parameter n is related to the non homogeneity of the surface, such as roughness and homogeneity of the oxide. In this paper, Q_p , n_p , and R_p are used to represent the single-layer oxide and the inner layer of the dual-layer oxide. Q_{por} , n_{por} , and R_{por} are used to represent the outer layer of the dual-layer oxide.

Comparison of the experimental data with the theoretical EEC data showed that the curves were comparable, with all chi-square values less than 4×10^{-3} . The results for Q_p , n_p , and R_p are given in Table 2; those for Q_{por} , n_{por} , and R_{por} are given in Table 3.

The “na” results in Table 3 refer to the fact that those groups were fitted by using a single-layer model, so that there were no results for an outer oxide.

In general, the Ultrasonic groups had higher Q_p and n_p results than the Static and 160Ti groups did, with some of the differences being statistically significant. The R_p results showed some of the groups to be sensitive to the concentration, with the 40% nitric acid groups having statistically significant higher R_p results. The results in Table 3 for the outer oxide parameters were indicative of a very thin, porous oxide layer with little to no resistance.

The Q , n , and R_p results for the 60-grit samples are given in Table 4. In addition, the results for the 600-grit samples are included for comparison purposes.

In general, the results for the cpTi and Ti-6Al-4V groups showed higher Q values and lower n and R_p values for the 60-grit samples than for the 600-grit samples. The Ti-15Mo groups showed the 60-grit groups to have lower Q values and higher n values than the 600-grit samples did in both the Clean and passivated conditions. The Ti-15Mo R_p results were mixed. Differences between the 60- and 600-grit groups were statistically significant for the both the Q and n values for the passivated cpTi groups, the Q values for the passivated Ti-6Al-4V groups, and the R_p values for the passivated Ti-15Mo groups.

Potentiodynamic polarization corrosion testing

The potentiodynamic polarization curves for all groups were characteristic of highly passive systems. The I_{pass} results were of the order of 3.3 to 9.1 $\mu\text{A}/\text{cm}^2$.

TABLE 2
Qp, np, and Rp Values for cpTi, Ti-6Al-4V, and Ti-15Mo

Treatment Group	Q ($\mu\text{F}/\text{cm}^2$)	n	Rp ($\text{K}\Omega\cdot\text{cm}^2$)
cpTi Clean Only	27.6 ± 0.7 ^{qz}	0.930 ± 0.002 ^{qrz}	579 ± 109
cpTi-Static-10%	27.6 ± 1.8 ^q	0.915 ± 0.012 ^{qC}	560 ± 268
cpTi-Ultra-10%	35.0 ± 5.9 ^q	0.916 ± 0.007 ^C	455 ± 52 ^C
cpTi-160Ti-10%	30.8 ± 3.9 ^q	0.920 ± 0.008 ^{qr}	739 ± 317
cpTi-Static-40%	24.2 ± 1.0 ^{qz}	0.946 ± 0.007 ^{aqCz}	846 ± 465
cpTi-Ultra-40%	28.9 ± 3.0 ^q	0.936 ± 0.002 ^{bC}	1008 ± 41 ^{Cz}
cpTi-160Ti-40%	26.2 ± 2.1 ^q	0.914 ± 0.007 ^{abz}	598 ± 261
Ti64 Clean Only	28.1 ± 3.4 ^{rz}	0.910 ± 0.005 ^q	443 ± 97
Ti64-Static-10%	30.3 ± 1.7 ^r	0.917 ± 0.005 ^{ar}	316 ± 33
Ti64-Ultra-10%	35.8 ± 0.1 ^{rz}	0.918 ± 0.003 ^b	423 ± 126 ^C
Ti64-160Ti-10%	32.7 ± 2.4 ^q	0.896 ± 0.002 ^{abqC}	837 ± 419
Ti64-Static-40%	31.1 ± 2.2 ^{aq}	0.918 ± 0.001	1020 ± 537
Ti64-Ultra-40%	38.3 ± 1.3 ^{abqz}	0.921 ± 0.014	973 ± 316 ^C
Ti64-160Ti-40%	31.5 ± 1.4 ^{br}	0.912 ± 0.002 ^C	1120 ± 646
Ti15 Clean Only	43.6 ± 2.1 ^z	0.902 ± 0.007 ^r	356 ± 46 ^z
Ti15-Static-10%	52.6 ± 4.1 ^{qrCz}	0.896 ± 0.005 ^{qr}	323 ± 43
Ti15-Ultra-10%	61.2 ± 5.3 ^{qrz}	0.907 ± 0.002	384 ± 78
Ti15-160Ti-10%	57.5 ± 11.0 ^{qr}	0.905 ± 0.010 ^r	350 ± 42 ^C
Ti15-Static-40%	43.1 ± 2.4 ^{aCq}	0.902 ± 0.007 ^q	409 ± 79
Ti15-Ultra-40%	68.1 ± 3.4 ^{abqz}	0.915 ± 0.056	561 ± 255
Ti15-160Ti-40%	45.5 ± 4.5 ^{bqr}	0.904 ± 0.007	692 ± 80 ^{Cz}

The values are the mean ± standard deviation (n = 3).

Statistically significant differences are denoted with superscripts, which correspond to specific comparisons.

Results with the same superscripts are significantly different ($p < 0.05$).

z superscript denotes differences between Clean Only result and passivated groups (t-test, $p < 0.05$).

ab superscripts denote differences due to passivation treatment only (one-way ANOVA, $p < 0.05$).

qr superscripts denote differences due to materials within same passivation treatment (one-way ANOVA, $p < 0.05$).

C superscripts denote differences due to concentration of passivation only (t-test, $p < 0.05$).

TABLE 3
Qpor, npor, and Rpor Values for cpTi, Ti-6Al-4V, and Ti-15Mo

Treatment Group	Qpor ($\mu\text{F}/\text{cm}^2$)	npor	Rpor ($\Omega\cdot\text{cm}^2$)
cpTi Clean Only	na	na	na
cpTi-Static-10%	na	na	na
cpTi-Ultra-10%	na	na	na
cpTi-160Ti-10%	1671 \pm 2268	0.545 \pm 0.173	0 \pm 0
cpTi-Static-40%	na	na	na
cpTi-Ultra-40%	2851 \pm 1589	0.310 \pm 0.140	0 \pm 0
cpTi-160Ti-40%	458 \pm 328	0.588 \pm 0.052	0 \pm 0
Ti64 Clean Only	na	na	na
Ti64-Static-10%	na	na	na
Ti64-Ultra-10%	1216 \pm 1875	0.408 \pm 0.124	3 \pm 6
Ti64-160Ti-10%	645 \pm 961	0.579 \pm 0.114	0 \pm 0
Ti64-Static-40%	na	na	na
Ti64-Ultra-40%	670 \pm 734	0.610 \pm 0.040	0 \pm 0
Ti64-160Ti-40%	3074 \pm 1114	0.522 \pm 0.057	0 \pm 0
Ti15 Clean Only	na	na	na
Ti15-Static-10%	na	na	na
Ti15-Ultra-10%	1022 \pm 1164	0.478 \pm 0.214	0 \pm 0
Ti15-160Ti-10%	2880 \pm 2458	0.542 \pm 0.116	2 \pm 2
Ti15-Static-40%	na	na	na
Ti15-Ultra-40%	54 \pm 13	0.683 \pm 0.275	4 \pm 8
Ti15-160Ti-40%	1996 \pm 341	0.565 \pm 0.013	0 \pm 0

Values are mean \pm standard deviation ($n = 3$).

“na” indicates that the group was fitted by using a single-layer model.

No statistical analysis was performed because not all groups were modeled as dual-layer oxide.

TABLE 4
Q, n, and Rp Results for 60- and 600-Grit Groups

Treatment Group	Q ($\mu\text{F}/\text{cm}^2$)	n	Rp ($\text{K}\Omega\cdot\text{cm}^2$)
cpTi-60-Clean	31.2 \pm 2.7	0.917 \pm 0.011	389 \pm 20
cpTi-600-Clean	27.6 \pm 0.7	0.927 \pm 0.002	517 \pm 101
cpTi-60-Pass	30.2 \pm 0.5*	0.929 \pm 0.008*	648 \pm 423
cpTi-600-Pass	24.2 \pm 1.0*	0.946 \pm 0.007*	846 \pm 465
Ti64-60-Clean	33.6 \pm 4.9	0.892 \pm 0.015	328 \pm 432
Ti64-600-Clean	28.6 \pm 2.1	0.918 \pm 0.001	1020 \pm 537
Ti64-60-Pass	39.6 \pm 1.8*	0.905 \pm 0.010	682 \pm 251
Ti64-600-Pass	31.1 \pm 2.2*	0.918 \pm 0.001	1020 \pm 537
Ti-15Mo-60-Clean	40.5 \pm 8.5	0.890 \pm 0.029	331 \pm 75
Ti-15Mo-600-Clean	43.7 \pm 3.0	0.904 \pm 0.008	377 \pm 39
Ti-15Mo-60-Pass	41.3 \pm 3.9	0.898 \pm 0.004	953 \pm 109*
Ti-15Mo-600-Pass	43.1 \pm 2.4	0.902 \pm 0.007	409 \pm 79*

Results are mean \pm standard deviation ($n = 3$).

Pass = 40% nitric acid at 20°C for 1 h.

* indicates statistically different between different grits within the same material and treatment group (one-way ANOVA, $p < 0.05$).

The low passive currents, typical of a passive system, persisted throughout the experiment; all curves exhibited negative hysteresis, indicating no localized corrosion. The E_{corr} , I_{corr} , and I_{pass} corrosion results for the potentiodynamic polarization tests are given in Table 5.

In general, compared with non passivated sample groups, samples that had been passivated showed better corrosion resistance properties in terms of more noble E_{corr} values and lower I_{corr} and I_{pass} results. Treatment group comparisons within each material group showed no obvious trends. The Ultrasonic groups for both Ti-6Al-4V-40 % and Ti-15Mo-40 % did have statistically significantly more noble E_{corr} results than the

160Ti groups had, and the 160Ti group for cpTi-10% had significantly lower Icorr than the Static and Ultrasonic groups did.

Comparisons between the similarly treated material groups showed all three material groups to exhibit excellent corrosion resistance, with cpTi and Ti-6Al-4V groups having relatively similar corrosion properties, which were slightly better than those of the Ti-15Mo group.

The Ecorr, Icorr, and Ipass results for the 60-grit samples are given in Table 6. As with the EIS results, the results for the 600-grit samples are included for comparison purposes.

The Ecorr results showed no consistent trend as the 60-grit groups were both more and less noble than similarly treated 600-grit groups were. Trends were shown, however, for the Icorr and Ipass results for cpTi and Ti-6Al-4V groups, with the 60-grit groups having slightly higher Icorr and Ipass results than similarly treated 600-grit groups did. For the Ti-15Mo groups, the opposite was shown: the 60-grit groups had lower Icorr and Ipass results than the 600-grit groups had. However, none of the differences due to grit size were statistically significant ($p < 0.05$).

Activation test

The activation test involved placing samples in 3-M sulfuric acid and recording the open-circuit corrosion potential of the sample until an active corrosion potential was obtained. The time it takes the sample to reach the active corrosion potential is taken to be the activation time or breakdown period. The active corrosion potential occurs when

TABLE 5
Ecorr, Icorr, and Ipass Results for cpTi, Ti-6Al-4V, and Ti-15Mo

Treatment Group	Ecorr (mV)	Icorr (nA/cm ²)	Ipass (μA/cm ²)
cpTi Clean Only	-223 ± 52 ^z	56 ± 8	4.60 ± 0.22 ^q
cpTi-Static-10%	-66 ± 152	83 ± 22 ^{abC}	4.15 ± 0.46 ^q
cpTi-Ultra-10%	-256 ± 20 ^C	45 ± 12 ^{aC}	4.40 ± 0.16 ^q
cpTi-160Ti-10%	-243 ± 73	33 ± 19 ^b	4.67 ± 0.63 ^q
cpTi-Static-40%	-83 ± 40 ^z	26 ± 9 ^{zC}	3.81 ± 0.24 ^{qz}
cpTi-Ultra-40%	-38 ± 63 ^{qCz}	17 ± 3 ^{Cz}	3.33 ± 0.43 ^q
cpTi-160Ti-40%	-127 ± 64 ^z	29 ± 31	9.19 ± 9.32
Ti64 Clean Only	-216 ± 57	46 ± 11	4.77 ± 0.41 ^r
Ti64-Static-10%	-160 ± 59	80 ± 54	4.83 ± 0.28 ^r
Ti64-Ultra-10%	-237 ± 4 ^C	62 ± 23	5.02 ± 0.35 ^r
Ti64-160Ti-10%	-264 ± 98	25 ± 17	4.63 ± 0.59 ^r
Ti64-Static-40%	-102 ± 8 ^a	27 ± 24	3.96 ± 0.92 ^r
Ti64-Ultra-40%	-20 ± 27 ^{abrCz}	26 ± 19	3.72 ± 0.36 ^{rz}
Ti64-160Ti-40%	-97 ± 38 ^{bz}	29 ± 21	4.19 ± 0.55
Ti15 Clean Only	-253 ± 23 ^z	70 ± 33	7.26 ± 0.50 ^{qr}
Ti15-Static-10%	-257 ± 41 ^{aC}	62 ± 16	7.68 ± 0.88 ^{qr}
Ti15-Ultra-10%	-238 ± 3 ^{bC}	43 ± 10	8.20 ± 0.53 ^{qr}
Ti15-160Ti-10%	-332 ± 24 ^{abCz}	55 ± 20	8.55 ± 1.07 ^{qr}
Ti15-Static-40%	-124 ± 14 ^{zC}	51 ± 24	6.83 ± 0.63 ^{qr}
Ti15-Ultra-40%	-135 ± 38 ^{qrCz}	35 ± 9	6.63 ± 0.61 ^{qr}
Ti15-160Ti-40%	-154 ± 23 ^C	39 ± 11	7.36 ± 0.42

The values are mean ± standard deviation ($n = 3$).

Statistically significant differences are denoted with superscripts, which correspond to specific comparisons.

Results with the same superscripts are significantly different ($p < 0.05$).

z superscript denotes differences between Clean Only result and passivated groups (t-test, $p < 0.05$).

ab superscripts denote differences due to passivation treatment only (one-way ANOVA, $p < 0.05$).

qr superscripts denote differences due to materials within same passivation treatment (one-way ANOVA, $p < 0.05$).

C superscripts denote differences due to concentration of passivation only (t-test, $p < 0.05$).

TABLE 6
E_{corr}, I_{corr}, and I_{pass} Results for 60- and 600-Grit Groups

Treatment Group	E _{corr} (mV)	I _{corr} (nA/cm ²)	I _{pass} (μA/cm ²)
cpTi-60-Clean	-256 ± 10	58 ± 8	5.16 ± 0.67
cpTi-600-Clean	-223 ± 52	56 ± 23	4.60 ± 0.69
cpTi-60-Pass	-81 ± 38	55 ± 43	4.59 ± 0.60
cpTi-600-Pass	-83 ± 40	26 ± 8	3.81 ± 0.24
Ti64-60-Clean	-54	267	9.33
Ti64-600-Clean	-216 ± 57	46 ± 11	4.77 ± 0.41
Ti64-60-Pass	-62 ± 22	40 ± 20	4.29 ± 0.62
Ti64-600-Pass	-79 ± 8	28 ± 24	2.59 ± 0.92
Ti-15Mo-60-Clean	-275 ± 4	48 ± 11	7.20 ± 1.05
Ti-15Mo-600-Clean	-253 ± 23	70 ± 33	7.26 ± 0.50
Ti-15Mo-60-Pass	-139 ± 29	25 ± 18	5.55 ± 0.39
Ti-15Mo-600-Pass	-124 ± 14	51 ± 24	6.83 ± 0.63

Results are mean ± standard deviation ($n = 3$, except Ti64-60-Clean group, where $n = 1$). Pass = 40% nitric acid at 20°C for 1 h.

the surface oxide has been completely dissolved from the specimen and the specimen is in a state of active dissolution. The activation test is a simple method for assessing the protectiveness of the surface oxide. Figure 6 shows representative activation curves for each of the cpTi and Ti-6Al-4V treatment groups. (The Ti-15Mo groups all had activation times of over 24 h, at which time the experiment was stopped. Thus, Ti-15Mo curves are not included in Figure 6 and are not included in any of the statistical analyses.) The results for the activation times are given in Table 7. For both cpTi and Ti-6Al-4V, the Ultrasonic group had the longest activation time, followed by the Static and 160Ti groups and then the Clean group, which had the shortest times. Comparisons between cpTi and Ti-6Al-4V within the same treatment group showed all the cpTi groups to have longer

activation times than the corresponding Ti-6Al-4V groups had. All these differences were statistically significant, except for the Ultrasonic group.

TABLE 7
Activation Times for cpTi, Ti-6Al-4V, and Ti-15Mo Passivation Treatment Groups

Material	Clean (h)	Static (h)	Ultrasonic (h)	160Ti (h)
cpTi	2.00 ± 0.24 ^{ab*}	4.72 ± 0.92 ^{a*}	6.79 ± 1.04 ^{ab}	4.01 ± 0.08 ^{b*}
Ti-6Al-4V	1.19 ± 0.03 ^{ab}	2.14 ± 0.32 ^a	5.06 ± 0.68 ^{ab}	2.18 ± 0.03 ^b
Ti-15Mo	>24	>24	>24	>24

The values are the mean ± standard deviation ($n = 3$).

Statistically significant differences are denoted with superscripts, which correspond to specific comparisons.

Results with the same superscripts are significantly different ($p < 0.05$).

ab superscripts denote differences due to passivation treatment only within each material group (one-way ANOVA, $p < 0.05$).

* denotes differences due to material group within each treatment group (t-test, $p < 0.05$).

XPS results

Surface chemistry

XPS analysis was used to determine the surface chemistry of the samples. It included initial survey spectra followed by high-resolution spectra for Ti 2p, O 1s, C 1s, and N 1s for all three material groups. In addition, the Al 2p and V 2p spectra were obtained for the Ti-6Al-4V groups, and the Mo 3d spectra were obtained for the Ti-15Mo groups. Argon ion sputtering was used to obtain depth profiles for the elemental composition. Analysis of high-resolution spectra yielded elemental composition (atomic %) of the surface region.

Survey spectra confirmed the presence of the constituent elements for each material, as well as carbon and nitrogen, which are ubiquitous surface contaminants. All the

survey spectra had dominant titanium and oxygen peaks with a relatively large carbon peak. There were also present smaller peaks for the alloy constituents, Al and V for the Ti64 groups and Mo for the Ti-15Mo groups.

The surface chemistry throughout the oxide layer was quantified by analyzing the high-resolution spectra taken after argon etching for specific time intervals. Tables 8-10 give the elemental compositions (atomic %) after the various etch times for the cpTi, Ti64, and Ti-15Mo groups, respectively.

TABLE 8
Surface Composition (at%) by XPS Analysis of Various Passivation Treatment Groups of cpTi After Different Etch Times

Element	cpTi Clean	cpTi Static	cpTi Ultrasonic	cpTi 160Ti
Ti 0s	14.8 ± 1.7	17.0 ± 0.1	18.8 ± 1.6	15.9 ± 1.6
Ti 30s	45.0 ± 5.7	41.2 ± 2.1	40.4 ± 0.9	35.6 ± 1.5
Ti 60s	--	--	48.7 ± 0.4	55.6 ± 7.9
Ti 90s	--	64.6 ± 4.8	--	--
Ti 120s	69.4	--	68.0 ± 1.6	67.3 ± 6.7
Ti 150s	--	72.6 ± 4.2	--	--
Ti 180s	66.2	--	72.3 ± 1.5	77.1 ± 2.7
O 0s	33.6 ± 1.3	40.8 ± 7.3	48.1 ± 5.2	45.2 ± 1.8
O 30s	52.5 ± 2.2	55.9 ± 1.8	58.8 ± 1.2	59.6 ± 0.8
O 60s	--	--	51.3 ± 0.4	44.4 ± 7.9
O 90s	--	35.4 ± 4.8	--	--
O 120s	30.6	--	32.0 ± 1.6	32.7 ± 6.7
O 150s	--	27.4 ± 4.2	--	--
O 180s	33.8	--	27.7 ± 1.5	22.9 ± 2.7
C 0s	46.4 ± 3.9	40.2 ± 5.5	31.7 ± 6.4	36.8 ± 2.7
C 30s	1.3 ± 1.9	2.4 ± 0.3	0.1 ± 0.2	4.4 ± 0.1
N 0s	5.2 ± 0.9	2.0 ± 1.9	1.4 ± 0.4	2.1 ± 0.7
N 30s	1.2 ± 1.7	0.5 ± 0.7	0.6 ± 0.1	0.4 ± 0.6

The values are mean ± standard deviation (at%; $n = 2$ specimens per group, except $n = 1$ where result has no standard deviation).

TABLE 9
Surface Composition (at%) by XPS Analysis of Various Passivation Treatment
Groups of Ti-6Al-4V After Different Etch Times

Element	Ti64 Clean	Ti64 Static	Ti64 Ultrasonic	Ti64 160Ti
Ti 0s	16.8 ± 0.0	15.0 ± 1.4	17.3 ± 1.0	17.9 ± 0.4
Ti 15s	32.8 ± 1.1	30.9 ± 0.0	32.0 ± 2.0	29.6 ± 2.2
Ti 30s	35.6 ± 0.8	34.7 ± 0.0	35.5 ± 0.0	33.9 ± 0.9
Ti 60s	49.6 ± 0.9	45.1 ± 2.3	45.4 ± 1.0	43.2 ± 0.0
Ti 120s	73.5 ± 1.6	62.1 ± 4.3	65.9 ± 10.5	55.5 ± 1.3
Ti 180s	77.1 ± 0.8	71.7 ± 2.3	67.6 ± 2.7	71.6 ± 0.1
O 0s	48.2 ± 0.9	43.2 ± 2.1	50.0 ± 2.9	49.9 ± 0.8
O 15s	58.7 ± 1.0	56.5 ± 1.3	65.0 ± 1.3	61.9 ± 0.3
O 30s	54.3 ± 2.3	53.9 ± 1.8	60.1 ± 2.4	60.4 ± 2.6
O 60s	41.9 ± 0.2	44.8 ± 1.8	48.8 ± 1.7	50.2 ± 0.9
O 120s	15.3 ± 0.4	24.3 ± 3.8	22.9 ± 1.4	30.3 ± 4.4
O 180s	8.4 ± 0.7	12.6 ± 1.2	14.7 ± 1.5	18.0 ± 2.4
Al 0s	2.8 ± 0.1	3.4 ± 0.7	2.8 ± 0.5	3.4 ± 0.8
Al 15s	4.5 ± 0.9	5.7 ± 0.7	2.7 ± 3.8	4.7 ± 0.0
Al 30s	4.9 ± 1.4	5.5 ± 1.1	4.0 ± 2.5	3.8 ± 2.0
Al 60s	6.0 ± 1.2	7.2 ± 1.6	4.7 ± 2.9	4.9 ± 1.1
Al 120s	7.7 ± 0.9	10.3 ± 0.2	8.1 ± 10.5	11.0 ± 5.5
Al 180s	10.6 ± 1.2	11.6 ± 0.1	13.0 ± 1.0	5.9 ± 1.3
V 0s	0.1 ± 0.1	0.6 ± 0.1	0.2 ± 0.3	0.5 ± 0.5
V 15s	0.5 ± 0.3	1.1 ± 1.0	0.3 ± 0.4	1.7 ± 0.1
V 30s	1.1 ± 0.5	1.6 ± 0.6	0.1 ± 0.2	0.1 ± 0.1
V 60s	2.6 ± 0.1	2.9 ± 1.1	1.1 ± 0.3	1.7 ± 0.2
V 120s	3.5 ± 0.3	3.3 ± 0.7	3.2 ± 1.3	3.2 ± 0.2
V 180s	4.0 ± 1.0	4.1 ± 0.9	4.6 ± 3.2	4.6 ± 1.0
C 0s	28.3 ± 1.5	35.6 ± 4.5	28.2 ± 3.2	27.4 ± 3.0
C 15s	3.3 ± 1.4	5.0 ± 1.5	0.0 ± 0.0	2.2 ± 2.0
C 30s	3.3 ± 0.6	4.2 ± 2.2	0.0 ± 0.0	0.5 ± 0.6
N 0s	3.8 ± 0.8	2.3 ± 0.4	1.5 ± 0.0	0.9 ± 1.3
N 15s	0.2 ± 0.2	0.9 ± 0.4	0.1 ± 0.1	0.0 ± 0.0
N 30s	0.7 ± 0.5	0.1 ± 0.1	0.2 ± 0.3	1.5 ± 2.0

The values are mean ± standard deviation (at%; $n = 2$ specimens per group).

TABLE 10
Surface Composition (at%) by XPS Analysis of Various Passivation Treatment
Groups of Ti-15Mo After Different Etch Times

Element	Ti-15Mo Clean	Ti-15Mo Static	Ti-15Mo Ultrasonic	Ti-15Mo 160Ti
Ti 0s	14.6 ± 0.5	14.3 ± 0.4	16.4 ± 1.5	14.9 ± 1.2
Ti 15s	31.8 ± 0.5	30.3 ± 0.7	29.7 ± 0.2	30.0 ± 0.8
Ti 30s	35.2 ± 1.3	35.8 ± 1.4	33.9 ± 0.7	33.6 ± 0.1
Ti 60s	45.0 ± 2.5	42.8 ± 1.0	39.3 ± 0.1	42.0 ± 0.2
Ti 120s	53.1 ± 0.3	56.2 ± 0.4	54.2 ± 2.6	54.9 ± 0.9
Ti 180s	59.5 ± 7.1	64.6 ± 0.0	65.1 ± 4.5	62.1 ± 0.7
O 0s	43.3 ± 2.5	45.4 ± 0.8	46.3 ± 2.4	43.8 ± 3.0
O 15s	54.6 ± 1.3	59.6 ± 1.4	62.3 ± 0.5	58.7 ± 0.6
O 30s	51.8 ± 0.2	54.5 ± 3.3	59.0 ± 0.7	55.8 ± 0.5
O 60s	49.1 ± 2.8	51.4 ± 0.3	55.5 ± 0.1	52.7 ± 0.3
O 120s	38.1 ± 1.3	34.9 ± 0.8	37.3 ± 2.8	36.7 ± 1.1
O 180s	29.9 ± 7.4	24.6 ± 0.2	25.1 ± 3.2	27.3 ± 1.1
Mo 0s	1.0 ± 0.1	1.6 ± 0.2	1.9 ± 0.1	1.4 ± 0.1
Mo 15s	2.5 ± 0.1	3.0 ± 0.1	3.2 ± 0.1	2.8 ± 0.4
Mo 30s	3.2 ± 0.1	3.7 ± 0.2	4.1 ± 0.0	3.3 ± 0.0
Mo 60s	5.9 ± 0.3	5.7 ± 0.7	5.2 ± 0.1	5.2 ± 0.1
Mo 120s	8.8 ± 0.9	8.9 ± 0.4	8.5 ± 0.3	8.3 ± 0.3
Mo 180s	10.6 ± 0.3	10.8 ± 0.3	9.9 ± 1.3	10.5 ± 0.4
C 0s	36.8 ± 3.5	35.1 ± 0.3	32.0 ± 0.3	36.5 ± 2.8
C 15s	10.6 ± 1.5	7.1 ± 0.7	4.5 ± 0.2	8.4 ± 2.1
C 30s	9.2 ± 0.3	5.9 ± 1.9	2.9 ± 0.0	7.3 ± 0.4
N 0s	4.3 ± 0.4	3.7 ± 1.2	3.4 ± 4.3	3.5 ± 1.4
N 15s	0.4 ± 0.6	0.0 ± 0.0	0.2 ± 0.3	0.2 ± 0.3
N 30s	0.6 ± 0.9	0.1 ± 0.2	0.0 ± 0.0	0.0 ± 0.0

The values are mean ± standard deviation (at%; $n = 2$ specimens per group).

The results from Tables 8-10 show all groups to follow the same basic trends in changes of chemical composition as a function of etch time. To illustrate this pattern graphically, representative depth profiles for the three material groups that had undergone ultrasonic passivation are shown in Figure 7. These profiles show the titanium atomic percentage to increase with longer etch times, while the oxygen atomic percentage in-

creases for the first 15-s etch time and then gradually decreases. The alloy constituents for Ti-6Al-4V and Ti-15Mo groups are seen to increase gradually with longer etch times.

The normalized atomic percentages of the different alloy constituents in the surface region are shown in Figures 8-10. Figures 8 and 9 show normalized atomic percentages of aluminum and vanadium for the Ti-6Al-4V groups. Figure 10 shows the normalized atomic percentage of molybdenum for the Ti-15Mo groups. The normalized atomic percentages were calculated by taking the atomic percentage of one of the alloy constituents and dividing by the sum of the atomic percentages of all metallic elements in the alloy; for example, the normalized atomic percentage of aluminum for Ti-6Al-4V is equal to $100 * [Al] / ([Ti] + [Al] + [V])$, where [] indicates atomic percentage.

In general, Figure 8 shows higher percentages of aluminum for all the nitric-acid-passivated groups than for the non passivated group (Clean). In addition, the highest percentages are shown to be at the outermost surfaces (0-s etch time), with subsequent decreases (15-s and 30-s etch times), which are then followed by relatively constant percentages of aluminum. The vanadium percentages shown in Figure 9, unlike those for aluminum, have the lowest percentages at the outermost surface and tend to increase with subsequent etch times. As for aluminum, however, the nitric-acid-passivated groups show higher percentages of vanadium than the non passivated group (Clean) does.

Figure 10 shows the normalized atomic percentage of molybdenum to be higher for all the passivated groups in the outer regions (0-s to 30-s etch times) compared to the non passivated group, with the Ultrasonic group having the highest molybdenum percentage in this region. All groups show the molybdenum percentages gradually increasing in

the outer regions (0-s to 30-s etch time) and then having larger increases from the 30 s to 180-s etch times, with all groups exhibiting similar percentages at each etch time.

Surface oxide stoichiometry

Analysis of the pre-etched (0-s etch time) Ti 2p spectra enabled the quantification of the different oxidation states present at the outermost surface of the oxide, specifically, Ti^{0+} (metallic Ti), Ti^{4+} (TiO_2), Ti^{3+} (Ti_2O_3) and Ti^{2+} (TiO). Common features for all the spectra included the presence of a dominant Ti $2p_{3/2}$ peak at a binding energy of 459.0 eV and a smaller and broader Ti $2p_{1/2}$ peak at a binding energy of 464.6 eV. These peaks both correspond to Ti^{4+} (TiO_2). The spectra also usually had a small Ti $2p_{3/2}$ peak at a binding energy of 453.9 eV, which corresponds to Ti^{0+} (metallic Ti). In addition, the peaks in these spectra exhibited shoulders to various extents. These shoulders represent the titanium suboxide states Ti^{3+} (Ti_2O_3) and Ti^{2+} (TiO). Subtle differences can be seen for the spectra of the different groups, indicating varying effects of the different passivation treatments.

A curve-fitting program was used on the high-resolution Ti 2p spectra to quantify the four oxidation states present in the surface oxide. Figure 11 shows representative high-resolution Ti 2p spectra for Ti-15Mo Clean and Ultrasonic samples. The figure shows the fitted curves for Ti^{0+} (metallic Ti), Ti^{2+} (TiO), Ti^{3+} (Ti_2O_3), and Ti^{4+} (TiO_2). The spectra show a higher Ti^{0+} peak for the Clean sample than for the Ultrasonic sample. The percentages of the different oxides are given in Table 11. The results in Table 11 show subtle differences in the percentages of oxide states for the different groups. The biggest differences between treatment groups within the material groups were between

the non passivated Ti-15Mo group (Clean) and the three nitric-acid-passivated Ti-15Mo groups, Static, Ultrasonic, and 160Ti. The passivated groups had higher TiO₂ percentages and lower percentages of suboxides Ti₂O₃ and TiO, as well as metallic Ti, than the non-passivated group did.

TABLE 11
Percentage of Oxidation States for cpTi, Ti-6Al-4V, and Ti-15Mo After Different Nitric Acid Passivation Treatments

Group	TiO ₂	Ti ₂ O ₃	TiO	Ti
cpTi-Clean	84.0	3.1	3.2	9.5
cpTi-Static	80.3 ± 0.8	6.9 ± 1.1	3.7 ± 1.1	9.2 ± 0.7
cpTi-Ultrasonic	78.0 ± 3.3	8.8 ± 1.8	4.0 ± 1.6	9.4 ± 0.1
cpTi-160Ti	80.1	7.4	5.6	7.0
Ti64-Clean	79.1 ± 1.1	6.2 ± 0.4	2.9 ± 0.2	12.0 ± 0.5
Ti64-Static	78.9 ± 1.4	7.1 ± 0.6	3.1 ± 0.8	11.0 ± 0.1
Ti64-Ultrasonic	80.4 ± 6.4	6.7 ± 4.7	3.6 ± 2.5	10.3 ± 0.5
Ti64-160Ti	81.4 ± 0.8	6.3 ± 1.2	3.1 ± 1.3	9.2 ± 1.0
Ti-15Mo-Clean	81.0 ± 2.9	6.5 ± 1.6	4.6 ± 0.5	8.1 ± 0.9
Ti-15Mo-Static	92.3 ± 3.7	1.4 ± 1.1	1.6 ± 0.8	4.6 ± 1.7
Ti-15Mo-Ultrasonic	92.0 ± 1.2	3.7 ± 2.5	1.2 ± 0.2	3.2 ± 1.5
Ti-15Mo-160Ti	90.5 ± 3.3	4.4 ± 1.2	1.4 ± 1.2	3.8 ± 1.0

The values are mean ± standard deviation (at%; *n* = 2 specimens, except *n* = 1 where no standard deviation is shown).

Cell culture

As in the Part I paper, hexosaminidase activity of the SaOS-2 cells was determined after 1 h, 4 h, 24 h, 3 days, and 7 days of incubation with the experimental samples. Quantification of the hexosaminidase activity was used to characterize the cell numbers at the different time periods to assess cellular attachment and proliferation. Proliferation is taken in this study as the percentage difference between the most recent result and the former result and is calculated as the most recent result less the former result, di-

vided by the former result; an example is $(100 \cdot [4 \text{ h} - 1 \text{ h}] / 1 \text{ h})\%$. The cell culture results are given in Tables 12 and 13. All results here are reported as percentage of control, where the control was blank tissue culture wells. The test groups for the cell culture tests included Clean, Static-40%, Ultrasonic-40%, and 160Ti-40% but did not include any 10% groups or 60-grit groups.

TABLE 12
Cell Number Results for the Different Treatment Groups at Different Time Points
Percent of Control (Tissue Culture Plastic)

	1 h	4 h	24 h	3 Days	7 Days
cp-Clean	91 ± 16	80 ± 13	73 ± 14	89 ± 11	91 ± 7
cp-Static-40%	100 ± 13	83 ± 15	81 ± 7	96 ± 8	93 ± 6
cp-Ultrasonic-40%	95 ± 10 ^{mn}	86 ± 9	82 ± 8	97 ± 9	96 ± 5
cp-160Ti-40%	94 ± 11	93 ± 11	81 ± 5	94 ± 9	90 ± 10
64-Clean	100 ± 24	82 ± 13	78 ± 14	92 ± 10	95 ± 9
64-Static-40%	101 ± 15	83 ± 10	84 ± 12	91 ± 7	92 ± 6
64-Ultrasonic-40%	89 ± 19 ⁿ	83 ± 16	79 ± 10	94 ± 8	95 ± 9
64-160Ti-40%	105 ± 20	81 ± 12	79 ± 10	91 ± 6	90 ± 9
15-Clean	102 ± 12	88 ± 12	81 ± 9	95 ± 15	92 ± 14
15-Static-40%	106 ± 20	88 ± 11	82 ± 9	94 ± 11	93 ± 13
15-Ultrasonic-40%	112 ± 27 ^{mn}	89 ± 7	84 ± 7	93 ± 10	94 ± 12
15-160Ti-40%	104 ± 15	84 ± 13	78 ± 6	95 ± 14	93 ± 12

Results are mean ± standard deviation ($n = 4$).

Statistical comparisons were made between specific groups.

Results with the same superscript denote statistically significant differences.

mn superscripts denote statistically significant difference between material groups within a specific treatment group and time point (one-way ANOVA, $p < 0.05$).

abc superscripts denote statistically significant difference between treatment groups within a specific material group and time point (one-way ANOVA, $p < 0.05$).

Comparisons of the cell number results for each of the experimental time periods showed no statistical differences between any of the treatment groups within each material group and only one statistical difference between any of the material groups within a

TABLE 13
Proliferation Results for the Different Treatment Groups at Different Time Periods:
Percentage of Control (Tissue Culture Plastic)

Group	1-4 h	4-24 h	1-3 Days	3-7 Days
cp-Clean	91 ± 18	89 ± 18	116 ± 10 ^{abc}	96 ± 9
cp-Static-40%	90 ± 18	100 ± 12	97 ± 7 ^a	98 ± 6
cp-Ultrasonic-40%	94 ± 9	95 ± 8	98 ± 8 ^b	100 ± 6
cp-160Ti-40%	101 ± 10 ^m	88 ± 7	97 ± 8 ^c	89 ± 21
64-Clean	84 ± 19	95 ± 18	108 ± 15	94 ± 8
64-Static-40%	83 ± 12	101 ± 20	107 ± 8	101 ± 6
64-Ultrasonic-40%	95 ± 24	96 ± 15	101 ± 7	103 ± 9
64-160Ti-40%	78 ± 10 ^m	98 ± 18	98 ± 7	99 ± 9
15-Clean	91 ± 16	93 ± 12	105 ± 17	98 ± 17
15-Static-40%	90 ± 23	93 ± 11	100 ± 15	99 ± 14
15-Ultrasonic-40%	89 ± 27	95 ± 11	98 ± 11	102 ± 13
15-160Ti-40%	87 ± 24	94 ± 12	103 ± 19	98 ± 14

Results are mean ± standard deviation (n = 4).

Statistical comparisons were made between specific groups.

Results with the same superscript denote statistically significant differences.

mn superscripts denote statistically significant difference between material groups within a specific treatment group and time point (one-way ANOVA, p<0.05).

abc superscripts denote statistically significant difference between treatment groups within a specific material group and time point (one-way ANOVA, p<0.05).

specific treatment group. The 1-h results for 15-Ultrasonic-40% were significantly greater than those for similarly treated cpTi and Ti-6Al-4V were. Trends were evident, however. Typically, the highest percentages of control results were shown at 1 h, and the Ti-15Mo groups had greater numbers at 1 h and 4 h. Results showed small differences between the different treatment groups within a material group and showed no obvious trends.

The proliferation results, like the cell number results, showed small differences between the groups, with only two differences being statistically significant. The cpTi-Clean group at the 1- to 3-day period had a significantly higher proliferation rate than the

other cpTi groups did in the same interval. The other difference was between material groups over the 1- to 4-h interval, where the cpTi-160Ti group had a significantly higher proliferation rate than the Ti-6Al-4V-160Ti group did.

DISCUSSION

Surface morphology

Samples were prepared with 60-grit and 600-grit finishes to better understand the effect of the surface roughness on the surface oxide properties and corrosion properties. Part I of this study²² showed that the 600-grit finish for Ti-15Mo was much rougher than the 600-grit cpTi and Ti-6Al-4V finishes were and that the rougher surface affected the surface oxide properties and corrosion.

The fact that the 600-grit Ti-15Mo was rougher is attributed to the fact that Ti-15Mo is a relatively soft material that tends to smear when polished. Ahmad²⁴ reported a smearing effect for softer cpTi Grade 1 that was not found for cpTi Grade 4 despite the use of identical surface preparation techniques (600-grit SiC). Figure 3 shows the smear effect for the 600-grit Ti-15Mo. It was also interesting that the 600-grit Ti-15Mo surface appeared rougher than the 60-grit Ti-15Mo surface did despite the fact that 60-grit is a coarser polishing paper. The 60-grit Ti-15Mo had relatively larger groove tracks but not as many of the secondary surface characteristics (i.e., small, island-like smear features and non groove indentations) that were seen on the 600-grit Ti-15Mo surface. The 60-grit versus 600-grit comparisons for cpTi and Ti-6Al-4V showed the 60-grit finishes being rougher, as expected.

Comparisons of the 60-grit surfaces for the three materials showed cpTi and Ti-15Mo to have a slightly rougher appearance than Ti-6Al-4V had. The cpTi and Ti-15Mo samples tended to have smear-like features on the groove edges, while the Ti-6Al-4V samples had sharper edges. As with the 600-grit Ti-15-Mo, the 60-grit differences can be attributed to the softer nature of the cpTi and Ti-15Mo materials when compared with Ti-6Al-4V.

Another interesting finding was the increased prevalence of relatively larger pit-like features on the surfaces of the materials that had been passivated in nitric acid and that contained additional titanium ions (160 mg Ti/L). This effect appeared on all the material groups but was more pronounced on the cpTi groups. It is not clear why this effect would occur. Robin stated that the addition of titanium ions in nitric acid decreased the corrosion of titanium and attributed the effect to faster formation of the surface oxide.¹² One explanation may be that a faster oxidation rate with the increased titanium ions was not uniform across the surface and thus resulted in pit-like features. This issue will be discussed further later in the paper.

Ultrasonic passivation effects

An ultrasonic wave passing through a solution can cause cavitations, the formation and collapse of voids, which can result in the generation of very high temperatures and pressures.¹¹ The presence of a solid surface near a collapsing void is predicted to result in asymmetric collapse with the formation of a high-velocity liquid jet directed toward the surface. This, in turn, can lead to cavitation damage to the metal surface, and

microstructural changes can occur.¹¹ Thus, it is reasonable to expect passivation processes to be affected by ultrasonication.

Whillock¹¹, in his work with 304L stainless steel in nitric acid, showed that, on initiation of ultrasonication, the alloy, which was in a passive state (i.e., exhibited a high or more noble corrosion potential), would immediately become more active (i.e., the corrosion potential would drop or become less noble) and remain in the more active state during ultrasonication. However, once the ultrasonication was stopped, the corrosion potential of the alloy would immediately increase to the previous passive level and remain until ultrasonication was started again, whereupon the cycle would be repeated as before. This phenomenon was attributed to shock waves from the collapsing cavities breaking the passive layer and increasing corrosion potential. In addition, Whillock showed that ultrasonication resulted in a three- to sixfold increase in corrosion rate, which implies that ultrasonication increased the rate of active metal dissolution. The depassivating effect of ultrasonication has also been reported for titanium.¹¹

In the present study, EIS and corrosion tests were conducted to determine the effects that ultrasonic passivation may have on the surface oxide. Unlike Whillock,¹¹ this study looked at the surface reactions in a physiological solution, HBSS, and not during the nitric acid passivation process. For the most part, the EIS and potentiodynamic polarization tests showed similar results for materials passivated statically or ultrasonically. One exception was the capacitance (Q) values, which showed higher values for the ultrasonicated groups. As mentioned in Part I of this study²², when the parallel-plate capacitor relation, $Q = \epsilon\epsilon_0 A/d_{ox}$, is used, the oxide thickness, d_{ox} , is seen to be inversely related to the capacitance, Q , and directly proportional to the dielectric constant, ϵ , and effective

surface area, A . Thus, if one assumes a constant dielectric constant and effective surface area, the higher Q value indicates a thinner oxide due to ultrasonic passivation. Callen reported a thinning of Ti-6Al-4V material that was ultrasonicated in nitric acid.⁴

However, in the present study, the XPS results showed no real changes in oxide thickness between statically and ultrasonically passivated materials. Thus, the increased Q values for the ultrasonicated materials appear to be due to a change in the dielectric constant or effective surface area rather than to a decrease in the surface oxide.

SEM analysis did not show any real differences between static and ultrasonic surface morphologies. It should be noted, however, that the SEM analysis was limited to one specimen per group, and others in the literature have shown rougher surfaces as a result of ultrasonication.¹¹

Hence, the most likely reason for the higher Q values for the ultrasonicated groups is an increase in the dielectric constant. Ohtsuka reported increases in the dielectric constant for surface oxides with a higher degree of hydration, which resulted from higher oxide formation rates.²⁵ Thus, an explanation for the higher Q values for the Ultrasonic groups may be that the oxides had a higher degree of hydration because of higher formation rates due to the ultrasonication process. The higher temperatures and pressures due to cavitation would be expected to increase the formation rate. Another reason for a higher oxide formation rate may be related to what Whillock¹¹ reported about the sample's becoming active upon ultrasonication and then immediately becoming more passive when the ultrasonication was stopped. This finding implies that the passive oxide grew almost instantaneously, which would result in a surface oxide with a higher degree of hydration.

In addition to EIS and potentiodynamic polarization tests, activation corrosion tests in 3-M sulfuric acid were conducted to help determine the protective properties of the surface oxides. Blackwood used activation corrosion tests to study the stability of the protective oxide films on porous titanium.²⁶ In general, the activation curves obtained in the present study exhibited the same characteristic regions as those reported by Blackwood.²⁶

The activation corrosion results from this study showed that, for cpTi and Ti-6Al-4V, the ultrasonically passivated groups had the longest breakdown times and thus the most protective oxide, followed by the statically passivated groups and then the non-passivated groups. None of the Ti-15Mo groups showed any breakdown up to 24 h. The improved protection seen for the statically and ultrasonically passivated cpTi and Ti-6Al-4V is consistent with the idea that nitric acid passivation dissolves the native air-formed oxide, which has been reported to be more defective,³ and grows in its place a less defective oxide. Furthermore, the increased protection for the ultrasonicated versus statically passivated samples suggests that the aggressive ultrasonication passivation may be more efficient in removing the original native oxide, which is then replaced with a less defective oxide. This suggestion is consistent with the results of Blackwood,²⁶ who found that a more protective oxide resulted when the native air-formed oxide had been removed prior to an anodic oxide was grown. It also agrees with the conclusions of Trepanier,³ who attributed improvements in corrosion properties of nitric-acid-passivated titanium and titanium alloys to the replacement of a native “deformed plastic” oxide with a more uniform oxide.

Another reason for the improved protection shown in the activation studies for the ultrasonicated groups is the oxide chemistry. The ultrasonicated Ti-6Al-4V had less aluminum at the outermost surface than the statically passivated Ti-6Al-4V did and then had similar amounts throughout. The presence of comparatively less aluminum at the outermost surface suggests a less defective oxide at the outermost regions and hence more protection.

The imperviousness of all the Ti-15Mo materials to sulfuric acid is explained by the presence of molybdenum in the surface oxide. The addition of molybdenum to titanium has been shown to increase the corrosion resistance 2000 to 4000 times in sulfuric acid.²⁷ However, there is some disagreement as to how molybdenum provides the protection. One theory credits the formation of a corrosion product overlayer that is insoluble in sulfuric acid.²⁸ Another explanation is that molybdenum covalently bonds with titanium, which increases the stability of the oxide.²⁹

The fact that the EIS Bode plots for some of the Ultrasonic groups exhibited two-phase maximums is indicative of two time constants and thus a dual-layered oxide.^{30, 31} The EIS results also showed that the outer oxide layer was extremely thin and porous. This finding may explain why some studies found increased titanium and aluminum ion release in serum solutions.⁴

Titanium ion passivation effects

Corrosion studies in the literature have shown that the addition of titanium ions in nitric acid decreased the corrosion rate of titanium and titanium alloys in nitric acid solutions.¹² Robin¹² showed that a critical concentration of titanium ions was necessary in or-

der to decrease the corrosion rates and that this effect was dependent on the concentration of the nitric acid and the material being corroded. For corrosion inhibition of Ti-4Al-4V alloy and cpTi, Robin found that 160 mg Ti/L and 45 mg Ti/L, respectively, were necessary for 40% and 50% nitric acid solutions.¹² Accordingly, 160 mg Ti/L used in the present study.

Robin also showed the corrosion potential to increase more quickly and to more noble levels when tested in nitric acid solutions containing added titanium ions and lower passive current densities.¹² Robin attributed the quicker and greater increase of the corrosion potential to a faster-growing passive film and attributed the lower passive current densities to a more stable surface oxide.¹² The increased oxide film formation was attributed to the presence of the additional titanium ions.

In the present study, the authors were interested in determining whether the presence of additional titanium ions in the nitric acid used to passivate the samples would alter the resultant oxide layer. Comparisons of the EIS and corrosion results for the groups that were passivated with additional titanium ions (160Ti) and for those passivated without additional titanium ions (Static) showed the two groups to be similar. Only a few of the differences between the groups were shown to be statistically significant. However, some trends were shown. The Q values were higher for the groups passivated with titanium ions, which could be the result of higher oxide formation rates due to the presence of additional titanium ions.¹² The corrosion results showed consistent trends for the individual parameters, showing, for the most part, lower (more active) E_{corr} values, lower I_{corr} results, and higher I_{pass} results for the 160Ti groups than for the Static groups. Un-

fortunately, these results conflict with respect to indicating better or worse corrosion properties.

A more consistent variation between the groups, however, was the appearance of two phase angle maximums in the EIS Bode plots. The two maximums indicate the presence of a dual oxide layer, typically a dense compact barrier layer covered with a porous oxide. The fit of the experimental EIS spectra with an appropriate dual-layer oxide model indicated that the outer layer was extremely thin and porous. The XPS results also tended to support the presence of a porous overlayer. Analysis of the oxidation states showed a smaller percentage of metallic titanium for the 160Ti group than for the Static groups, which suggests a thicker oxide. The thicker oxide is consistent with a barrier layer covered by a porous oxide layer. In addition, the Ti-6Al-4V and Ti-15Mo 160Ti groups showed lower percentages of aluminum and molybdenum, respectively, at the outermost surface region. This result is consistent with the formation of a porous titanium oxide layer on top of the barrier layer as a result of the higher concentration of titanium ions¹². The porous overlayer may be one reason for the appearance of pit-like features shown in the SEM analysis.

Roughness effects

Samples with rougher surfaces have increased effective surface area, which leads to increased corrosion. This effect was seen in this study in that the rougher 60-grit finishes of cpTi and Ti-6Al-4V samples showed more corrosion than the 600-grit samples did. The fact that the 60-grit Ti-15Mo samples had lower corrosion than the 600-grit fin-

ishes did agree with the surface area concept since the 60-grit Ti-15Mo samples appeared to be somewhat smoother than the 600-grit Ti-15Mo samples did.

What was of interest in this study, however, was how the roughness affected the EIS parameters. In this study, the groups with the rougher surfaces (i.e., the 60-grit cpTi and Ti-6Al-4V and the 600-grit Ti-15Mo) tended to have higher Q values, lower n values, and lower Rp values, a result that agreed with those of other studies^{32,33}. Mustafa showed that rougher grit-blasted cpTi disks had higher Q values and lower Rp values than smoother cpTi³³ disks had. The author attributed the differences entirely to the change in effective surface area since he assumed equal oxide thicknesses and dielectric constants for the oxides. One reason for the lower Rp values is that the Rp value is equal to the total resistance of the oxide film per geometric area of the specimen and not per effective surface area. As the effective area increases, the active anodic areas in the surface increase³⁴; as a result, the total resistance of the oxide layer decreases.³²

Comparisons between the passivated and non passivated rougher specimens showed higher Q, n, and Rp values for the passivated specimens; these values were similar to the results found for the groups with the smoother surfaces. This result indicates that the passivation treatment had similar effects on samples with different roughness.

Cell culture

The effect of nitric-acid-passivated titanium and titanium alloys on cellular response has been reported in the literature. Faria³⁵ showed no differences in cell attachment and proliferation of cells on non passivated and passivated cpTi and Ti-6Al-4V.

Ku³⁶ also showed negligible effects when comparing passivated and non passivated Ti-6Al-4V. On the other hand, Mante³⁷ showed increased cellular attachment for nitric-acid-passivated cpTi specimens. In Part I of the present study, the results showed differences due to passivation parameters and roughness.²² Passivated samples tended to have higher cell numbers than non passivated samples did, and the rougher Ti-15Mo samples showed significantly higher cell attachment at the early time periods.

In the present study, the cellular attachment and proliferation results for all the groups demonstrated good compatibility. Because similar results were shown for all the treatment groups, it was not possible to discriminate among the effects of the different treatments. This uniformity indicates that ultrasonic passivation and passivation with additional titanium ions did not affect the biological response more than static passivation did. However, these tests were conducted over a 1-week time period; thus, long-term effects cannot be excluded.

Material effects

Studies by Callen⁴ and others⁵ found that Ti-6Al-4V samples that had been ultrasonically passivated released more titanium, aluminum, and vanadium ions than non-passivated samples did. In contrast, cpTi samples did not show any effect on the release of ions. They attributed the increased ion release for the Ti-6Al-4V to a thinner oxide and the presence of aluminum in the oxide.⁴

As in Callen and as in Part I of this study,^{4, 22} the effects of the passivation treatments differed according to which material was being treated. Furthermore, passivating samples ultrasonically or with the addition of titanium ions demonstrated similar mate-

rial-specific effects, as was reported in Part I of this study. One interesting apparent difference among the materials was the appearance of pit-like features on the surfaces. This effect seemed to be more prevalent and pronounced on samples that had been passivated with additional titanium ions and still more prevalent and pronounced for the cpTi sample. It is unclear why the cpTi sample would be more affected; an explanation may involve the lack of alloy elements within its oxide.

Another interesting difference was that the Ti-15Mo samples exhibited fewer variations between treatment groups and generally had better repeatability (i.e., smaller standard deviations) within each study group. The most likely explanation is that the molybdenum interacted with the titanium to form a more stable passive layer²⁹ and that molybdenum oxide is relatively insoluble.²⁸

CONCLUSIONS

The following conclusions were drawn from the results of this study:

1. A rougher surface morphology resulted from identical polishing procedures for the softer Ti-15Mo materials because of a smearing effect than resulted for cpTi and Ti-6Al-4V.
2. Rougher surfaces affected EIS parameters, resulting in higher capacitance (Q) values, lower n values, and lower oxide resistance (Rp) values than were found for similar smoother materials.
3. Ultrasonic nitric acid passivation resulted in higher capacitance (Q) values and lower atomic percentages of aluminum at the outermost surface than were found for static passivation.

4. The addition of titanium ions to the nitric acid passivation solutions resulted in minimal effects on the analyzed surface and corrosion properties, but it did increase the appearance of pit-like features on the surface.
5. Cell attachment and proliferation results for the different treatment groups were similar and comparable to the tissue culture plastic control regardless of surface treatments. However, because of the relatively short time period (1 week) used in this study, no assessments of long-term cellular response could be made.
6. The presence of molybdenum in Ti-15Mo made it less sensitive to nitric acid passivation than cpTi and Ti-6Al-4V were found to be.

References

1. ASTM F86-91 standard practice for surface preparation and marking of metallic surgical implants. Annual Book of ASTM Standards 1995; 13.01:6-7.
2. Petersen D, Lemons JE, Lucas LC, Comparative evaluations of surface characteristics of cp Titanium, Ti-6Al-4V and Ti-15Mo-2.8Nb-0.2Si (Timetal 21SRX). Titanium, niobium, zirconium and tantalum for medical and surgical applications, ASTM STP. 2005, West Conshohocken: ASTM International.
3. Trepanier C, Tabrizian M, Yahia LH, Bilodeau L, Piron DL. Improvement of the corrosion resistance of niti stents by surface treatments. Mater Res Soc Symp Proc 1997; 459:363-368.
4. Callen BW, Lowenberg BF, Lugowski S, Sodhi RNS, Davies JE, Nitric acid passivation of Ti6Al4V reduces thickness of surface oxide layer and increases trace element release. J Biomed Mater Res 1995; 29(3):279.
5. Lowenberg BF, Lugowski S, Chipman M, Davies JE, ASTM-F86 passivation increases trace element release from ti6al4v into culture medium. J Mater Sci: Mater Med 1994; 5(6-7):467.
6. Lee TM, Chang E, Yang CY, Effect of passivation on the dissolution behavior of Ti6Al4V and vacuum-brazed Ti6Al4V in Hank's ethylene diamine tetra-acetic acid solution part I Ion release. J Mater Sci: Mater Med 1999; 10(9):541.

7. Browne M, Gregson PJ, Surface modification of titanium alloy implants. *Biomaterials* 1994; 15(11):894.
8. Wisbey A, Gregson PJ, Peter LM, Tuke M, Effect of surface treatment on the dissolution of titanium-based implant materials. *Biomaterials* 1991; 12(5):470.
9. Kilpadi DV, Lemons JE. Effect of surface and heat treatments on corrosion of unalloyed titanium implants. 1997. Shreveport, LA, USA: IEEE, Piscataway, NJ, USA.
10. Wan GJ, Yang P, Leng YX, Sun H, Chen JY, Wang J, Huang N, Enhanced corrosion resistance of Ti6Al4V with Ti-O film deposited by dc metal vacuum arc deposition. *IEEE International Conference on Plasma Science* 2003: p.419.
11. Whillock GOH, Harvey BF, Preliminary investigation of the ultrasonically enhanced corrosion of stainless steel in the nitric acid/chloride system. *Ultrasonics Sonochemistry* 1996; 3(2):111-118.
12. Robin A, Sandim HRZ, Rosa JL, Corrosion behavior of the Ti-4%Al-4%V alloy in boiling nitric acid solutions. *Corr Sci* 1999; 41:1333-1346.
13. Cabrini M, Cigada A, Rondelli G, Vicentini B, Effect of different surface finishing and of hydroxyapatite coatings on passive and corrosion current of Ti6Al4V alloy in simulated physiological solution. *Biomaterials* 1997; 18(11):783.
14. Rammelt U, Reinhard, G., The influence of surface roughness on the impedance data for iron electrodes in acidic solutions. *Corr Sci* 1987; 27:373-382.
15. Schultze JW, Davepon B, Karman F, Rosenkranz C, Schreiber A, Voigt O, Corrosion and passivation in nanoscopic and microscopic dimensions: The influence of grains and grain boundaries. *Corr Eng Sci Tech* 2004; 39(1):45.
16. Venugopalan R, George MA, Weimer JJ, Lucas LC, Surface topography, corrosion and microhardness of nitrogen-diffusion-hardened titanium alloy. *Biomaterials* 1999; 20(18):312.
17. Cavin R, Ong JL, Cardenas HL, Carnes DL. Effect of titanium roughness and BMP-2 on osteoblast progenitor cells in vitro. *Trans Soc Biomat* 1996; 1:943.
18. Kanagaraja S, Wennerberg A, Eriksson C, Nygren H, Cellular reactions and bone apposition to titanium surfaces with different surface roughness and oxide thickness cleaned by oxidation. *Biomaterials* 2001; 22(13):1809.
19. Ponsonnet L, Comte V, Othmane A, Lagneau C, Charbonnier M, Lissac M, Jaffrezic N, Effect of surface topography and chemistry on adhesion, orientation

- and growth of fibroblasts on nickel-titanium substrates. *Mater Sci Eng* 2002; 21(1-2):157.
20. Shin D, Lee K, Ong JL, Effects of dental implant roughness on mechanical adhesiveness of boneforming cells. *Ann Biomed Eng* 2000; 28(SUPPL 1):19.
 21. Soares GA, Fernandes MH, Diniz MG, Coelho MJ, Surface topography modulates the osteogenesis in human bone marrow cell cultures grown on titanium samples prepared by a combination of mechanical and acid treatments. *J Mater Sci: Mater Med* 2002; 13(4):421.
 22. Petersen D, Lemons JE, Effects of nitric acid passivation parameters on titanium and titanium alloys related to corrosion, surface chemistry and cell culture. Part I: Effects of nitric acid concentration, temperature and time. To Be Submitted 2005.
 23. Landegren U, Measurement of cell numbers by means of the endogenous enzyme hexosaminidase. Applications to detection of lymphokines and cell surface antigens. *J Immun Methods* 1984; 67:379-388.
 24. Ahmad M, Gawronski, D, Blum, J, Golderg, J, Gronowicz, Differential response of human osteoblast-like cells to commercially pure (cp) titanium grades 1 and 4. *J Biomed Mater Res* 1999; 46:121-131.
 25. Ohtsuka T, Otsuki T, The influence of the growth rate on the semiconductive properties of titanium anodic oxide films. *Corr Sci* 1998; 40(6):951-958.
 26. Blackwood DJ, Chooi SKM, Stability of protective oxide films formed on a porous titanium. *Corr Sci* 2002; 44(3):395.
 27. Malyshev VV, Hab AL, Electrochemical and corrosion behavior of titanium with molybdenum-carbide coatings in solutions of sulfuric acid. *Mater Sci* 2003; 39(6):901-904.
 28. Popa MV, Vasilescu E, Drob P, Vasilescu C, Mirza-Rosca J, Lopez AS, Corrosion behavior of some titanium base alloys in acid solutions. *EUROCORR* 2005; 20(1):35-45.
 29. Tomashov ND, Chernova GP, Ruscol YS, Ayuyan GA, The passivation of alloys on titanium bases. *Electrochim Acta* 1974; 19(4):159-172.
 30. Pan J, Thierry D, Leygraf C, Electrochemical impedance spectroscopy study of the passive oxide film on titanium for implant application. *Electrochimica Acta* 1996; 41(7-8):1143.

31. Metikos-Hukovic M, Tkalacec E, Kwokal A, Piljac J, An in vitro study of Ti and Ti-alloys coated with sol-gel derived hydroxyapatite coatings. *Surf and Coat Tech* 2003; 165(1):42.
32. Aparicio C, Gil FJ, Fonseca C, Barbosa M, Planell JA, Corrosion behaviour of commercially pure titanium shot blasted with different materials and sizes of shot particles for dental implant applications. *Biomaterials* 2003; 24(2):184.
33. Mustafa K, Pan J, Wroblewski J, Leygraf C, Arvidson K, Electrochemical impedance spectroscopy and x-ray photoelectron spectroscopy analysis of titanium surfaces cultured with osteoblast-like cells derived from human mandibular bone. *J Biomed Mater Res* 2002; 59(4):655.
34. Solar RJ, Pollack SR, Korostoff E, Titanium release from implants: A proposed mechanism. *J Biomed Mater Res* 1979(684):161.
35. Faria AC, Beloti MM, Rosa AL, Nitric acid passivation does not affect in vitro biocompatibility of titanium. *Int J Oral Maxillofac Implants* 2003; 18(6):820-825.
36. Ku CH, Pioletti DP, Browne M, Gregson PJ, Effect of different Ti-6Al-4V surface treatments on osteoblasts behaviour. *Biomaterials* 2002; 23:1447-1454.
37. Mante M, Daniels B, Golden E, Diefenderfer D, Reilly G, LeBoy PS, Attachment of human marrow stromal cells to titanium surfaces. *J Oral Implantol* 2003; 29(2):66-72.

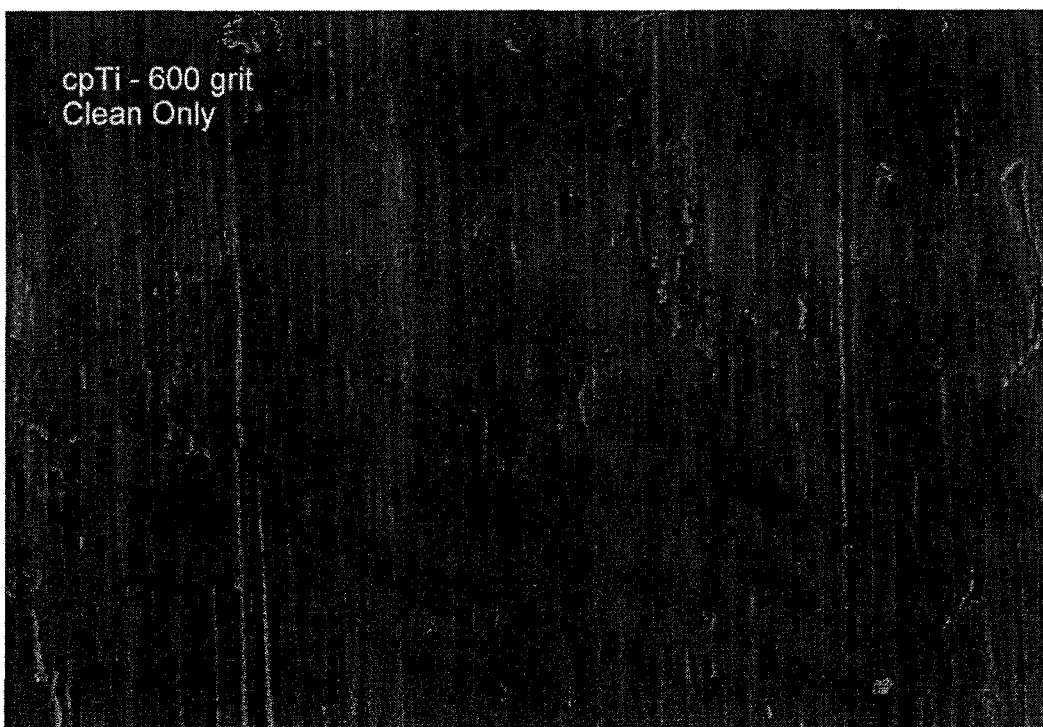
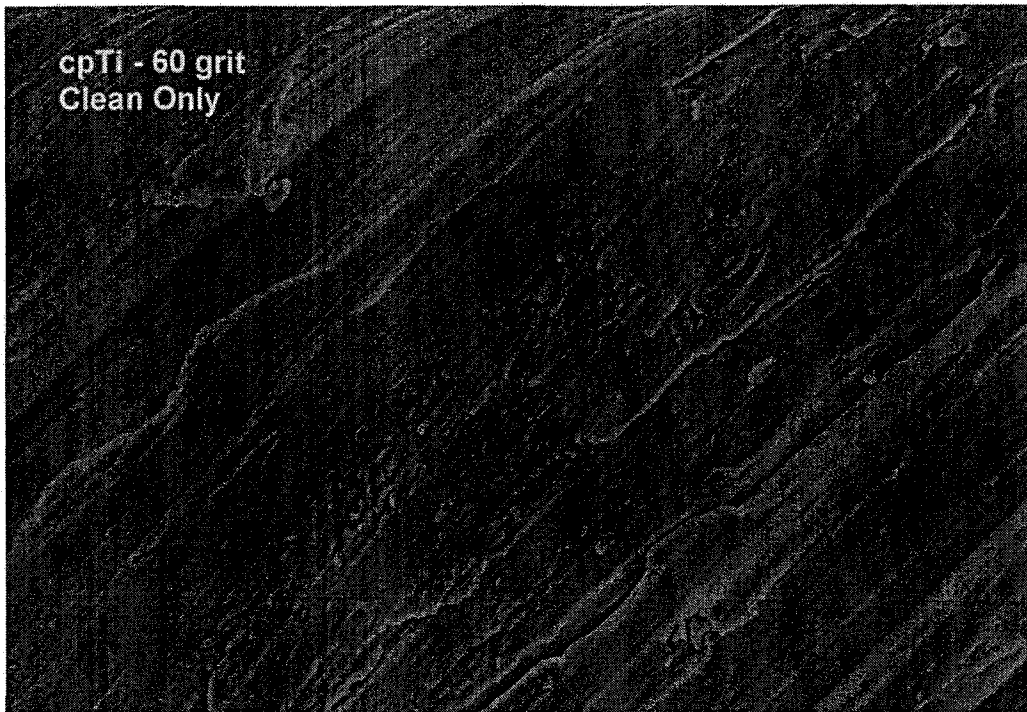


Figure 1. Representative SEM micrographs of cpTi material with 60-grit and 600-grit finish in the Clean condition (original magnifications of top and bottom micrographs x1000).

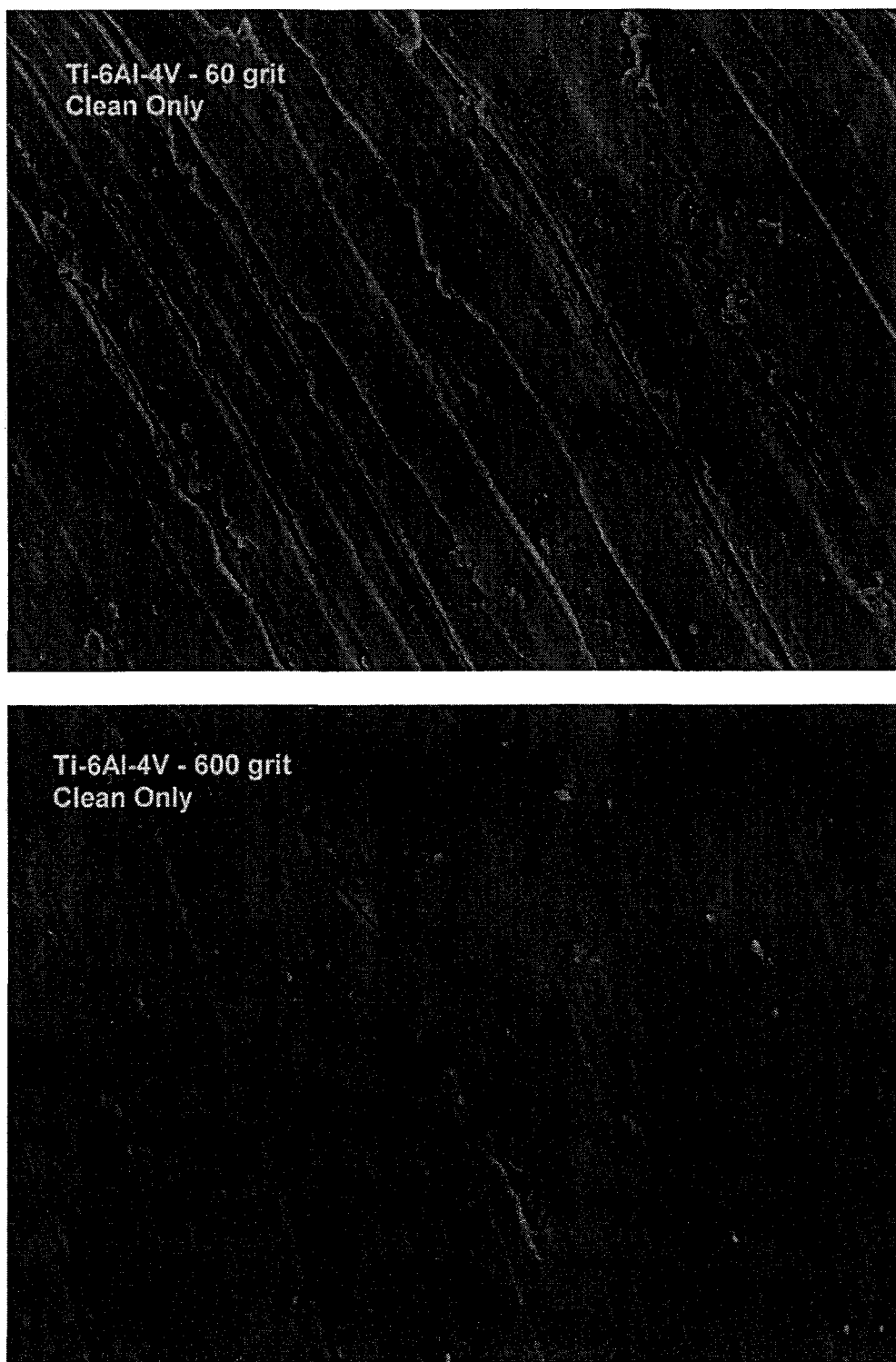


Figure 2. Representative SEM micrographs of Ti-6Al-4V material with 60-grit and 600-grit finish in the Clean condition (original magnifications of top and bottom micrographs x1000).

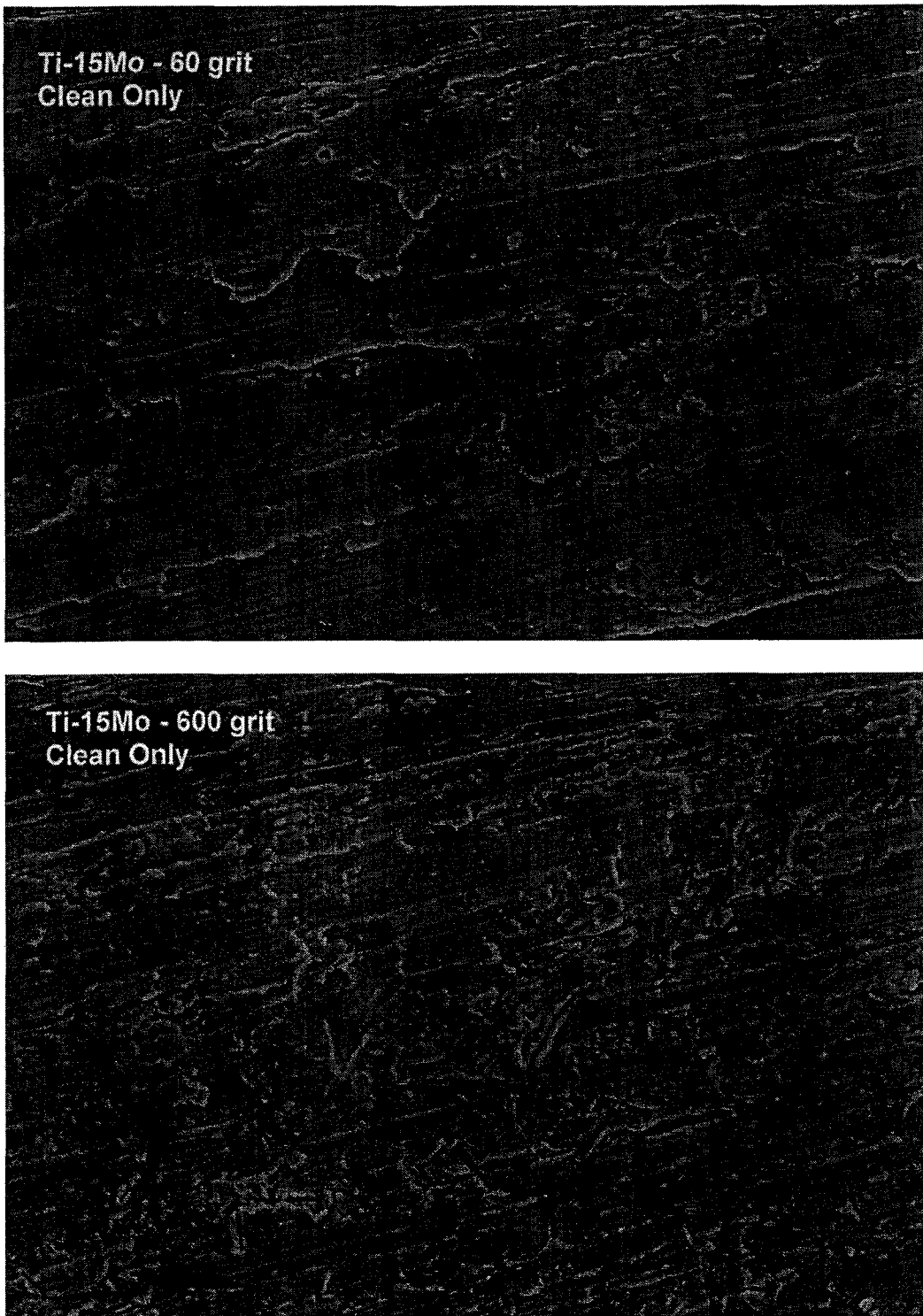


Figure 3. Representative SEM micrographs of Ti-15Mo material with 60-grit and 600-grit finish in the Clean condition (original magnifications of top and bottom micrographs x1000).

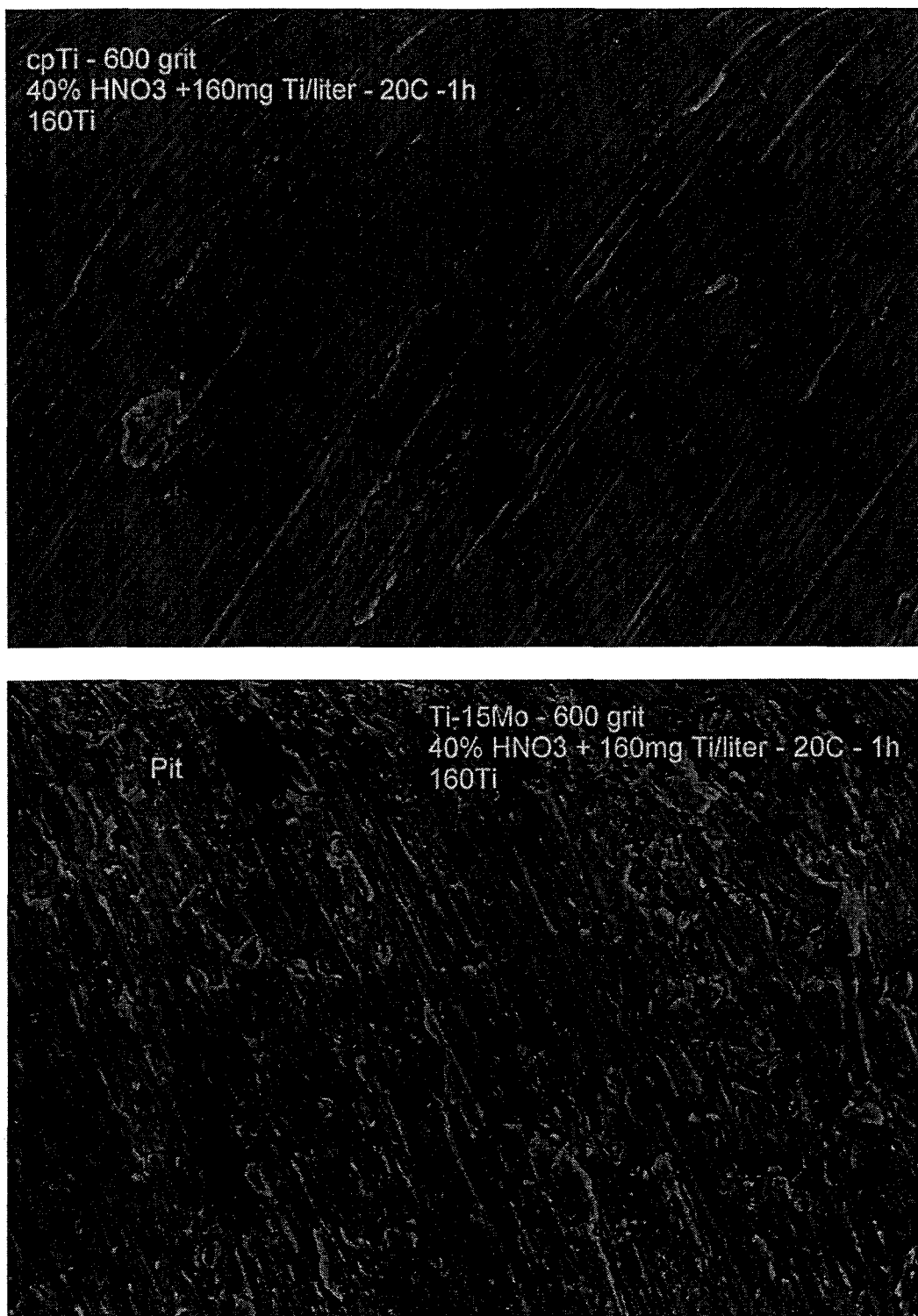


Figure 4. SEM micrographs of cpTi and Ti-15Mo materials with 600-grit finish that had been passivated with 40% nitric acid with the addition of 160 mg Ti/L. Micrographs show pit-like features that were more prevalent and larger on the surfaces of the 160Ti groups (original magnifications of top and bottom micrographs x1000).

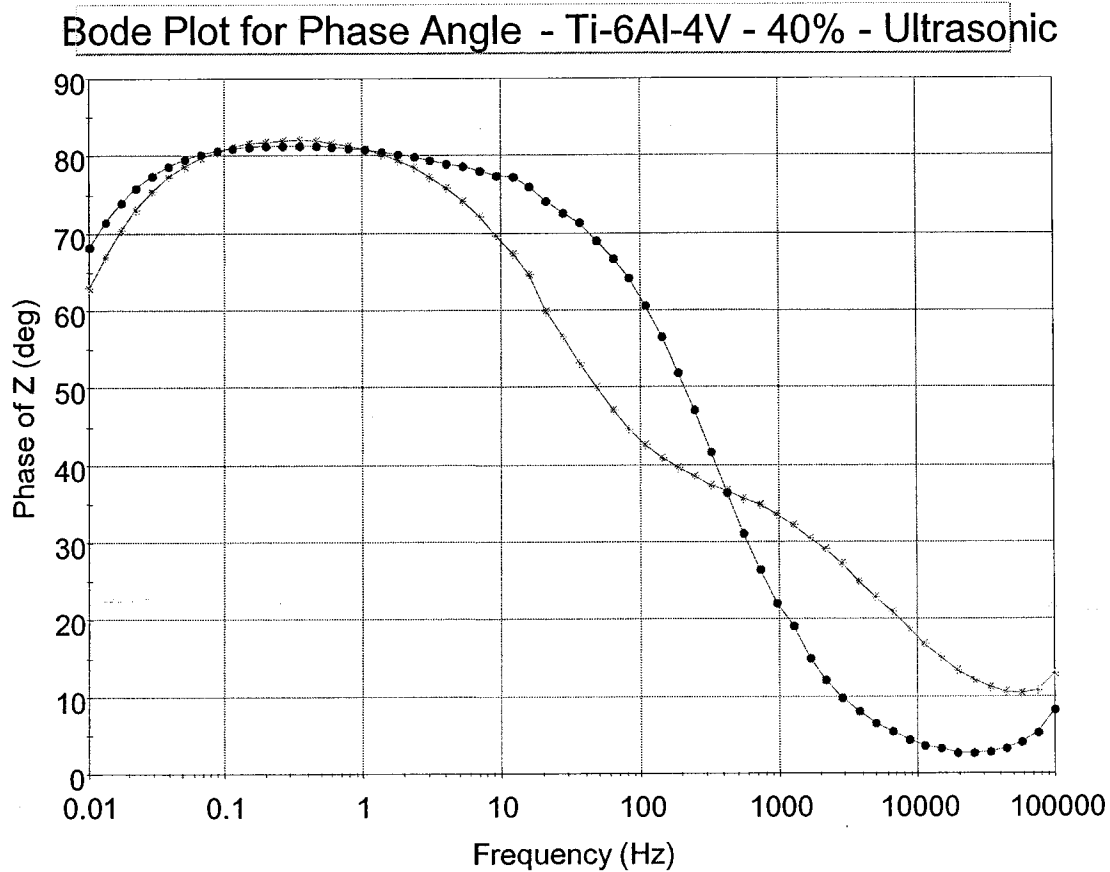


Figure 5. Phase angle Bode plot for two Ti-6Al-4V-40%-Ultrasonic samples. The samples show two distinct spectra, one having two maximum phase angles indicative of a dual-layer oxide. Similar variations in spectra were shown for the other Ultrasonic and 160Ti groups.

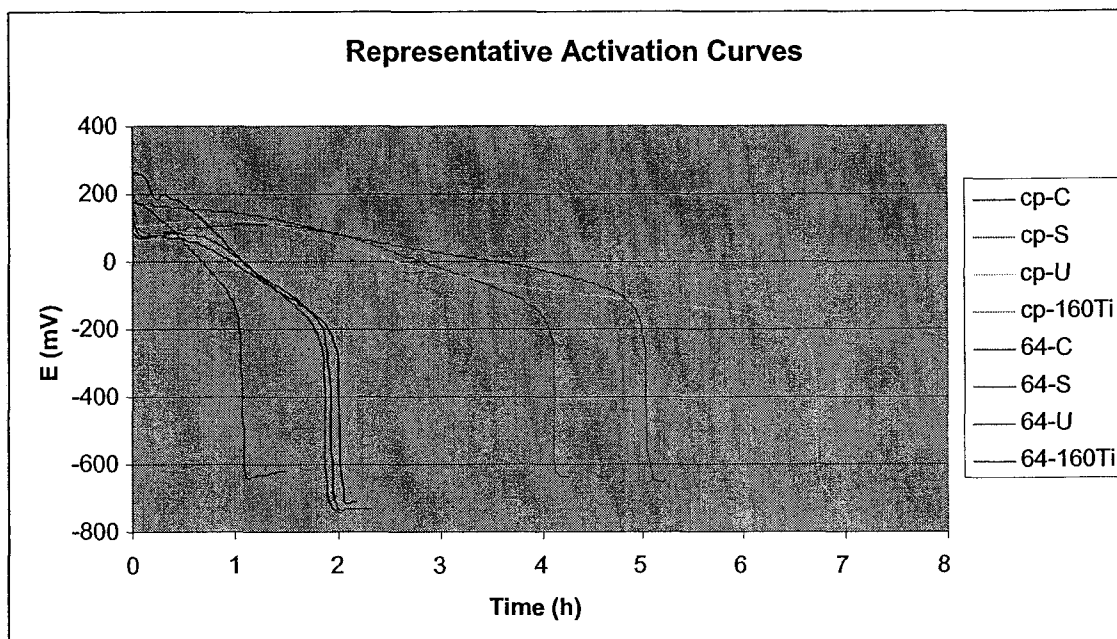


Figure 6. Representative activation curves for cpTi (cp) and Ti-6Al-4V (64) samples from all the treatment groups. Samples were immersed in 3M H_2SO_4 at 37°C. Activation time is the time taken to reach active dissolution of the metal, which is the point at the end of the extreme drop in potential and where it begins to level off at the activation potential (~650-750 mV). Treatments: C = Clean Only, S = Static, U = Ultrasonic, and 160Ti = 160Ti.

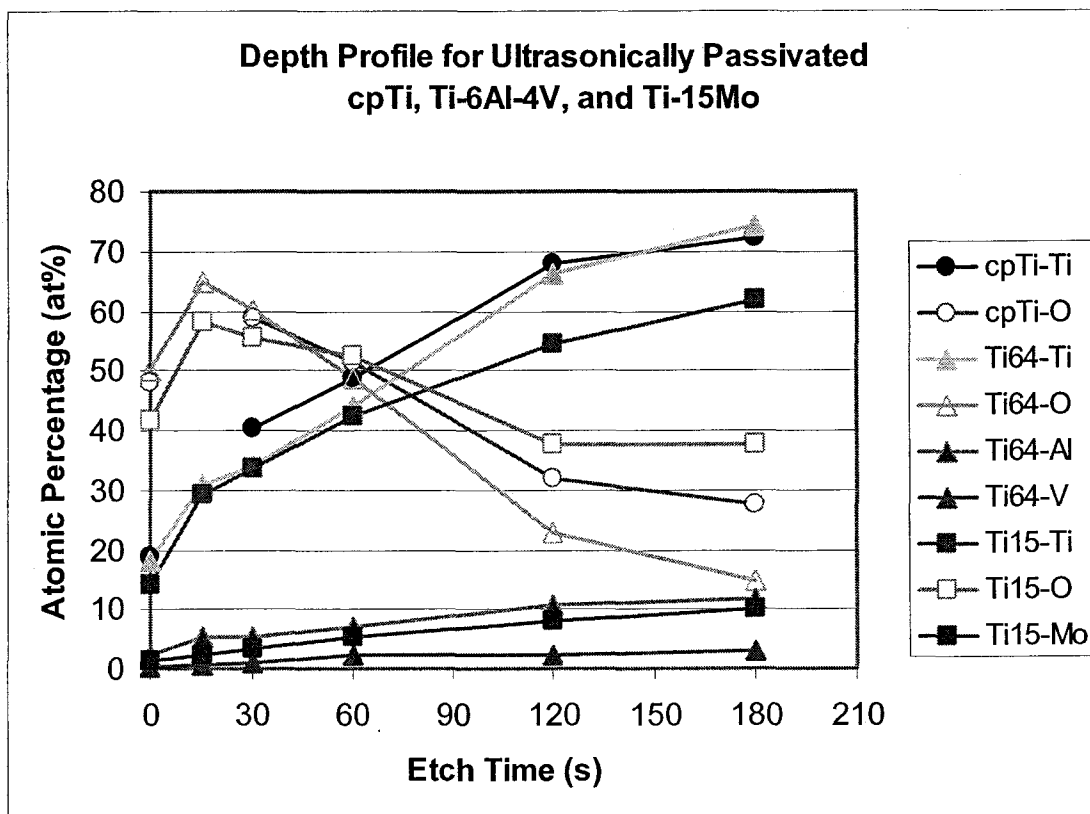


Figure 7. Depth profiles of elemental composition in the surface region for ultrasonically passivated cpTi, Ti-6Al-4V, and Ti-15Mo.

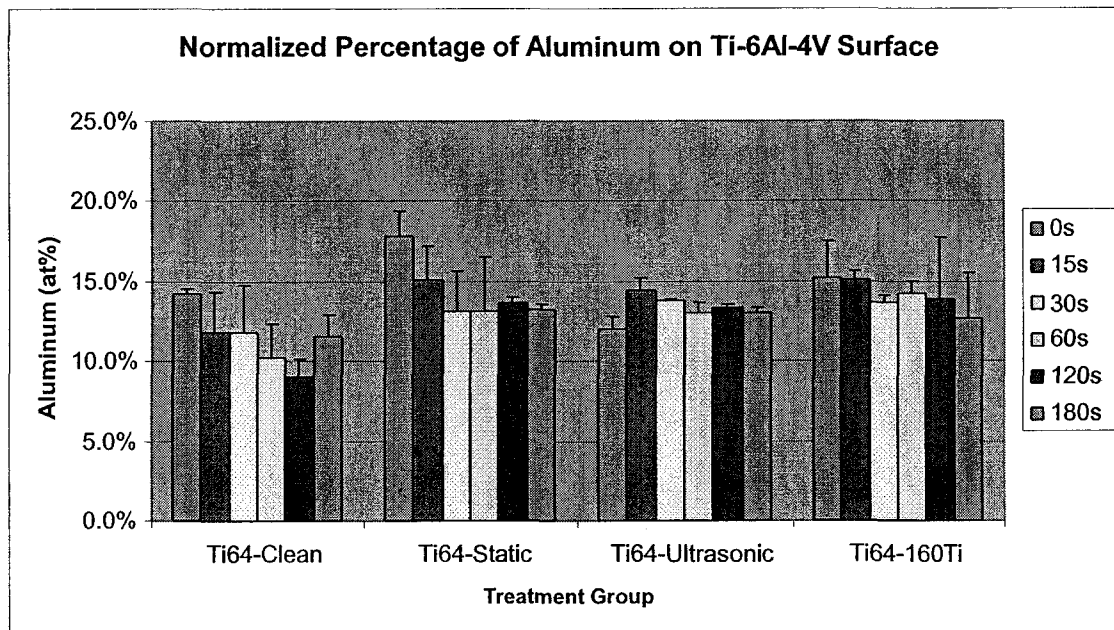


Figure 8. Normalized percentage of aluminum in the surface region for the different treatment groups of Ti-6Al-4V as a function of etch time. Graph illustrates the enrichment of aluminum throughout the surface for the nitric-acid-passivated groups compared with the non passivated group (Clean). Graph also shows highest aluminum percentages at the outermost regions of the surface (etch time = 0-s), except for the Ultrasonic group.

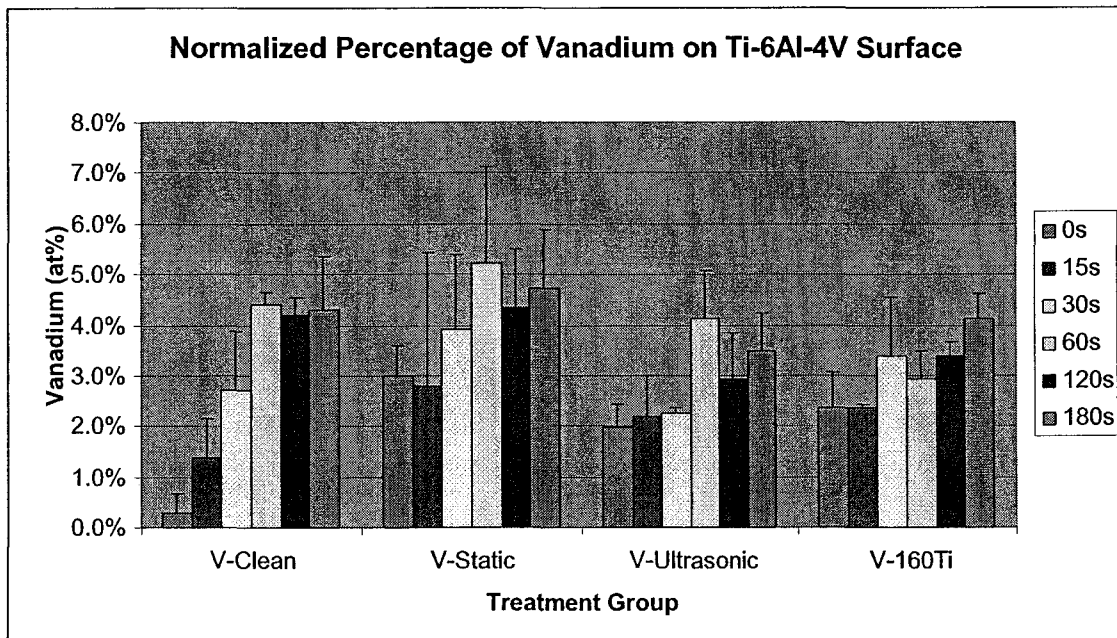


Figure 9. Normalized percentage of vanadium in the surface region for the different treatment groups of Ti-6Al-4V as a function of etch time. Graph illustrates the enrichment of vanadium at the outer regions of the surface (0-s and 15-s etch times) for the nitric-acid-passivated groups compared with the non passivated group (Clean). Graph also shows lower vanadium percentages at the outermost regions of the surfaces and peak percentages at 60 s, except for the 160Ti group.

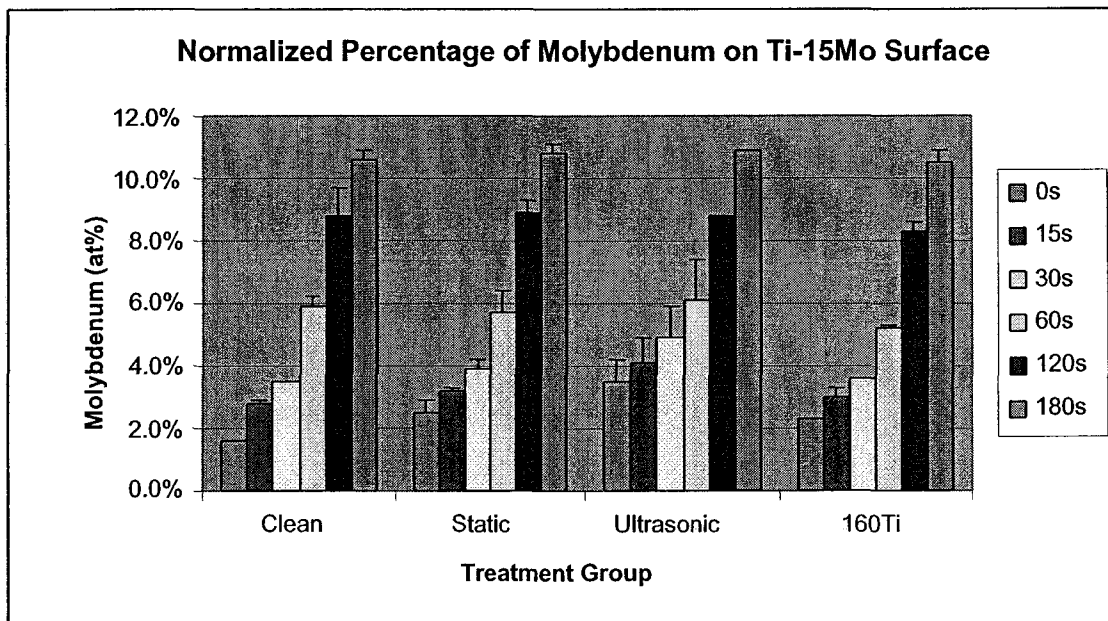


Figure 10. Normalized percentage of molybdenum in the surface region for the different treatment groups of Ti-15Mo as a function of etch time. Graph illustrates the enrichment of molybdenum at the outer regions of the surface (0-s and 15-s etch times) for the nitric-acid-passivated groups compared with the non passivated group (Clean). Graph also shows lower molybdenum percentages at the outermost regions of the surfaces, followed by a gradual increase with subsequent etch times.

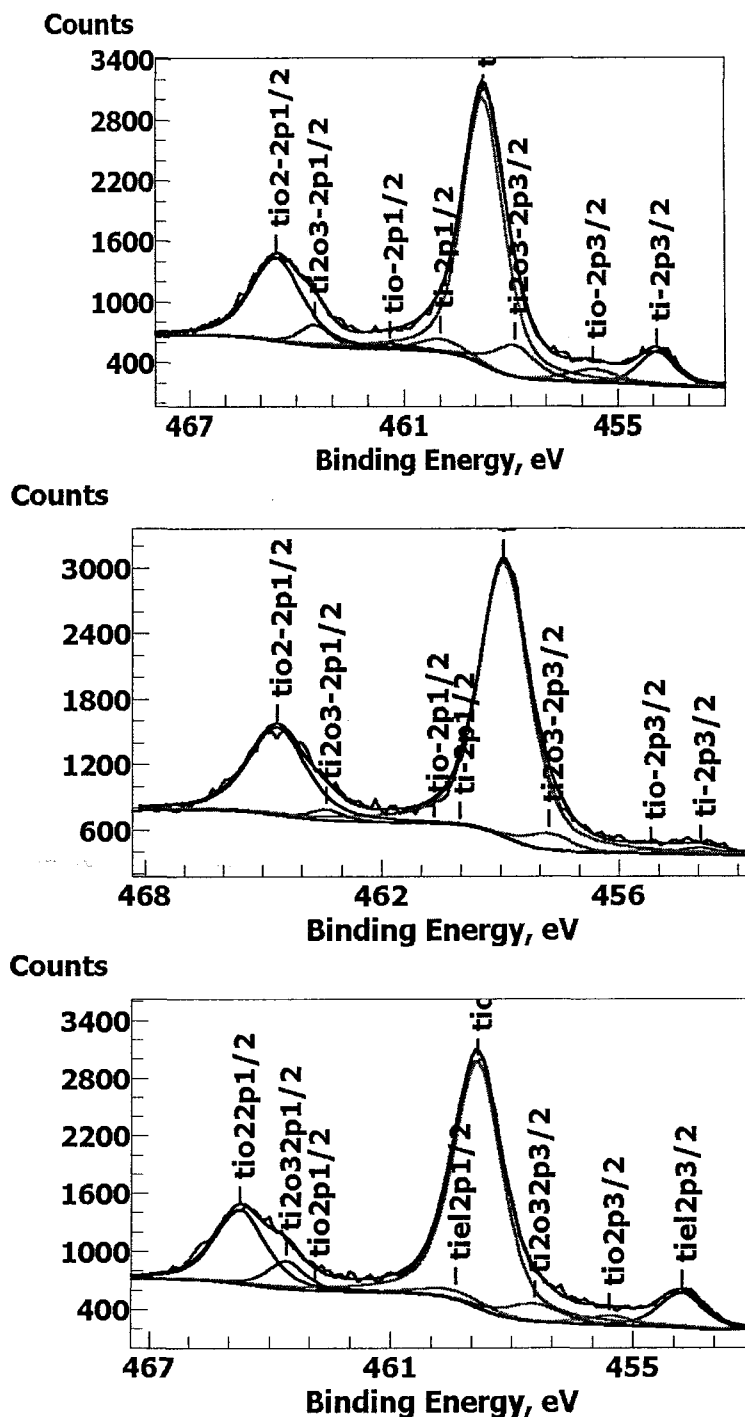


Figure 11. Representative Ti 2p high-resolution spectra for cpTi (top), Ti-6Al-4V (middle), and Ti-15Mo (bottom) samples that had been passivated ultrasonically (40% nitric acid at 20°C for 1 h).

SUMMARY DISCUSSION

Hypothesis 1

This hypothesis stated that heat treatment (350°C for 1 h in air) and nitric acid passivation (40 vol% nitric acid at room temperature for 30 min) will improve the corrosion properties of cpTi, Ti-6Al-4V, and beta-titanium, Ti-15Mo-2.8Nb-0.2Si (Timetal[®] 21SRx).

Corrosion results for this part of the study showed nitric-acid-passivated and heat-treated samples to have significantly better corrosion properties than non passivated samples had in terms of more noble corrosion potentials (E_{corr}) values and lower corrosion current (I_{corr}) values ($p < 0.05$). The passive current density (I_{pass}) results showed the heat-treated groups and nitric-acid-passivated groups to be lower; however, only the heat-treated groups were significantly lower ($p < 0.05$).

Thus, Hypothesis 1 was proven.

Ong¹⁸ showed nitric acid passivation of cpTi to increase corrosion resistance, but the differences were not statistically significant. Kilpadi⁸ showed similar corrosion properties for nitric-acid-passivated and heat-treated cpTi samples. Trepanier¹² showed greater corrosion resistance for passivated Ti-Ni alloys than for non passivated Ti-Ni. Thus, most studies show similar to improving corrosion properties for nitric-acid-passivated samples. In this study, the improvements in corrosion properties were statistically significant. However, it should be noted that all materials studied showed excellent

corrosion properties, with I_{corr} results of 2-61 nA/cm² and I_{pass} results typically less than 1 $\mu\text{A}/\text{cm}^2$.

Heat treatment of titanium and titanium alloys has been shown in the literature to improve the corrosion properties of the materials.^{12, 29-31} Heat treatments also have been shown to increase the thickness and crystallinity of the oxide, with the extent of such increases depending on the temperature and duration of the heat treatment.^{8, 9} It is generally thought that the thicker oxides that result from oxidation at higher temperatures improve corrosion resistance.^{12, 29-31}

Hypothesis 2

Hypothesis 2 stated that heat treatment (350°C for 1 h in air) and nitric acid passivation (40 vol% nitric acid at room temperature for 30 min) will increase the oxide thickness of cpTi, Ti-6Al-4V, and beta-titanium, Ti-15Mo-2.8Nb-0.2Si (Timetal[®] 21SRx).

The method used to determine the oxide thickness of the samples has been used by others in the literature. The thicknesses of the surface oxides were determined by using Auger electron spectroscopy (AES) in conjunction with continuous argon ion etching to obtain a depth profile for the titanium and oxygen elements. A sputter rate of 0.2 nm/s was determined by sputtering through a 100-nm-thick tantalum oxide film. The oxide thickness was calculated by multiplying the sputter rate of 0.2 nm/s by the time it took the oxygen Auger signal to reach one-half its maximum intensity. Comparisons of the AES results for oxide thickness showed the heat-treated samples to be significantly thicker than both the non passivated and nitric-acid-passivated groups were but showed

no statistically significant differences between the non passivated and nitric-acid-passivated groups ($p < 0.05$).

Thus, Hypothesis 2 was not proven.

The oxide thickness values obtained by AES for the heat-treated samples are consistent with a logarithmic growth rate, which has been reported to govern titanium and its alloys at the temperature (350°C) used in this study.³² In addition, the AES oxide thickness results are in agreement with the golden interference coloration shown by the heat-treated samples. A golden interference color has been reported to correspond to a thermal oxide thickness of 10-25 nm³², which agrees with the values of 8.8-16.8 nm found in this study.

However, contrary to Hypothesis 2, the oxide thicknesses of the nitric-acid-passivated samples did not show any significant differences when compared with those of the non-passivated samples. This result is not entirely surprising since conflicting reports exist in the literature on the oxide thicknesses of nitric acid passivated titanium and titanium alloys. Smith^{33, 34} reported an increase in oxide thickness for Ti-6Al-4V with passivation, while Callen¹⁵ showed a thinner oxide to result for passivated Ti-6Al-4V and no change for cpTi.

One interesting aspect of this result is the fact that the passivated samples exhibited improved corrosion resistance but not an increase in oxide thickness when compared with the non passivated samples. This finding suggests that surface oxide properties besides thickness can significantly influence the corrosion properties of the materials. The oxide property responsible for the improvement is unclear. Trepanier¹² found improved corrosion properties for nitric-acid-passivated Ti-Ni alloy and attributed the improvement

to the dissolution of a “deformed plastic” native oxide and its replacement by a more uniform oxide. This topic will be discussed in more detail in the sections on Hypotheses 4-6.

Hypothesis 3

Hypothesis 3 stated that the surface oxides of cpTi, Ti-6Al-4V, and Ti-15Mo-2.8Nb-0.2Si (Timetal[®] 21SRx) materials undergoing similar surface treatments will have similar thicknesses but different chemistries.

Results from AES analysis showed similar oxide thickness results for non-passivated and nitric-acid-passivated materials, with oxide thicknesses of 3.0-5.4 nm, which are consistent with the values reported in the literature^{4, 15, 18, 35}. The heat-treated cpTi and Ti-6Al-4V also exhibited similar oxide thicknesses of 16.8 nm and 14.8 nm; however, the heat-treated 21SRx had a significantly thinner oxide of 8.8 nm.

Thus, Hypothesis 3 was not proven.

The thinner oxide for the 21SRx was attributed to the material's larger grain sizes (Fig. 3 of first paper). Oxide growth in thermal treatments is controlled in large part by mass diffusion through the grain boundaries.³⁶ Thus, mass transport is greater in the fine-grained structures of the cpTi and Ti-6Al-4V materials than in the larger-grained 21SRx, which leads to thicker oxides for the fine-grained structured materials, cpTi and Ti-6Al-4V, than for the larger-grained 21SRx.

The surface chemistries for the different material groups exhibited similarities but ultimately were distinct because of the inclusion of alloy elements on the surfaces of the alloys. Similarities in surface chemistries for all the material groups included a ubiquitous carbonaceous layer, which is routinely found on surfaces analyzed by AES³, and the pres-

ence of titanium dioxide, TiO_2 , which was attributed to all the surfaces' having AES spectra with large Ti and O peaks, with the Ti (LMV) peak at ~ 420 eV demonstrating a shape that corresponded closely to that of TiO_2 .³⁷

However, the alloy materials also showed the presence of alloying elements in the surface oxide. Aluminum peaks were found for all Ti-6Al-4V surfaces, but no vanadium peaks were found. These results are consistent with the literature^{4, 15, 35}, although the presence of vanadium has been reported by others using XPS.^{4, 15, 38} One reason for not detecting vanadium with AES in this study is that the vanadium AES peaks overlap those of titanium and oxygen.³⁹

The AES spectra for the 21SRx showed molybdenum throughout the oxides. The presence of molybdenum on surfaces of various Ti-Mo alloys has been reported by other researchers using AES^{40, 41}. Although no niobium peaks were shown in any of the 21SRx spectra, the presence of niobium cannot be ruled out since niobium peaks overlap molybdenum peaks.

Hypothesis 4

This hypothesis stated that increasing the time of passivation used in the nitric acid passivation process will improve the protective properties of the surface oxides and the corrosion resistance of cpTi, Ti-6Al-4V, and Ti-15Mo.

The results of this study showed the protective properties of the material groups to change with time of passivation. The time effect was sensitive to concentration; the samples passivated in 10% nitric acid exhibited less protective oxides initially at 15 min and 1 h but then improvements at 2 h. This pattern was in contrast to the samples passivated

in 40% nitric acid, which showed immediate improvement at 15 min and more improvement at 1 h but then a decrease in protective properties at 2 h.

Thus, Hypothesis 4 was not proven.

Previous studies by Wallinder¹³ and Noh¹⁴ have shown longer passivation times to improve the corrosion properties of stainless steels; however, such studies for titanium or titanium alloys are limited. The time response shown in this study indicates that passivation in 10% nitric acid initially dissolves and/or degrades the surface oxide at 15 min and 1 h but then improves the oxide at 2 h. This conclusion is based on the EIS and corrosion results, which showed the oxide resistance (R_p) and corrosion resistance to decrease at the first two time periods and then improve at 2 h.

The surface chemistry results also support this conclusion. The XPS results showed the samples passivated in 10% nitric acid at 20°C for 1 h to have increases in the atomic percentages for the suboxides Ti_2O_3 and TiO and in the metallic Ti when compared with the non passivated groups (Clean). Increases in suboxide amounts have been associated in the literature with decreased corrosion resistance⁹, while increases in metallic Ti have been interpreted as indicative of a thinner oxide.^{9, 15, 42} Another surface chemistry result that supports this conclusion is the more irregular distribution of alloy elements within the oxide of the alloys passivated with 10% nitric acid for 1 h than within the non passivated (Clean) groups (Figs. 13 and 14 in paper 2). A more irregular compositional gradient indicates a more defective oxide due to point defects introduced by mismatches in ionic radii of the different elements.⁴³

The samples passivated in 40% nitric acid showed a different time response than those passivated in 10% nitric acid did. Initially, the 40% groups showed improved oxide

properties, with increased oxide resistance and improved corrosion resistance culminating in maximum protection at 1 h. However, after 2 h, the oxides were shown to become less protective, with lower R_p values and lower oxide n values and corrosion resistance. The physical meaning of the n EIS parameter has been associated with surface roughness⁴⁴, the presence of a porous corrosion product layer⁴⁵, and/or the homogeneous nature of the surface oxide.⁴⁶ Thus, a decrease in the n value at 2 h indicates a rougher, less uniform oxide with the additional presence of a porous corrosion product layer, which could play a role in the observed increased corrosion. As with the 10%-1h groups, the 40%-2h groups exhibited irregular compositional gradients for the alloying elements within the oxide, which also could explain the less protective oxide properties at 2 h. However, it should be noted that the variation in time response was less pronounced for the Ti-15Mo alloy.

The mechanisms for the different time responses are unclear. The time response for the 10% nitric acid groups may be due to the fact that more dilute acid solutions are less oxidizing than higher acid concentrations are.^{13, 14} Thus, one might hypothesize that, at the shorter times, the chemical reactions at the oxide surface for the 10% nitric acid groups are less uniform, leading to a less uniform oxide (i.e., increased percentages of suboxides) and a more irregular compositional gradient. For groups passivated at the higher concentration (40%), the oxidation reactions are more prevalent and stronger, leading initially to uniform dissolution and oxidation over the surface and thus to a more uniform oxide. However, after a certain time (i.e., 1 h), a less uniform oxide may result because of the formation of an outer porous corrosion product layer.

Hypothesis 5

This hypothesis stated that increasing the nitric acid concentration used in the nitric-acid-passivation process will improve the protective properties of the surface oxides and the corrosion resistance of cpTi, Ti-6Al-4V, and Ti-15Mo.

In the present study, nitric acid concentration was shown to have a significant effect on the surface properties of the titanium and titanium alloys studied. In general, the samples passivated with 40% nitric acid showed higher oxide resistance and improved corrosion resistance than with similar groups treated with 10% nitric acid showed. The only exceptions were the Ti-15Mo groups passivated for 1 h and 2 h at 50°C.

Thus, Hypothesis 5 is not proven.

Wallinder¹³ and Noh¹⁴, in addition to showing the time effects, have shown that the concentration of nitric acid has a major effect on the corrosion resistance of stainless steel. Wallinder showed greater concentration effects at shorter passivation times, and Noh demonstrated the existence of an optimum concentration, which if exceeded would result in poorer corrosion properties of the stainless steel. In the present study, concentration effects were more pronounced at the shorter passivation times of 15 min and 1 h than at 2 h, much as Wallinder showed. Because only two concentrations were tested in the present study, a conclusion as to “peak” concentration was not possible.

Surface chemistry results supported the conclusion of improved protective properties for the 40% groups when compared with those properties of the 10% groups. The stoichiometry results from the XPS showed that the 40% groups had lower percentages of suboxides and metallic Ti than the 10% groups did, which, as mentioned earlier, suggests improved corrosion properties⁹ and thicker oxides^{9, 15, 42}, respectively. However, as with

the effect of time, the most important surface chemistry differences due to concentration for the alloys may have been the compositional gradient within the oxide. Figure 13 in the second paper shows that, in comparison with the 10%-Ti-6Al-4V groups, the 40%-Ti-6Al-4V groups had a higher percentage of Al and V at each etch time, and, more important, displayed more constant gradients for both elements throughout the oxide layer. Figure 14 in the second paper shows similar results for the percentages of Mo throughout the Ti-15Mo groups. These results were consistent with the EIS and corrosion results, which showed in general that the 40% groups had more protective oxides and less corrosion than the 10% groups did.

As described in the Hypothesis 4 discussion on the effects of time, the most likely mechanism for the production of more protective oxides by higher acid concentrations is their increased oxidizing power. A more oxidizing environment would result in more pronounced and uniform surface reactions, which would lead to a more uniform oxide, as well as a thicker oxide.

The only exception to the general trend was the Ti-15Mo groups passivated for 1 h and 2 h at 50°C. The reason for this result is unclear. The probable explanation is that the Ti-15Mo groups were not as sensitive to nitric acid treatments.

Hypothesis 6

Hypothesis 6 stated that increasing the nitric acid temperature used in the nitric acid passivation process will improve the protective properties of the surface oxides and the corrosion resistance of cpTi, Ti-6Al-4V, and Ti-15Mo.

The increases in passivation temperature tended to result in improved protective oxide properties and lower corrosion. In all but a couple of instances, the EIS parameters, Q , n , and R_p , increased, the E_{corr} results became more noble, and the I_{pass} results decreased with the higher temperature.

Thus, Hypothesis 6 is proven.

The stoichiometry for all three material groups had similar changes due to the higher passivation temperature. All the changes were slight and showed the 50°C groups to have slightly more TiO_2 , slightly less total suboxides, and slightly less metallic Ti than the groups passivated at 20°C had. These results are consistent with those found in other studies in the literature, which have attributed increased oxidation reactions to the higher temperatures. As a result of the increased oxidation, thicker oxides are formed with more TiO_2 and less suboxides.^{15, 16}

As with the time and concentration effects, the passivation temperature was shown to affect the distribution of alloy elements in the oxides of the two alloys. Figure 13 in the second paper shows that the 50°C-Ti-6Al-4V groups had smaller percentages of Al and V elements throughout the surface oxide layer than the 20°C-Ti-6Al-4V groups did. The lower concentrations of alloying elements agree with the consistently higher n and R_p results for the 50°C-Ti-6Al-4V groups, which indicate greater oxide homogeneity and hence a more protective oxide and lower corrosion.

Hypothesis 7

Hypothesis 7 stated that nitric acid passivation using ultrasonication will decrease the protective properties of the surface oxides of cpTi, Ti-6Al-4V, and Ti-15Mo and increase corrosion.

The study showed samples passivated with ultrasonication to have EIS and potentiodynamic polarization corrosion results similar to those of statically passivated samples. In the activation corrosion tests, the ultrasonicated passivated cpTi and Ti-6Al-4V groups had significantly longer breakdown times than non passivated and statically passivated groups had.

Thus, Hypothesis 7 is not proven.

The propagation of an ultrasonic wave through a liquid generates voids and the collapse of voids, which are called cavitations. The collapse of the void can generate higher temperatures and pressures. Additionally, when the void comes in contact with a solid surface, the collapse of the void results in a high-velocity fluid stream directed toward the surface. These events can lead to cavitation damage to the surface, and microstructural changes can occur.²⁰ In fact, Whillock²⁰ showed that, during ultrasonication in nitric acid, stainless steel had three- to sixfold increases in corrosion. On the basis of these facts, Hypothesis 7 was developed.

However, contrary to Hypothesis 7, the surface oxides and corrosion properties were not adversely affected by the ultrasonic process and even showed increased protection in the activation corrosion studies. Examining the results revealed that, most were similar; however, a few differences were shown. One difference was the compositional gradient in the Ti-6Al-4V groups. The ultrasonicated group had less aluminum at the outermost region than the statically passivated group did and then had similar amounts

ermost region than the statically passivated group did and then had similar amounts throughout the rest of the surface. Comparatively less aluminum at the outermost surface suggests a less defective oxide at the outermost regions and hence more protection.⁴³

Another interesting result for the ultrasonic groups was their consistently higher capacitance (Q) values. As discussed in the third paper, on the basis of the parallel-plate capacitor equation, $Q = \epsilon\epsilon_0A/d_{ox}$ (where ϵ_0 is permittivity of vacuum, ϵ is the dielectric constant of the oxide, A is the effective area, and d_{ox} is the thickness of the oxide), the Q value is inversely related to oxide thickness, d_{ox} , and directly related to the effective area and dielectric constant. In the literature, many authors assume a constant dielectric constant and effective area in order to calculate an oxide thickness. If those assumptions were made for the results from the present study, the higher Q values for the ultrasonic groups would suggest a thinner oxide. However, the XPS results indicate that the oxide thicknesses were similar. Thus, the change in Q values must result from changes in effective area or dielectric constant. SEM analysis showed similar surface topographies for ultrasonic and static groups, which would lead one to assume similar effective areas. Thus, it would appear that the change in Q values must be related to changes in the dielectric constant of the oxides.

Ohtsuka reported increases in the dielectric constant for surface oxides with a higher degree of hydration, which resulted from higher oxide formation rates.⁴⁷ Thus, the higher Q values may indicate that ultrasonication results in more hydrated oxides. The higher temperature and pressures due to cavitation might be expected to increase the oxide formation rate.

Another possible reason for a higher oxide formation rate is related to what Whillock reported in his study on ultrasonication of stainless steel in nitric acid.²⁰ Whillock²⁰ reported that, upon the initiation of ultrasonication, the stainless steel went from a passive state (i.e., a more positive corrosion potential) to a more active corrosion state (i.e., a lower corrosion potential) and remained there until ultrasonication was stopped, whereupon the sample immediately became more passive (i.e., the corrosion potential returned to passive levels). The fact that the sample became passive immediately upon the stopping of ultrasonication implies an instantaneous growth of the oxide, which, as Ohtsuka⁴⁷ reported, would result in an oxide with a higher degree of hydration and hence increased dielectric constant and higher Q values.

Hypothesis 8

This hypothesis stated that nitric acid passivation with the addition of titanium ions will improve the protective properties of the surface oxides of cpTi, Ti-6Al-4V, and Ti-15Mo and decrease corrosion.

Comparisons of the EIS and corrosion results for the groups that had been passivated with additional titanium ions (160Ti) with those results for the groups passivated without additional titanium ions (Static) showed the two groups to be similar. Only a few of the differences between the groups were shown to be statistically significant.

Thus, Hypothesis 8 is not proven.

Corrosion studies in the literature have shown that the addition of titanium ions in nitric acid decreased the corrosion rate of titanium and titanium alloys in nitric acid solutions.²² Robin²² showed that a critical concentration of titanium ions was necessary in or-

der to decrease the corrosion rates. For Ti-6Al-4V, Robin²² found the critical concentration to be 160 mg Ti/L for 40% nitric acid; accordingly, that concentration was used in the present study.

In nitric acid solutions containing additional titanium ions, Robin found that the corrosion potential increased more quickly and to more noble levels and that the samples had lower passive current densities. Robin attributed the quicker and greater increase in corrosion potential to a faster-growing passive film and attributed the lower passive current densities to a more stable surface oxide. The increased oxide formation rate was attributed to the presence of additional titanium ions.²²

In the present study, the Q values for the 160Ti groups were only slightly higher than those of the Static groups were, which indicates similar oxide hydration levels and, by extension as outlined in the Hypothesis 7 discussion, similar oxide formation rates.

An interesting result for the 160Ti groups was the more prevalent and pronounced appearance of pit-like features on the surfaces. This result may be due to the formation of a porous outer oxide layer since the EIS spectra exhibited two phase angle maximums, which are indicative of a dual oxide layer.⁴⁸ The dual oxide layer is assumed to consist of a dense barrier layer on the substrate and a porous layer on top of the barrier layer. XPS analysis of the groups tended to support the presence of a porous outer oxide, with the 160Ti groups demonstrating smaller percentages for metallic Ti and alloy elements at the outermost surface, which would be consistent with a thicker oxide layer resulting from the presence of a porous outer oxide.

Hypothesis 9

Hypothesis 9 stated that the nitric acid treatments for cpTi, Ti-6Al-4V, and Ti-15Mo will not reduce cell attachment and proliferation compared to those properties of non passivated materials.

In both investigations in which cell culture studies were performed, comparisons between the non passivated and passivated groups did not show the passivated groups to exhibit a diminished cellular response.

Thus, Hypothesis 9 is proven.

SaOS-2 osteoblast-like cells were used to determine the cellular response to the different treatment groups. Hexosaminidase assay was used to quantify the cell numbers at various time points. This assay measures the amount of hexosaminidase enzyme, which has been shown to be directly proportional to the number of attached cells.⁴⁹ In addition to cell numbers, cell proliferation between successive time points was quantified.

The effect of nitric-acid-passivated titanium and titanium alloys on cellular response has been reported in the literature. Faria⁵⁰ showed no differences in cell attachment and proliferation of cells on non passivated and passivated cpTi and Ti-6Al-4V. Ku⁵¹ also showed negligible effects when comparing passivated and non passivated Ti-6Al-4V. On the other hand, Mante⁵² showed increased cellular attachment for nitric-acid-passivated cpTi specimens. The studies in this dissertation showed similar results. Passivated samples had results as good as if not better than those of non passivated samples.

In the second paper, a report on studying the effects of time, concentration, and temperature of nitric acid passivation, the initial attachment results showed the Ti-15Mo

to have significantly higher cell numbers. However, these increases could be attributed to the rougher surface of the Ti-15Mo samples since rougher surfaces have been linked to increased cellular attachment in the literature.⁵³⁻⁵⁵

In the same paper, the Ti-15Mo groups also showed significant differences within the treatment groups for the 1-h cell attachment results. All the passivated Ti-15Mo groups were significantly higher than the non passivated group (Clean) was. The reason for this result is not clear. The EIS, corrosion, and XPS results for these groups did not show a consistent change in a single variable or a set of variables that would explain this difference. However, although the SEM analysis did not show any obvious differences in surface morphology between the passivated and non passivated Ti-15Mo groups, perhaps the nitric acid passivation treatments enhanced cell attachment by removing or altering some irregular surface features that may not have been noticeable with the SEM analysis.

Another interesting result in the studies was that the cell numbers seemed to follow the Q values of the treatment groups, with more cells shown for groups with higher Q values. As has been discussed previously, the Q value is a function of not only the oxide thickness but also the effective area (i.e., roughness) and dielectric constant of the surface oxide. In these studies, the changes in Q values seem to be associated more with differences in roughness and dielectric constant than with oxide thickness since large changes in Q values were shown with no significant changes in oxide thickness. Thus, the trend of increased cell numbers with higher Q values would seem to reflect changes in roughness or dielectric constant.

However, large changes in Q values were documented for similar material groups, which had comparable surface roughness. Hence, this finding suggests that the observed

higher Q values were related to a higher dielectric constant and thus that changes in the dielectric constant were affecting the cellular trends. This interpretation agrees with studies from the literature, which show increased surface bioactivity for specimens with oxides that have a higher degree of hydration.^{56, 57} As was mentioned earlier, Ohtsuka⁴⁷ showed that more highly hydrated oxides have higher dielectric constant.

Future Research

The results of these studies demonstrated that passivation parameters do affect the surface oxide and corrosion properties of titanium and titanium alloys. However, like all research, answering one question raised many more in the process. The following subjects are suggested future research areas that would further improve the understanding of the passivation process and resultant oxides for titanium and titanium alloys.

First, a better understanding is needed of the processes that are occurring during the nitric acid passivation itself. Corrosion analysis during the process would help identify the passivation mechanisms occurring when different passivation parameters are used. Performing simple corrosion potential tests and EIS testing while passivating the samples would help determine how the oxide is responding to the various nitric acid environments.

Second, roughness effects were shown to confound some of the comparisons between material groups; thus, the surface topographies should be normalized, perhaps by using a more highly polished surface. Also, quantifiable analysis of the surface topography should be done in addition to the qualitative SEM analysis.

Third, the capacitance, or Q value, obtained from the fitted Equivalent Electrical Circuit (EEC) models was shown to be sensitive to the various passivation treatments with good reproducibility. However, it was unclear whether the changes in Q value were due to oxide thickness, effective area, or dielectric constant. Controlled studies isolating each of these three parameters would help future analysis using EIS.

Fourth, the potentiodynamic polarization corrosion tests and EIS tests do not provide direct information as to the dissolution properties of the materials and dissolution products. Thus, dissolution tests would provide a more complete picture of how the passivation parameters are affecting the surfaces of the titanium and titanium alloys. In addition, dissolution studies would help clinicians make a better correlation between the surface treatments and biological outcomes.

Finally, more extensive and sensitive cell culture tests would help differentiate cellular responses to the various passivation treatments. Also, longer-term experiments would help identify possible passivation effects that are more time sensitive.

CONCLUSIONS

The following conclusions were drawn from the results of these studies:

1. The titanium and titanium alloy materials that were tested all exhibited excellent corrosion properties regardless of surface treatments.
2. Heat treatment and nitric acid passivation treatments significantly improved or resulted in similar corrosion properties compared with non-passivated titanium and titanium alloys.
3. Titanium and titanium alloys with similar oxide thicknesses could have significantly different corrosion properties.
4. Time of passivation and nitric acid concentration and temperature affected the surface oxide properties and corrosion resistance of titanium and titanium alloys.
5. Effects of passivation time were dissimilar for different nitric acid concentrations.
6. More highly oxidizing nitric acid environments (i.e., higher concentrations and temperatures) resulted in more uniform surface oxides that were more corrosion resistant for most treatment groups.
7. Nitric acid passivation with ultrasonication did not adversely affect the surface oxide or corrosion properties of titanium and titanium alloys.
8. Addition of titanium ions to the nitric acid solution did not improve the surface properties or corrosion properties of titanium and titanium alloys.
9. Titanium and titanium alloys undergoing nitric acid passivation treatments had similar biological responses that were comparable to those of non passivated mate-

-rials and tissue culture controls. The rougher Ti-15Mo surfaces resulted in higher cell numbers at the initial time period.

10. The overall results indicated that the optimal combination of parameters for nitric acid passivation of titanium and titanium alloys tested in this study was 40% nitric acid for 1 h at 50°C.

GENERAL LIST OF REFERENCES

1. Tomashov ND, *Theory of corrosion and protection of metals the science of corrosion*, ed. B.H. Tytell. 1966, New York: McMillan Company.
2. Lomonosov MV, *Collected Works*. 1950, Moscow: Academy of Sciences.
3. Lausmaa J, Kasemo B, Mattsson H, Odellius H, Multi-technique surface characterization of oxide films on electropolished and anodically oxidized titanium. *Applied Surface Science* 1990; 45(3):189.
4. Ask M, Lausmaa J, Kasemo B, Preparation and surface spectroscopic characterization of oxide films on ti6al4v. *Applied Surface Science* 1989; 35(3):283.
5. Fraker AC, "*Corrosion of Metallic Implants and Prosthetic Devices*", in *Metals Handbook*. 1987, ASM International: Metals Park, Ohio. p. 1324-1335.
6. Williams DF, "*Titanium and Titanium Alloys*", in *Biocompatibility of Clinical Implant Materials*, D.F. Williams, Editor. 1981, CRC Press: Boca Raton, Florida. p. Ch. 2.
7. Zitter H, Plenk H, The electrochemical behavior of metallic implant materials as an indicator of their biocompatibility. *J Biomed Mater Res* 1987; 21(7):881-96.
8. Kilpadi DV, Raikar GN, Liu J, Lemons JE, Vohra Y, Gregory JC, Effect of surface treatment on unalloyed titanium implants: Spectroscopic analyses. *Journal of Biomedical Materials Research* 1998; 40(4):128.
9. Lee TM, Chang E, Yang CY, Surface characteristics of Ti6Al4v alloy: Effect of materials, passivation and autoclaving. *Journal of Materials Science: Materials in Medicine* 1998; 9(8):439.
10. Browne M, Gregson PJ, Surface modification of titanium alloy implants. *Biomaterials* 1994; 15(11):894.
11. Wisbey A, Gregson PJ, Peter LM, Tuke M, Effect of surface treatment on the dissolution of titanium-based implant materials. *Biomaterials* 1991; 12(5):470.
12. Trepanier C, Tabrizian M, Yahia LH, Bilodeau L, Piron DL, Effect of modification of oxide layer on NiTi stent corrosion resistance. *Journal of Biomedical Materials Research* 1998; 43(4):433.

13. Wallinder D, Pan J, Leygraf C, Delblanc-Bauer A, EIS and XPS study of surface modification of 316lvm stainless steel after passivation. *Corrosion Science* 1999; 41(2):275.
14. Noh JS, Laycock NJ, Gao W, Wells DB, Effects of nitric acid passivation on the pitting resistance of 316 stainless steel. *Corrosion Science* 2000; 42(12):2069.
15. Callen BW, Lowenberg BF, Lugowski S, Sodhi RNS, Davies JE, Nitric acid passivation of ti6al4v reduces thickness of surface oxide layer and increases trace element release. *Journal of Biomedical Materials Research* 1995; 29(3):279.
16. Lowenberg BF, Lugowski S, Chipman M, Davies JE, Astm-f86 passivation increases trace element release from ti6al4v into culture medium. *Journal of Materials Science: Materials in Medicine* 1994; 5(6-7):467.
17. ASTM F86-91 standard practice for surface preparation and marking of metallic surgical implants. *Annual Book of ASTM Standards* 1995; 13.01:6-7.
18. Ong JL, Lucas LC, Raikar GN, Gregory JC, Electrochemical corrosion analyses and characterization of surface-modified titanium. *Applied Surface Science* 1993; 72(1):7.
19. Kilpadi DV, Weimer JJ, Lemons JE, Effect of passivation and dry heat-sterilization on surface energy and topography of unalloyed titanium implants. *Colloids and Surfaces A: Physicochemical and Engineering Aspects* 1998; 135(1-3):89.
20. Whillock GOH, Harvey BF, Preliminary investigation of the ultrasonically enhanced corrosion of stainless steel in the nitric acid/chloride system. *Ultrasonics Sonochemistry* 1996; 3(2):111-118.
21. Robin A, Rosa JL, Sandim HRZ, Corrosion behavior of Ti-4Al-4V alloy in nitric, phosphoric and sulfuric acid. *J Appl Electrochemistry* 2001; 31:455-460.
22. Robin A, Sandim HRZ, Rosa JL, Corrosion behavior of the Ti-4%Al-4%V alloy in boiling nitric acid solutions. *Corrosion Science* 1999; 41:1333-1346.
23. Turner TM, Sumner DR, Urban RM, Igloria R, Galante JO, Maintenance of proximal cortical bone with use of a less stiff femoral component in hemiarthroplasty of the hip without cement. An investigation in a canine model at six months and two years. *J Bone Joint Surg Am* 1997; 79(9):1381-90.
24. Thompson GJ, Puleo DA, Ti-6Al-4V ion solution inhibition of osteogenic cell phenotype as a function of differentiation timecourse in vitro. *Biomaterials* 1996; 17(20):1949-54.

25. van der Voet GB, Marani E, Tio S, De Wolff FA, *Aluminum neurotoxicity*, in *Histo- and cytochemistry as a tool in environmental toxicology*, W. Graumann and J. Drukker, Editors. 1991, Stuttgart. p. 235-242.
26. Rae T, The toxicity of metals used in orthopaedic prostheses. An experimental study using cultured human synovial fibroblasts. *J Bone Joint Surg Br* 1981; 63-B(3):435-40.
27. Wataha JC, Hanks CT, Craig RG, The effect of cell monolayer density on the cytotoxicity of metal ions which are released from dental alloys. *Dent Mater* 1993; 9(3):172-6.
28. Blumenthal NC, Cosma V, Inhibition of apatite formation by titanium and vanadium ions. *Journal of Biomedical Materials Research* 1989; 23(A1 SUPPL):13.
29. Garcia-Alonso MC, Saldana L, Valles G, Gonzalez-Carrasco JL, Gonzalez-Cabrero J, Martinez ME, Gil-Garay E, Munuera L, In vitro corrosion behaviour and osteoblast response of thermally oxidised Ti6Al4V alloy. *Biomaterials* 2003; 24(1):19.
30. Lee TM, Chang E, Yang CY, Effect of passivation on the dissolution behavior of ti6a14v and vacuum-brazed Ti6A14V in hank's ethylene diamine tetra-acetic acid solution Part I Ion release. *Journal of Materials Science: Materials in Medicine* 1999; 10(9):541.
31. Park YJ, Shin MS, Yang HS, Ong JL, Rawls HR. *Effect of heat treatment on microstructural and electrochemical properties of titanium and ti alloy*. 1998. San Antonio, TX, USA: IEEE, Piscataway, NJ, USA.
32. Velten D, Biehl V, Aubertin F, Valeske B, Possart W, Breme J, Preparation of Tio(2) layers on cp-Ti and Ti6Al4V by thermal and anodic oxidation and by sol-gel coating techniques and their characterization. *J Biomed Mater Res* 2002; 59(1):18-28.
33. Smith DC, Pilliar RM, Chernenky R, Dental implant materials. I. Some effects of preparative procedures on surface topography. *Journal of Biomedical Materials Research* 1991; 25(9):1045.
34. Smith DC, Pilliar RM, Metson JB, McIntyre NS, Dental implant materials. II. Preparative procedures and surface spectroscopic studies. *Journal of Biomedical Materials Research* 1991; 25(9):1069.
35. Lausma J, Ask M, Rolander U, Kasemo B, Preparation and analysis of Ti and alloyed Ti surfaces used in the evaluation of biological response. *Materials Research Society Symposia Proceedings* 1989; 110:647-653.

36. Leyens C, Peters M, Kaysser WA, Influence of microstructure on oxidation behaviour of near-alpha titanium alloys. *Materials Science and Technology* 1996; 12:213-218.
37. Lausmaa J, Mattsson L, Rolander U, Kasemo B, Chemical composition and morphology of titanium surface oxides. *Materials Research Society Symposia Proceedings* 1986; 55:351.
38. Sodhi RN, Weninger A, Davies JE, X-ray photoelectron spectroscopic comparison of sputtered Ti, Ti6Al4V, and passivated bulk metals for use in cell culture techniques. *Journal of Vacuum Science Technology* 1991; A9(3):1329-1333.
39. Lausmaa J, Kasemo B, Mattsson H, Surface spectroscopic characterization of titanium implant materials. *Applied Surface Science* 1990; 44(2):133.
40. Kim YJ, Oriani RA, Effect of the microstructure of Ti-5Mo on the anodic dissolution in H₂SO₄. *Corrosion* 1987; 43(4):418.
41. Laser D, Marcus HL, Auger electron spectroscopy depth profile of thin oxide on a Ti-Mo alloy. *Journal Electrochemical Society* 1980; 127(3):763-765.
42. Sodhi RNS, Sahi VP, Mittelman MW, Application of electron spectroscopy and surface modification techniques in the development of anti-microbial coatings for medical devices. 2001; 121(1-3):249.
43. Metikos-Hukovic M, Kwokal A, Piljac J, The influence of niobium and vanadium on passivity of titanium-based implants in physiological solution. *Biomaterials* 2003; 24(21):3765.
44. Rammelt U, Reinhard, G., The influence of surface roughness on the impedance data for iron electrodes in acidic solutions. *Corrosion Science* 1987; 27:373-382.
45. Park JR, MacDonald, D.D., Impedance studies on the growth of porous magnetite films on carbon steels in high temperature aqueous systems. *Corrosion Science* 1983; 23(4):295-315.
46. MacDonald DD, *Impedance spectroscopy*, ed. W.B. Johnson. 1987, New York: John Wiley. 154-156.
47. Ohtsuka T, Otsuki, T, The influence of the growth rate on the semiconductive properties of titanium anodic oxide films. *Corrosion Science* 1998; 40(6):951-958.
48. Pan J, Thierry D, Leygraf C, Electrochemical impedance spectroscopy study of the passive oxide film on titanium for implant application. *Electrochimica Acta* 1996; 41(7-8):1143.

49. Landegren U, Measurement of cell numbers by means of the endogenous enzyme hexosaminidase. Applications to detection of lymphokines and cell surface antigens. *J Immun Methods* 1984; 67:379-388.
50. Faria AC, Beloti MM, Rosa AL, Nitric acid passivation does not affect in vitro biocompatibility of titanium. *Int J Oral Maxillofac Implants* 2003; 18(6):820-825.
51. Ku CH, Pioletti DP, Browne M, Gregson PJ, Effect of different Ti-6Al-4V surface treatments on osteoblasts behaviour. *Biomaterials* 2002; 23:1447-1454.
52. Mante M, Daniels B, Golden E, Diefenderfer D, Reilly G, LeBoy PS, Attachment of human marrow stromal cells to titanium surfaces. *J Oral Implantol* 2003; 29(2):66-72.
53. Ahmad M, Gawronski, D, Blum, J., Golderg, J, Gronowicz, Differential response of human osteoblast-like cells to commercially pure (cp) titanium grades 1 and 4. *J Biomed Mater Res* 1999; 46:121-131.
54. Feng B, Weng J, Yang BC, Qu SX, Zhang XD, Characterization of surface oxide films on titanium and adhesion of osteoblast. *Biomaterials* 2003; 24(25):4663.
55. Stanford CM, Keller JC, Solursh M, Bone cell expression on titanium surfaces is altered by sterilization treatments. *J Dent Res* 1994; 73(5):1061-71.
56. Li P, Ohtsuki C, Kokubo T, Nankanishi K, Soga N, de Groot K, The role of hydrated silica, titania and alumina in inducing apatite on implants. *J Biomed Mater Res* 1994; 28:7-15.
57. Ohtsuki C, Iida H, Hayakawa S, Osaka A, Bioactivity of titanium treated with hydrogen peroxide solutions containing metal chlorides. *J Biomed Mater Res* 1997; 35:39-47.

**GRADUATE SCHOOL
UNIVERSITY OF ALABAMA AT BIRMINGHAM
DISSERTATION APPROVAL FORM
DOCTOR OF PHILOSOPHY**

Name of Candidate Donald William Petersen

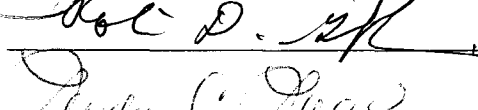
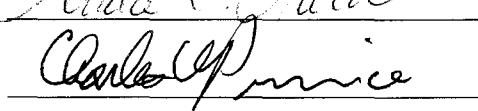
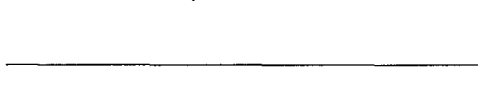
Graduate Program Biomedical Engineering

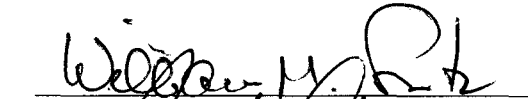
Title of Dissertation Effects of Passivation on Surface Properties of

Titanium and Titanium Alloys

I certify that I have read this document and examined the student regarding its content. In my opinion, this dissertation conforms to acceptable standards of scholarly presentation and is adequate in scope and quality, and the attainments of this student are such that he may be recommended for the degree of Doctor of Philosophy.

Dissertation Committee:

Name	Signature
<u>Jack E. Lemons</u> , Chair	
<u>John M. Cuckler</u>	
<u>Robin D. Griffin</u>	
<u>Linda C. Lucas</u>	
<u>Charles W. Prince</u>	

Director of Graduate Program 

Dean, UAB Graduate School 

Date _____